Error rate performance metrics for digital communications systems.

Hassanien, Mohamed A. M

Error Rate Performance Metrics for Digital Communications Systems

Swansea University
Prifysgol Abertawe

Mohamed A. M. Hassanien

College of Engineering

Swansea University

Submitted to Swansea University in fulfillment of the requirements for the degree of

Doctor of Philosophy (Ph.D.)

August. 2011

ProQuest LLC.
789 East Eisenhower Parkway
P.O. Box 1346
Ann Arbor, MI 48106 – 1346

Abstract

In this thesis, novel error rate performance metrics and transmission solutions are investigated for delay limited communication systems and for co-channel interference scenarios. The following four research problems in particular were considered.

The first research problem is devoted to analysis of the higher order ergodic moments of error rates for digital communication systems with time-unlimited ergodic transmissions and the statistics of the conditional error rates of digital modulations over fading channels are considered. The probability density function and the higher order moments of the conditional error rates are obtained. Non-monotonic behavior of the moments of the conditional bit error rates versus some channel model parameters is observed for a Ricean distributed channel fading amplitude at the detector input. Properties and possible applications of the second central moments are proposed.

The second research problem is the non-ergodic error rate analysis and signaling design for communication systems processing a single finite length received sequence. A framework to analyze the error rate properties of non-ergodic transmissions is established. The Bayesian credible intervals are used to estimate the instantaneous bit error rate. A novel degree of ergodicity measure is introduced using the credible interval estimates to quantify the level of ergodicity of the received sequence with respect to the instantaneous bit error rate and to describe the transition of the data detector from the non-ergodic to ergodic zone of operation. The developed non-ergodic analysis is used to define adaptive forward error correction control and adaptive power control policies that can guarantee, with a given probability, the worst case instantaneous bit error rate performance of the detector in its transition from the non-ergodic to ergodic zone of operation.

In the third research problem, novel retransmission schemes are developed for delay-limited retransmissions. The proposed scheme relies on a reliable reverse link for the error-free feedback message delivery. Unlike the conventional automatic repeat request schemes, the proposed scheme does not require the use of cyclic redundancy check bits for error detection. In the proposed scheme, random permutations are exploited to locate the bits for retransmission in the predefined window within the packet. The retransmitted bits are combined using the maximal-ratio combining. The complexity-performance trade-offs of the proposed scheme is investigated by mathematical analysis as well as computer simulations. The bit error rate of the proposed scheme is independent of the packet length

while the throughput is dependent on the packet length. Three practical techniques suitable for implementation are proposed. The performance of the proposed retransmission scheme was compared to the block repetition code corresponding to a conventional ARQ retransmission strategy. It was shown that, for the same number of retransmissions, and the same packet length, the proposed scheme always outperforms such repetition coding, and, in some scenarios, the performance improvement is found to be significant. Most of our analysis has been done for the case of AWGN channel, however, the case of a slow Rayleigh block fading channel was also investigated. The proposed scheme appears to provide the throughput and the BER reduction gains only for the medium to large SNR values.

Finally, the last research problem investigates the link error rate performance with a single co-channel interference. A novel metric to assess whether the standard Gaussian approximation of a single interferer underestimates or overestimates the link bit error rate is derived. This metric is a function of the interference channel fading statistics. However, it is otherwise independent of the statistics of the desired signal. The key step in derivation of the proposed metric is to construct the standard Gaussian approximation of the interference by a non-linear transformation. A closed form expression of the metric is obtained for a Nakagami distributed interference fading amplitude. Numerical results for the case of Nakagami and lognormal distributed interference fading amplitude confirm the validity of the proposed metric.

The higher moments, interval estimators and non-linear transformations were investigated to evaluate the error rate performance for different wireless communication scenarios. The synchronization channel is also used jointly with the communication link to form a transmission diversity and subsequently, to improve the error rate performance.

Declarations and statements

DECLARATION

This work has not previously been accepted in substance for any degree and is not being concurrently submitted in candidature for any degree.

Signed.. candidate)
Date....21/11/2011.....

STATEMENT 1

This thesis is the result of my own investigations, except where otherwise stated. Where correction services have been used, the extent and nature of the correction is clearly marked in a footnote(s).

Other sources are acknowledged by footnotes giving explicit references. A bibliography is appended.

Signed (candidate)
Date.....21/11/2011.....

STATEMENT 2

I hereby give consent for my thesis, if accepted, to be available for photocopying and for inter-library loan, and for the title and summary to be made available to outside organizations.

Signed. candidate)
Date....21/11/2011.....

Contents

Acknowledgment

I express my sincere gratitude and appreciation to my learned supervisor Dr. Pavel Loskot for his relentless and continuous enlightening support during the process of this research. I am certainly aware and appreciative for his patience, inspiring ideas, his encouraging enthusiasm and his immense knowledge. His guidance indeed inspired and helped me at all stages of this research when it was just an idea until its conclusions as a presentable thesis.

I also express my gratitude to the school of engineering (institute of advanced telecommunication previously) of Swansea university for awarding me Master degree and full scholarship for the first year on my PhD work.

I also express my sincere thanks to my family members,especially my parents Ali Mahmoud and Samira Kamil, for their support and encouragement to continue my PhD work. I really needed such encouragement to finish my research.

List of figures

List of tables

Acronyms

ARQ automatic repeat request, (17)

AWGN additive white Gaussian noise, (28)

BEP bit error probability, (14)

BER bit error rate, (14)

BPSK binary phase shift keying, (34)

BSC binary symmetric channel, (41)

CRC cyclic redundancy check, (17)

DLC delay-limited capacity, (22)

DOE degree of ergodicity, (41)

FEC forward error correction, (17)

FER frame error rate, (40)

HARQ hybrid automatic repeat request, (18)

MGF moment generating function, (30)

MIMO multiple-input multiple-output, (23)

MISO multiple-input single-output, (23)

MRC maximal ratio combining, (18)

MSE mean square error, (14)

OFDM orthogonal frequency division multiplexing, (23)

PDF probability density function, (11)

PE error probability, (14)

QAM quadrature amplitude modulation, (33)

QoE quality-of-experience, (3)

QoS quality-of-service, (3)

RNG random number generator, (19)

RV random variable, (11)

SER symbol error rate, (14)

SIMO single-input multiple-output, (23)

SIR signal-to-interference ratio, (109)

SNR signal-to-noise ratio, (13)

WSS wide-sense stationary, (12)

Notation

$\lvert x \rvert$	absolute value
$\lceil x \rfloor$	rounding function
$\binom{N}{k}$	binomial coefficient
$\beta(x, y)$	beta function
$\beta(x; y, z)$	incomplete beta function
$\Gamma(x)$	gamma function
$\mathrm{erf}(x)$	error function
$\mathrm{erfc}(x)$	complementary error function
$\mathrm{erf}^{-1}(x)$	inverse error function
$\mathrm{E}[X]$	expectation
${}_p\mathrm{F}_q(a_1, \ldots, a_p; b_1, \ldots, b_q; z)$	generalized hypergeometric function
${}_p\bar{\mathrm{F}}_q(a_1, \ldots, a_p; b_1, \ldots, b_q; z)$	regularized generalized hypergeometric function
$I_x(y, z)$	regularized beta function
$I_k(x)$	k-th order modified Bessel function of the first kind
$Q(x)$	Q function
$\mathrm{sign}(x)$	sign of real number

1

Introduction

A performance metric is a standard definition of the measurable quantity that indicates some aspects of the system performance. These quantities are called performance measurements. The performance metric should [1]:

- be measurable,
- have a clear definition, including boundaries of the measurements,
- indicate progress towards a performance goal,
- answer specific questions about the performance.

Several performance metrics are used in communication systems. The error rate analysis is one of the most important indicators of the system performance in wireless communication systems. The error rate is a measure of the number of errors in the received sequence (of bits, packets or frames) normalized by the sequence length. Thus, it is an indicator of the transmission quality.

The traditional error rate analysis in wireless communication systems is based on a number of assumptions which are chosen for some transmission scenarios in order to evaluate the system performance in terms of the average or expected values. The modern and upcoming future wireless communication systems operate in different transmission scenarios due to a large demand on the wireless communication services.

Such increasing demand creates a need to develop optimum transmission solutions under limited resources such as the transmission power and the transmission spectrum. In addition, there are concerns about other transmission constraints such as the delay.

The optimization in the mathematical sense refers to the selection of the best solution available. In wireless communication systems, the optimization usually refers to designing of algorithms that aim to either minimize the error rate, or to increase the system throughput or both of them. Therefore, it is important to obtain the error rate metrics that are capable to describe accurately the actual system performance and can be used to develop optimum transmission solutions.

In this thesis, novel error rate performance metrics and transmission solutions were investigated for delay limited communication systems and for co-channel interference scenarios. The following four research problems were considered. The first research problem is devoted to analysis of the higher order ergodic moments of error rates for digital communication systems with time-unlimited ergodic transmissions, and it is presented in Chapter 3. The second research problem is the non-ergodic error rate analysis and signaling design for communication systems processing a single finite length received sequence; it is presented in Chapter 4. In the third research problem, novel retransmission schemes are developed for delay-limited retransmissions, and these results are presented in Chapter 5. Finally, the last research problem investigates the link error rate performance with a single co-channel interference , and it is presented in Chapter 6.

The rest of this first chapter introduces the research that has been carried out. Chapter 1 content is organized as follows. Section 1.1 discusses the motivation of the thesis. Section 1.2 explains the thesis structure. Section 1.3 presents the thesis work methodology. Finally, Section 1.4 lists the thesis contributions and where they have been published.

1.1 Motivation

Since the error rate is a function of the channel random parameters (e.g., fading and noise), it is a random variable. The random variable statistics can be either fully de-

scribed by its distribution or partially through its moments. This motivated us to consider the statistics of the error rates for different digital modulation schemes in order to answer several questions such as: How to compute the error rate distributions and the moments of the error rate over fading channels? What is the impact of the used modulation schemes on these moments? What is the impact of the fading parameters on these moments? What are the possible applications of the error rate higher moments?

One of the inspiring motivations for this thesis research is the difference between the analytical and practical measurements of the wireless communication systems. In particular, in telecommunications networks, quality-of-service (QoS) and quality-of-experience (QoE) are used to define the required information transmission properties. In broad terms, the QoS is a set of objective measures, and the QoE is a set of subjective measures. Importantly, although the QoS and QoE measurements are correlated, good QoS measurements do not necessarily imply satisfactory QoE. Since the QoS measures are usually defined as the average or expected quantities, the instantaneous measures are rarely considered as QoS measures. The average QoS measurements often appear satisfactory even though the instantaneous values of the performance measurements are occasionally unacceptable. Such situation can explain why the QoS requirements can be met although the users's perceived QoE is considered to be poor. Although we did not consider the QoS and the QoE measurements in the thesis, similar analogy inspired us to consider the notion of the difference between the instantaneous error rate and the expected error rate and their relationship.

The traditional error rate metrics are based on a set of statistical assumptions where the delay is assumed unconstrained. Thus, the importance of the instantaneous error rate analysis in wireless communication systems is emphasized under the transmission delay constraint. This is the main motivation to consider the error rate analysis under delay constraints. This part of work aims to answer a number of questions such as: How to evaluate the instantaneous error rate in practical systems? What is the impact of considering the traditional error rate metrics in such cases and how to measure this impact? How to control and improve the error rate performance under delay constraints?

Another motivational fact, is that many of the wireless communication systems today rely on the time synchronization. The synchronized transmission is usually

achieved in mobile systems by using a set of synchronized clocks where the master clock is located at the base station. Although the synchronization signal is usually a very low frequency signal that is not suitable for data communications, it still represents an additional channel that may be used jointly with the communication link to improve the system performance. This is the motivation to answer several questions such as: Is it possible to use the synchronization channel to improve the system performance without using forward error correction or cyclic redundancy check bits for delay-limited retransmissions? How to develop and to implement such transmission scheme? What are the advantages and disadvantages of such scheme?

Another motivational fact, is that many research and development efforts are focusing on combating the channel impairments especially the channel interference. The resulting transmission techniques form a transmission environment with a limited number of interferers. For such environments, the traditional error rate analysis and its statistical assumptions are no longer valid. This is the motivation to answer several questions such as: What is the impact of eliminating the infinite number of interferers to a finite one? How to evaluate the system performance in such scenario? How to compare the new metrics of the system performance to the traditional ones?

All above issues motivated us to consider novel error rate metrics and techniques to evaluate, and subsequently, to improve the system performance.

1.2 Thesis layout

The thesis structure is organized into individual topics based chapters to improve readability of the whole thesis. Each chapter can be read as a separate unit. The rest of the thesis is organized as follows.

- Chapter 2:
  This chapter is an overview of the background research topics for the work that has been done in the thesis and also provides a literature review of the research problems considered.

- Chapter 3:
  This chapter studies the higher moments of the error rates for different digital modulation schemes.

- Chapter 4:
  This chapter introduces a novel error rate metric to evaluate the error rate performance when transmitting a finite length sequence over a binary symmetric channel.

- Chapter 5:
  This chapter develops a novel automatic repeat request scheme to improve the wireless communication system reliability complexity trade-off.

- Chapter 6:
  This chapter introduces a novel error rate metric to assess the error rate performance of a link with a single interferer.

- Chapter 7:
  This chapter provides the overall thesis conclusions and suggestions for the future work.

- Appendix A
  This appendix summarizes the properties of some probability distributions that are used in the thesis.

1.3 Methodology

The research work has been carried out using mathematical analysis with "pen and paper". *Mathematica* software has been used to evaluate some symbolic mathematical operations such as integration. The obtained expressions were verified and compared with the relevant models through computer simulations based on Monte Carlo simulation method. *Matlab* software has been used extensively for simulations and numerical computations in the thesis work. Some *C++* mex files are used with *Matlab* scripts in order to improve the code speed performance when necessary. Many of the underlying

mathematical concepts used in the mathematical analysis are based on the probability theory; see and Appendix A.

1.4 Contributions and list of publications

1.4.1 Contributions

1. Contributions of Chapter 3:
   Statistics of the conditional error rates of digital modulations over fading channels are considered. The probability density function and the higher order moments of the conditional error rates are obtained using the Prony approximation. For a Ricean distributed channel fading amplitude at the detector input, non-monotonic behavior of the moments of the conditional bit error rates versus some channel model parameters is observed. Furthermore, the Bollinger bands for the first order non-central moment of the conditional bit error rate are obtained as an application of the second order moment of the conditional bit error rate. Our results indicate that, in line-of-sight communications links, smaller transmission powers can be used to reduce the average bit error rate as well as to reduce the variance of the conditional bit error rate. These contributions are published in [2].

2. Contributions of Chapter 4:
   A framework to analyze the error rate properties of non-ergodic transmissions is established. The frame error rate of a finite number of frames transmitted over a block fading channel is equivalently represented as the problem of instantaneous bit error rate of a single finite length sequence of bits transmitted over a binary symmetric channel. In computer simulations, the instantaneous bit error rate is estimated using the confidence intervals. However, in practical receivers, after estimating the binary symmetric channel crossover probability, the Bayesian credible intervals are proposed to estimate the instantaneous bit error rate. A novel degree of ergodicity measure is introduced using the credible interval estimates to quantify the level of ergodicity of the received sequence with respect to the instantaneous bit error rate and to describe the transition of the

data detector from the non-ergodic to ergodic zone of operation. It is shown that the channel uncertainty at the receiver reduces ergodicity, and that the optimum maximum-likelihood detector has the fastest transition from the non-ergodic to ergodic zone of operation. Finally, the developed non-ergodic analysis is used to define adaptive forward error correction control and adaptive power control policies that can guarantee, with a given probability, the worst case instantaneous bit error rate performance of the detector in its transition from the non-ergodic to ergodic zone of operation. These contributions have been published in [3] and in preparation to be submitted in [4].

3. Contributions of Chapter 5:
   In this chapter, a novel retransmission scheme that relies on a reliable reverse link for error-free feedback message delivery is proposed. Unlike the conventional automatic repeat request schemes, the proposed scheme does not require the use of cyclic redundancy check bits for error detection. In the proposed scheme, random permutations are exploited to locate the bits of small reliabilities in the predefined window within the packet. The bits in this window are retransmitted, and then, combined using the maximal-ratio combining. The complexity-performance trade-offs of the proposed scheme are investigated by mathematical analysis as well as by computer simulations. The bit error rate of the proposed scheme is independent of the packet length. However, the proposed scheme throughput is dependent on the packet length. Three strategies to select the parameters of the proposed retransmission scheme were considered. These parameters were optimized to achieve the minimum BER. The performance of the proposed retransmission scheme was compared to the block repetition code corresponding to a conventional ARQ retransmission strategy. It is found that, for the same number of retransmissions, and the same packet length, the proposed scheme always outperforms the conventional stop-and-wait automatic repeat request schemes in terms of the bit error rate as well as throughput, and, in some scenarios, the performance improvement can be significant. These contributions have been published in [5] and in preparation to be submitted in [6].

4. Contributions of Chapter 6:
   A novel metric to assess whether the standard Gaussian approximation of a sin-

gle interferer underestimates or overestimates the link bit error rate is derived. This metric is a function of the interference channel fading statistics. However, it is otherwise independent of the statistics of the desired signal. The key step in derivation of the proposed metric is to construct the standard Gaussian approximation of the interference by a non-linear transformation. A closed form expression of the metric is obtained for a Nakagami distributed interference fading amplitude. Numerical results for the case of Nakagami and lognormal distributed interference fading amplitude confirm the validity of the proposed metric. These contributions have been submitted on [7].

1.4.2 List of publications

During this research, we have published the three conference papers,

1. M. A. M. Hassanien and P. Loskot, "Higher Order Moments of Error Rates of Digital Modulations ," in *IEEE VTC-2010 Spring Conf. 71th* , May 2010, pp. 1–5.

2. M. A. M. Hassanien and P. Loskot, "Non-Ergodic Error Rate Analysis of Finite Length Received Sequences," in *Int. Conf. Wireless Comm. Signal Proces.*, Nov. 2009, pp. 1–5.

3. M. A. M. Hassanien and P. Loskot, "Improving Link Reliability Complexity Trade-Off by Exploiting Reliable Feedback Signaling," in *ISWCS* , Sep. 2010, pp. 775–779.

and the following three journal papers in preparation to be submitted,

1. M. A. M. Hassanien and P. Loskot, "Non-ergodic Error Rate Analysis of a Single Finite Length Sequence Over BSC," in *Preparation to be Submitted to IEEE Trans. Commun.*, Dec. 2011.

2. M. A. M. Hassanien and P. Loskot, "Improving Link Reliability Complexity Trade-Off by Exploiting Reliable Feedback Signaling," in *Preparation to be Submitted to IEEE Trans. Sign. Proc.*,Jan. 2012.

3. M. A. M. Hassanien and P. Loskot, "Assessment of the Link Performance with a Single Interferer," *Submitted to IEEE Trans. Commun.*, Jul. 2011.

2

Background and Literature Review

This chapter introduces fundamentals of the performance measurements in the wireless digital communication systems. This overview of concepts, techniques and systems assumed in this thesis is useful in order to state the design problems that are considered before providing their solutions in the following chapters. This chapter also summarizes the literature review for error rate performance analysis of the digital wireless communication systems and other relevant works to the thesis. Moreover, the references used are also provided in the introduction of each chapter.

This chapter is organized as follows. Section 2.1 explains fundamentals of the random processes with focus on ergodicity. Section 2.2 gives introduction to the basics of the average error rate performance metrics. Section 2.3 is introduction to the fundamentals of the estimation theory with focus on differences between the point estimators and the interval estimators. Section 2.4 introduces the concept of error correction techniques. Section 2.5 explains the concepts of random number generators (RNGs) and the pseudo-random sequences. Section 2.6 illustrates the concepts of diversity often employed in many wireless communication systems. Section 2.7 is the literature review for the delay limited transmission problem. Lastly, Section 2.8 is the literature review for the co-channel interference error rate analysis of wireless communication systems.

2.1 Stochastic processes and ergodicity

Many random phenomena occurring in nature can be represented as functions of time. Thus, a stochastic process $x(t)$ is defined as a function that assigns to every random outcome ζ a function $x(t,\zeta)$ [8, 9]. The time domain is represented by a variable t from a set of real numbers R, and the ζ-domain represents the set of all possible experimental outcomes. The process $x(t)$ is a continuous-time process when R is a set of continuous real numbers, and the process $x(t)$ is a discrete-time process when R is a set of discrete real numbers. The set of $x(t,\zeta)$ for all values t and ζ is referred to as an ensemble. Therefore, for a given time instance $t_0 \in R$, $x(t_0,\zeta)$ is a random variable (RV), and for a given ζ_0, the function $x(t,\zeta_0)$ is a time function referred to as the sample function of the given random process. The number of the sample functions in the ensemble is usually assumed to be extremely large or even infinite. When t and ζ are both fixed, then $x(t)$ is some real valued number.

2.1.1 Properties of stochastic processes and stationarity

For a random process $x(t)$, the random variables $x(t_i)$, $i = 1,2,\ldots,N$, can be obtained for any set of time instances $t_1 > t_2 > t_3 > \ldots > t_N$. For any value of n, these random variables are characterized statistically by the N-fold joint probability density function (PDF) , $f(x(t_1),x(t_2),x(t_3),\ldots,x(t_N))$. Based on the properties of the PDF $f(x(t_1),x(t_2),x(t_3),\ldots,x(t_N))$, we can classify the stochastic processes [10]. In particular, the most widely assumed class of the stochastic processes are the stationary processes. The random process is called stationary in the strict sense provided that,

$$f(x(t_1),x(t_2),x(t_3),\ldots,x(t_N)) = f(x(t_1+t),x(t_2+t),x(t_3+t),\ldots,x(t_N+t))$$

where t is an arbitrary time shift. In other words, the statistics of the stationary stochastic processes are invariant to any translation in the time axis. Thus, for stationary processes in the strict sense, all the stochastic moments are independent of time, and the correlation coefficient (or the covariance) depends only on the time differences [11]. When the statistics of the N-fold joint PDF are varying with the time shifts, the process is called non-stationary. There is a class of stochastic processes having the means

and variances independent of time, and their correlation coefficient (or the covariance) is a function of only the time differences whereas their N-fold joint PDF statistics depend on the choice of the time origin. Such stochastic processes are called wide-sense stationary (WSS) processes. The stationary process in the strict sense implies the stochastic process in the WSS. However, the inverse statement is not necessarily true except for the Gaussian random processes, since the N-fold joint Gaussian PDF is completely described in terms of the means, variances and the covariances of the random variables $x(t_1), x(t_2), x(t_3), \ldots, x(t_N)$.

2.1.2 Ergodicity

Since many parameters of the stochastic process $x(t)$ can be expressed in terms of the expected values of $x(t)$ (corresponding to the probability theory based on expected values; see [10]), the central problem of characterizing the stochastic processes is to obtain their statistical parameters in terms of the real measured data [9] (corresponding to the deterministic theory based on the time averages; see again [10]). Under certain conditions known as the ergodicity, the infinite time average and the expectation operations are interchangeable. Thus, the ergodic property guarantees equality between the ensemble averages and the infinite-time averages. Depending on the required order of the stochastic moments to be replaced by the time average, we can classify the ergodic precesses. The most widely used ergodicity processes are the mean ergodic processes [12]. In the mean ergodic processes, the infinite time average can be replaced by the first order ensemble moment. The Slutsky's theorem [9] states that a continuous process $x(t)$ is mean ergodic if and only if,

$$\frac{1}{T}\int_0^T C(\tau), d\tau \underset{T\to\infty}{\longrightarrow} 0$$

whereas the discrete process $x[n]$ is mean ergodic if and only if,

$$\frac{1}{M}\sum_{m=0}^{M} C[m] \underset{M\to\infty}{\longrightarrow} 0$$

where $C(\tau)$ and $C[m]$ are the auto-covariance of the processes $x(t)$ and $x[n]$, respectively.

2.2 Performance measures of transmission reliability

Evaluation of the performance of the communication systems is important for the design of modern communication systems [13]. For example, in employing wireless communication systems, it is important to optimize the transmitting powers while maximizing the system data throughput which is usually specified by the application used. There are several performance metrics that can be used. Most of these metrics are aiming at the average performance evaluation instead of the instantaneous performance evaluation. More importantly, the average performance is computed based on the probability theory (i.e., expectation), however it can also be computed by assuming a deterministic theory (i.e., the time averages) under ergodic conditions. We now introduce three most commonly used performance metrics of the wireless digital communication systems [10].

2.2.1 Average signal-to-noise ratio

The signal-to-noise ratio (SNR) is the most understood performance characteristic of the digital communication systems [13]. Generally, the SNR is the easiest to evaluate among the performance measures. It is a measure of the relative strength of the useful signal compared to the noise. Usually, the SNR is measured at the receiver, and therefore, it is directly connected to the data detection process. The SNR can be defined as a ratio of the squared mean to the variance or as a ratio of the mean squares. It is also a good measure of the overall fidelity of the communication system. The noise term in the SNR definition is traditionally used to refer to the thermal noise at the input of the receiver. However, in wireless communication environment where the fading often occurs, more appropriate performance measure can be the average SNR. In this SNR definition, the average refers to the statistical average over the fading distribution. Provided that γ is a RV denoting the instantaneous SNR at the detector input, the average SNR $\bar{\gamma}$ can be expressed as,

$$\bar{\gamma} = \int_0^\infty \gamma f_\gamma(\gamma) d\gamma$$

where $f_\gamma(\gamma)$ is the PDF of γ.

2.2.2 Mean square error (MSE)

The MSE is a well known measure of the difference between the estimated value at the output of the estimator and the actual value [14]. In other words, the MSE is a measure of the dissimilarity between the noisy distorted signal and the uncorrupted signal. The MSE is usually measured using the statistical averages. Thus, the second statistical moment of the measurement error incorporates the variance and the bias of the estimate, i.e., (see also Section 2.3),

$$\mathrm{MSE} = \mathrm{E}\big[(\bar{\theta} - \theta)^2\big]$$

where $\bar{\theta}$ is the estimated value of some parameter θ. Generally, the term parameter is used to refer to the properties of the signal which is not directly expressed or used as a performance measure. In addition, the MSE is the variance of the estimator for the unbiased estimators [15] where the bias of the estimator is a measure of the difference between the average estimate and the single parameter being estimated, i.e,

$$B(\bar{\theta}) = \mathrm{E}\big[\bar{\theta} - \theta\big]$$

where $B(\bar{\theta})$ is the bias of the estimator. The estimator is called unbiased if and only if, $B(\bar{\theta}) = 0$.

2.2.3 Bit error rate (BER)

The BER is one of the most important performance measures in wireless communications even though it is often the most difficult measure to evaluate. The main reason for this difficulty is that the BER is usually a non-linear function of the instantaneous SNR. Such non-linearity occurs due to non-linear operations of modulation and detection that are employed in the system. The BER is a measure of the likelihood of making an incorrect decision about the transmitted bits or symbols; in the latter case, we use the term symbol error rate SER . In some literature, the BER is called bit error probability (BEP) or just error probability (PE) . Note that all probabilities can be defined using the expected values. Therefore, the most evaluations of the BER are based on the expected or average values. The same discussion applies for the SER. More

generally, if a symbol of length N bits (i.e., a packet or a frame) is assumed to be in error, then at least one bit within the packet must be in error. Assuming that the bit errors in the packet are independent, the SER can be expressed in terms of the BER as,

$$\mathrm{SER} = 1 - (1 - \mathrm{BER})^N.$$

For small values of the BER, this expression can be approximated as,

$$\mathrm{SER} \approx N\mathrm{BER}.$$

2.3 Estimators of signal characteristics

It is useful to classify the signal reception problem as the two main sub-problems, i.e., the detection and the estimation. The detection operation aims to detect the presence of a particular signal among other candidate signals in a noisy background [16, 11]. The estimation process aims to estimate some characteristics of the signal that are usually assumed to be present in a noisy environment [17]. It is also useful to distinguish between the estimation and filtering operations. In particular, if the signal characteristics are time independent parameters such as a constant (either random or non-random), then this operation is referred to as the estimation. However, when the estimate is the waveform itself or it is a function of the waveform, the corresponding operation is called filtering [18]. In the following, we give an introduction to the point and the interval estimators.

In general, there are two types of estimators, the point estimators and the interval estimators [19, 20]. The term estimator usually denotes the point estimator. The point estimator is a function that uses the sample data to map a single value to the unknown parameter (either random or non-random), and this includes also a single vector or a single function. On the other hand, the interval estimator is a function that uses the sample data to obtain an interval of unknown parameters, i.e., either the confidence interval or the credible interval. In addition, assuming a stationary and mean-ergodic process, the mean-square error is becoming smaller with the increasing number of samples [10]. In case of estimating the mean of a mean-ergodic process, provided that the number of data samples is infinite, the optimum estimator corresponds to the point

estimator. On the other hand, if the number of data samples is finite, one prefers to obtain the interval estimator. The confidence intervals are based on the frequentest approach while the credible intervals are based on the Bayesian approach. However, even though both these approaches can be identical in some special cases [21], they are mathematically very different due to different interpretation of the relative frequency and the probability as a degree of belief. Furthermore, the credible intervals use the Bayesian theorem and exploit prior probabilities of the parameters to be estimated [22].

2.4 Error correction and ARQ

The main goal of the error correction is to reduce the probability of information error during the transmission. The transmission errors are happening due to distortions in the communication channel, for example, due to additive white Gaussian noise, fading, interference and attenuation of the transmitted signal.

There is no specific way to protect information against channel impairments [23]. The presence of the impairments of the transmission medium limits the information flow through the channel but not the quality of message reconstruction at the receiver. This is the main concept of the information theory that created channel coding concept. The channel error control coding techniques aim to enable a reliable delivery of information between a source and a destination. The error control techniques use additional information such as parity that the receiver can use in order to recover the original data. These additional or redundant parity bits are added to the original data by the encoder at the transmitter which also limits the flow of information to the value that is smaller than the channel capacity. Therefore, the channel coding aims to deliver reliable information from a source to a destination at the information flow rate reaching the channel capacity. Shannon suggested the fundamental concept of the channel coding and information theory [24]. Shannon theorem states that "by proper encoding of the information, errors caused by noise channel and channel impairments can be reduced to any desired level without sacrificing the information flow rate ". There exist extensive results in the literature how to design efficient encoding and decoding algorithms to achieve reliable communications for high speed transmissions [25].

The error control coding design problems are usually classified into two main categories.

1. Error detection: It is the ability to detect existence of errors caused by channel impairments. This design problem includes the design of additional parity bits to detect these errors such as the cyclic redundancy check (CRC) bits.

2. Error correction: It is the ability to detect transmission errors and recover the original data by correcting these errors. The error correction techniques are usually classified into the following three main categories.

   A) Forward error correction (FEC): It is an error control scheme where the source utilizes the encoder in order to encode the transmitted information bits by adding redundant bits in a systematic way. Thus, the decoder at the receiver side can detect and correct errors by using these redundant bits. In FEC, no feedback channel is used to request retransmission of data as in the case of ARQ schemes. Based on the method of adding the redundancy to the information bits, the FEC can be further divided into two classes, i.e., block coding [23, 25, 26] and convolutional coding.

   B) Automatic repeat request (ARQ): It is an error control scheme that uses acknowledgments to provide a reliable data transmission in two way channels, i.e., the forward and the feedback channels. The acknowledgments are sent from the destination to the source via a feedback channel after receiving the information from the source to the destination via a forward channel. The transmitter decides whether to retransmit the data, or send the new data depending on the received acknowledgment from the destination receiver. Usually, after a specific time period, the transmitter assumes negative acknowledgment and retransmits the data. The destination generates the acknowledgment message using additional parity bits to detect the errors such as the CRC bits. Based on the acknowledgment messages ordering protocols, the ARQ techniques are usually classified into three main classes, i.e., stop-and-wait ARQ [27], go-back-N ARQ [27, 28], and the selective-repeat ARQ [29].

C) Hybrid automatic repeat request (HARQ) [29, 30, 31]: It is an error control scheme that combines the usage of the FEC and the ARQ techniques in order to provide the reliable data transmission. The HARQ adds the FEC parity bits to the existing error detection parity information. The FEC parity bits are used to correct the errors while the error detection parity bits are used to detect the remaining errors. Therefore, the HARQ can perform better under poor SNR conditions at the expense of achieving lower transmission rates or throughput. This creates a trade-off between using the HARQ and the ARQ schemes which is dependent on the received signal conditions, the throughput and the BER. The HARQ types are usually classified into two classes. In particular, in the simple HARQ, the information received in error is simply discarded. On the other hand, type I HARQ provides the error detection and the FEC protection for each message. Type II HARQ is more complicated in order to improve the efficiency of using the FEC parity information bits. There also exists a HARQ scheme with soft combining. This retransmission scheme uses the incorrect received information with the retransmitted information by combining them in order to increase the chances of decoding the original information correctly. The main two types of this class are the Chase combining and the incremental combining. In the Chase combining, every retransmission contains the same information and the parities and it combines the original received information using the maximal ratio combining (MRC); see Section 2.6. The Chase combining can be considered as employing a repetition code. On the other hand, the incremental combining uses different information and parities in each retransmission. Therefore, the receiver can gain extra knowledge in each retransmission which in turn improves the BER performance.

2.5 Random number generators and pseudo-random sequences

The wireless communication links suffer from channel impairments which have random behavior. Modeling of this random behavior requires generation of random numbers to recreate distributions and other statistical properties of the channel impairments. A mathematical abstraction of random numbers used in computer simulations is often based on independent random variables, where each random experiment output can be modeled as an independent RV. The random number generator (RNG) is a computational or physical device that can generate symbols or numbers that appear to be random. For example, the RNG can be used to generate uniformally distributed RVs and then transformed them to the required distributions using the inversion method and the acceptance-rejection method. There are two classes of the RNGs depending on the used generation method.

1. Physical RNGs: The physical RNGs measure some physical quantity that is expected to be random and then compensates for possible biases in the measurement process.

2. Computational RNGs: The computational RNGs are deterministic models that generate long sequences of random results from the specified shorter sequences that are usually called a seed or an initial state [32]. This type of RNGs is called pseudo-random. However, since this type of RNG practically has a finite amount of memory, it has a finite number of initial states and outputs that can be reached or produced. The pseudo-random RNGs can be defined as a structure [33], (S, μ, f, U, g), where S is the set of finite states, μ is the PDF, S is used to select the initial state or seed s_0, the mapping $f : S \rightarrow S$ is the transition function, U is a finite set of output symbols, and $g : S \rightarrow U$ is the output function. Thus, the states can be computed by the recurrence, $s_n = f(s_{n-1})$, where the number of steps or iterations $n \geq 1$. The output at the iteration n can be expressed as, $u_n = g(s_n) \in U$, where u_n is the random number generated by the RNG. Since S is finite, the RNG will return to a state already passed, i.e. $s_{i+j} = s_i$, for $i \geq 0$ and $j > 0$. Therefore, $s_{n+j} = s_n$, for $n \geq i$. The smallest

j that satisfies this is called a period length ρ. The period length cannot exceed cardinality of S. In addition, if the number of bits that denotes the number of states is b, then $\rho \leq 2^b$. The designs of the RNGs are often trying to achieve this upper limit. The quality of the RNGs is measured using their output statistical properties.

2.6 Diversity in wireless communications

Diversity is a technique to improve reliability of message delivery by exploiting the random nature of radio propagation. The main idea behind diversity is to find independent signal paths that experience different levels of fading and interference, so that multiple versions of the transmitted signal can be received. Moreover, error correction techniques can be added to the transmitted message to improve its immunity against the channel impairments.

2.6.1 Diversity schemes

Diversity schemes can be classified as follows [8].

- Time diversity: This kind of diversity can be achieved in two ways, i.e., either by transmitting multiple versions of the original message at different time slots or the FEC is added to the message and spread in time by interleaving techniques.
- Frequency diversity: This kind of diversity is achieved either by transmitting multiple versions of the message over different frequency channels or by spreading the message over wide spectrum of frequencies.
- Space diversity or antenna diversity: The message is transmitted over different propagation paths using the antenna diversity. The multiple antennas are utilized at the receiver side in order to receive multiple versions of the transmitted message; this is called the receiver diversity. Or, multiple antennas are used at the transmitter side in order to send multiple versions of the message through different propagation paths.

- Polarization diversity: This kind of diversity is achieved when multiple versions of the message are transmitted and received with different polarization.
- Cooperative diversity [8, 34, 35, 36]: It is one of the diversity schemes that utilizes relays in order to improve reliability of the transmitted message. Such systems consist of the source, one or more relays, and the destination. The source broadcasts the signal to the relays and to the destination, and then the relays forwards the signal to the destination.

2.6.2 Diversity signal processing

Diversity combining schemes allow the destination to combine multiple received signals that are produced by different diversity schemes.

- Maximal-ratio combining (MRC): The MRC is often used in large phased array systems. The received signals from all paths are weighted according to their SNRs and then summed up.
- Equal gain combining: All the received signals are summed up coherently. In this case, the weights for signals from all the propagation paths are set to unity.
- Selection combining: The strongest signal among the received signals from all paths is selected.

2.7 Delay limited transmission

The Shannon capacity of communication channel is the ultimate limit of the rate that can be achieved [24]. Such capacity is achievable in an asymptotic sense as the delay goes to infinity. Thus, the Shanon capacity is not dependent on any delay considerations and sometimes it is called ergodic capacity or throughput capacity [37]. However, modern wireless communication systems are sensitive to the delay constraints where each time slot should have a certain rate [38]. Future wireless communication systems will use even more sensitive delay multimedia and streaming data which should

be successfully transmitted within a fixed time frame [39]. The assumption of delay limitation is included in many works, e.g. [40, 41, 42] assume that a desired signal-to-interference ratio must be met for every fading state, and this means that the user's mutual information is kept constant in time.

[43] defined a formal notion of delay-limited capacity for multi-access channels using the assumption of symmetric case with users having the same rate requirements.

There has been extensive research on system capacity or the maximum rate under delay constraints for different systems and scenarios. Such maximum rate is called the delay-limited capacity (DLC) or the zero outage capacity. Fig. 2.1 shows the structure of the code word in block fading channel [44], where the blocks of N symbols undergoes the same fading gain.

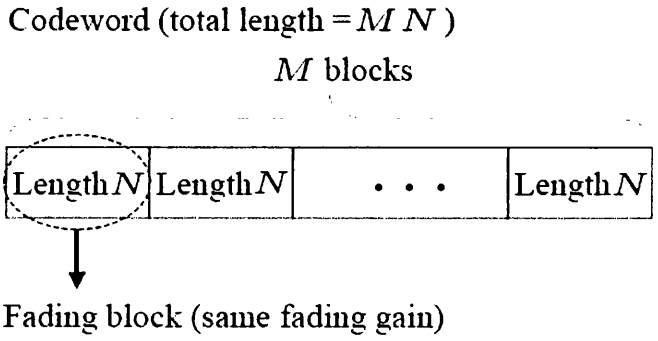

Figure 2.1: The codeword structure over fading blocks.

According to values of N and M, the capacity of the fading channel can be classified as,

- $N \leq \infty$ and $M = \infty$: ergodic capacity (delay unconstrained).
- $N = \infty$ and $M < \infty$: DLC, zero outage capacity.
- $N = \infty$ and $M = 1$: Outage capacity.

There are several examples on the DLC in literature. For example, [45] discusses the connection between the DLC to the compound channels. [37] studies the DLC

region for the multiuser muli-access channel (MAC). [46] derives the DLC for block-fading single-user diversity Rayleigh fading channels. [47] characterizes the DLC of block fading multiple antenna channels. [39] derives the expressions of the DLC of multiple-input multiple-output (MIMO) , multiple-input single-output (MISO), single-input multiple-output (SIMO), and parallel fading channels. [48] shows how to achieve the DLC in MIMO-OFDM without spatial power allocation, where OFDM stands for orthogonal frequency division multiplexing.

The delay limited transmission in modern communication systems studies are not limited to the DLC computation, but extended to the problem of communication of delay sensitive bits over wireless channels with all its design aspects. One of the studied problems is the power-delay trade-off. For example, [49, 50] address the trade-off between the minimum average power consumption and the average delay over a Markovian fading channel with channel state information (CSI) known at both the transmitter and the receiver. [51] derived optimal delay-bounded schedulers for transmission of constant-rate traffic over finite-state fading channels with CSI known at both the transmitter and the receiver. [52] find the code-rate allocation that maximizes the decay rate of the asymptotic probability of error for a given asymptotically large delay requirement known at both the transmitter and the receiver. [53] address the problem of minimizing the average delay, under average power constraints and fixed transmission rate where CSI is unknown to the transmitter but there is a mechanism for retransmission of codewords when the channel is in outage. [54] studied the problem of fixed transmission rate to maximize the decay rate of the probability of buffer overflow for ON-OFF channels and Markov-modulated arrivals, where CSI is unknown to the transmitter and the channel is considered OFF when outage occurs. [55] analyzed the high-SNR asymptotic error performance of outage-limited communications with fading, where the number of bits that arrives at the transmitter during any time slot is random but the delivery of bits at the receiver have a strict delay limitation.

Another studied problem is the throughput-delay trade-off. For example, [56] characterized the delay and determining the throughput-delay trade-off in ad hoc wireless networks, based on the fixed nodes ad hoc wireless network model introduced in [57] and mobility observations in [58, 59]. [60, 61] designed a scheduling scheme for multi-hop wireless networks to ensure end-to-end delays when the total throughput is within

a constant factor of the optimum throughput. [62] derived the network average delay bound for the max-weight scheduling. [63] studied the problem of throughput maximization in multi-hop wireless networks with end-to-end delay constraints for each session and developed algorithms to compute such trade-offs.

More importantly, in the thesis, we consider the error rate analysis for selected delay limited case in Chapter 4 based on the intervals estimators which have not been done before, where the delay constraint can be considered as a finite length codeword as in [64, 65]. It can also be limited by the number of the allowed retransmissions in the ARQ systems as in [66]. This type of the ARQ is also called a truncated ARQ [67, 68]. We also develop a novel delay limited ARQ transmission scheme in Chapter 5.

2.8 Co-channel interference error rate analysis

The cellular concept was developed to offer very high capacity within a limited spectral allocation without any major technological changes. It has been developed as a replacement in the system level to the idea of using a single in large cell with many low power transmitters in small cells, each providing coverage to a small portion of the service area [69]. The term cell is used in wireless cellular systems to denote a geographical area. In cellular systems, in each base station a portion of the total number of channels available to the entire system is allocated, and nearby base stations are assigned different groups of channels. Therefore, all the available channels are assigned to a relatively small number of neighboring base stations.

In order to reduce the interference between the base stations and mobile users under their control, neighboring base stations are assigned different groups of channels.

As a result of demand for more channels, the number of base stations may be increased with a reduction in the transmission power to reduce the interference, in order to provide additional radio capacity with the same radio spectrum [70]. The design process of selecting operating frequencies or channels, in order to reduce the interference for a group of cells called cluster (see Fig. 2.2 from [69]) is called frequency reuse or frequency planning [71]. Thus, the frequency reuse aims to increase the radio capacity and minimize the interference. The interference due to the usage of the same

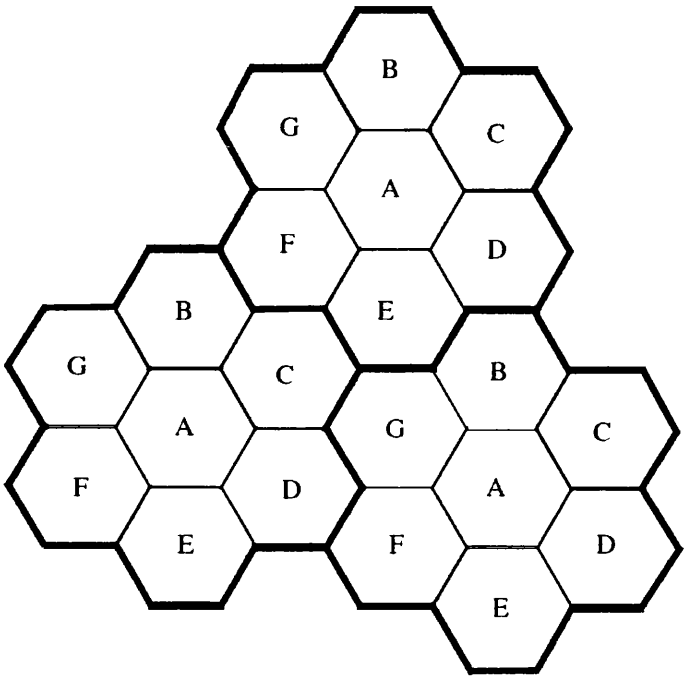

Figure 2.2: Illustration of the cellular frequency reuse concept. The cells with the same letter use the same set of frequencies. A cell cluster is outlined in bold and replicated over the coverage area. In this example, the cluster size, S, is equal to seven, and the frequency reuse factor is 1/7 since each cell contains one-seventh of the total number of available channels.

frequency in multiple cells is called co-channel interference. The co-channel interference adds unwanted signals to the received useful signal. There are several strategies to achieve the goals of the frequency reuse or channels assignment. These strategies are classified as fixed or dynamic. The selection of the strategy has impact on the system performance and decides how the mobile unit hands off between cells as in [72, 73, 74, 75].

One of the underlying assumptions to evaluate the error performance with a large number of co-channel interferes is the central limit theorem [76, 77] which states conditions under which the sum of a sufficiently large number of independent random variables, each with the finite mean and variance, will be approximately normally distributed [78, 79, 80]. However, there are several techniques to reduce the co-channel interference impacts on the system performance. Statistical modeling of the co-channel interference has been considered extensively, for example in [81, 82, 83, 84], in order to design transceivers with improved communication performance [85, 86]. Several co-channel interference suppression techniques studied in the literature for different systems and cases can be found, for example, in [87, 88, 89, 90]. Hence, there is a need to evaluate the error performance with a finite number of co-channel interferes or even a single interferer as we have done in Chapter 6.

3

Higher Order Moments of Error Rates of Digital Modulations

3.1 Introduction

The error rates of digital communication systems are random quantities due to a stochastic nature of the communication channel. The error rates are fully described by their probability density function (PDF). However, a full description of the error rate properties of the communication systems using the PDF is impractical. Thus, the first order non-central moment of the error rate corresponding to the expected value is the most frequently used performance measure [91]. The expected value of the error rate is considered to be one of the most important metric in designing the communication systems. On the other hand, in non-ergodic (e.g., delay limited) communication scenarios, one should use credible intervals rather than the expected values to describe the error rate properties of the communication systems [3]. The width of the credible interval can be used to define a degree-of-ergodicity of the received sequence with respect to the instantaneous bit error rate (BER), and consequently, to define the ergodic and non-ergodic zones of the detector operation.

In this chapter, we consider a particular case of the conditional BER; our results and conclusions remain valid also for the symbol and frame error rates. The conditional BER is, in general, a function of the modulation scheme used, and of the instantaneous

signal-to-noise ratio (SNR) at the detector input. Assuming a sum-of-exponentials approximation of the conditional BER referred to as the Prony approximation [92], we obtain the PDF of the conditional BER using the transformation of a random variable [93]. In addition, we describe the conditional BER using the higher order central and non-central moments. For our numerical examples, we assume a Ricean distributed channel fading amplitude at the detector input. We plot the second and the third order central moments of the conditional BER versus the standard deviation per dimension of the channel fading. These plots indicate that, over line-of-sight communication links, the average BER as well as the variance of the conditional BER are non-monotonic, and they can be reduced by reducing the transmission power. Finally, we investigate the Bollinger bands to characterize the random fluctuations of the conditional BER [94]. The Bollinger bands are defined using a deterministic function of the second order central moment of the conditional BER. The Bollinger bands are useful to characterize the error rates in non-ergodic scenarios, and they can be more easily determined than the credible intervals [3].

The rest of this chapter is organized as follows. The statistics of the error rates for digital modulations over a standard flat fading channel model are introduced in Section 3.2. Numerical examples of the PDF, of the moments and of the Bollinger bands of the conditional BER are presented in Section 3.3. Discussion in Section 3.4 concludes the chapter.

3.2 Error rates statistics

We investigate the error rates statistics for the particular case of the conditional BER. Assume an equivalent frequency flat fading channel model with an additive white Gaussian noise (AWGN) at the detector input. Denote as g the instantaneous fading amplitude; then, the instantaneous SNR at the detector input $\gamma \propto g^2$. In general, the average BER performance measure is defined as,

$$\bar{P}_{\mathrm{e}}(\Omega) = \int_0^\infty P_{\mathrm{e}}(\gamma)\ f_\gamma(\gamma;\Omega)\,\mathrm{d}\gamma \tag{3.1}$$

where $P_{\mathrm{e}}(\gamma)$ is the conditional BER corresponding to the transmission over a channel with a constant fading $g = 1$, $f_\gamma(\gamma;\Omega)$ is the PDF of γ, and Ω are the parameters of the

PDF (e.g., the variance of the fading amplitude g). The average BER (3.1) corresponds to the first order non-central moment, i.e., $\mathrm{E}[P_\mathrm{e}(\gamma)] = \bar{P}_\mathrm{e}(\Omega) = \bar{P}_\mathrm{e}$ where $\mathrm{E}[\cdot]$ is expectation. More importantly, at any given time instant, the value of g is random, and so is the value of γ. Consequently, the conditional BER can be considered to be a mapping,

$$g \mapsto \gamma \mapsto P_\mathrm{e}(\gamma)$$

representing the transformations of random variables [93]. In this chapter, we assume the following transformations,

$$\begin{aligned} \gamma &= g^2 \gamma_b \\ P_\mathrm{e}(\gamma) &= \sum_{i=1}^{p} A_i \mathrm{e}^{-a_i \gamma} \end{aligned} \tag{3.2}$$

where γ_b is the SNR per transmitted bit. The expression (3.2) is a highly accurate sum-of-exponentials approximation of the conditional BER referred to as the Prony approximation [92]. The order p (i.e., the accuracy) of the approximation in (3.2) is application dependent, and the coefficients $A_i > 0$ and $a_i > 0$ are modulation dependent. It has been shown in [92] that $p = 2$ is sufficient to efficiently evaluate the integral in (3.1). Since the PDF $f_g(g)$ of g can be usually obtained from the channel model being considered, the PDFs of γ and of the conditional BER $P_\mathrm{e} = P_\mathrm{e}(\gamma)$, respectively, are given as [93],

$$\begin{aligned} f_\gamma(\gamma) &= \frac{1}{\gamma_b \sqrt{\gamma/\gamma_b}} f_g\left(\sqrt{\gamma/\gamma_b}\right) \\ f_{P_\mathrm{e}}(P_\mathrm{e}) &= \frac{f_\gamma(P_\mathrm{e}^{-1})}{\left|\dot{P}_\mathrm{e}(P_\mathrm{e}^{-1})\right|} \end{aligned} \tag{3.3}$$

where $P_\mathrm{e}^{-1} = \gamma$ and $\dot{P}_\mathrm{e}(\gamma) = \frac{\mathrm{d}}{\mathrm{d}\gamma} P_\mathrm{e}(\gamma)$ are the inverse function and the derivative of the conditional BER $P_\mathrm{e}(\gamma)$, respectively, and $|\cdot|$ denotes the absolute value. Note that the PDF of $P_\mathrm{e}(\gamma)$ can be also expressed as,

$$f_{P_\mathrm{e}}(\gamma) = \frac{f_\gamma(\gamma)}{|\dot{P}_\mathrm{e}(\gamma)|}.$$

For the special case when $p = 1$ in (3.2), the conditional BER (3.2) is analytically invertible and its PDF can be written as,

$$f_{P_\mathrm{e}}(P_\mathrm{e}) = \frac{f_\gamma\left(-\frac{1}{a_1} \log \frac{P_\mathrm{e}}{A_1}\right)}{a_1 P_\mathrm{e}}.$$

3.2.1 Higher order moments of error rates

We investigate higher order central moments of the conditional BER. The k-th central moment operator $M_k[\cdot]$ is defined as [93],

$$M_k = M_k[P_e(\gamma)] = \mathrm{E}\Big[(P_e(\gamma) - \mathrm{E}[P_e(\gamma)])^k\Big] \tag{3.4}$$

so that the first moment, $M_1 = 0$, and the moment M_2 is the variance of the conditional BER $P_e(\gamma)$. Using the binomial theorem and substituting the Prony approximation of the conditional BER (3.2) into (3.4), we obtain,

$$\begin{aligned} M_k &= \sum_{i=0}^{k} \binom{k}{i} \left(-\bar{P}_e(\gamma)\right)^{k-i} \mathrm{E}\Big[(P_e(\gamma))^i\Big] \\ &= \sum_{i=0}^{k} \binom{k}{i} \left(-\sum_{i=1}^{p} A_i \Phi_\gamma(-a_i)\right)^{k-i} \mathrm{E}\left[\left(\sum_{i=1}^{p} A_i \mathrm{e}^{-a_i\gamma}\right)^i\right] \end{aligned} \tag{3.5}$$

where $\Phi_\gamma(t) = \mathrm{E}[\mathrm{e}^{t\gamma}]$ is the moment generating function (MGF) of γ, and t is an auxiliary complex-valued variable. Thus, in order to evaluate the central moments (3.5), we have to compute the i-th non-central moments, $\mathrm{E}\Big[(P_e(\gamma))^i\Big]$, $i = 0, 1, \cdots, k$, of the conditional BER.

The first non-central moment $\bar{P}_e(\gamma)$ corresponding to the average BER (3.1) can be expressed as [92],

$$\bar{P}_e = \mathrm{E}[P_e(\gamma)] = \sum_{i=1}^{p} A_i \Phi_\gamma(-a_i)$$

i.e., the average BER can be well-approximated by a weighted sum of the MGFs of the SNR γ. The second and the third non-central moments of the conditional BER $P_e(\gamma)$ can be expressed as,

$$\begin{aligned} \mathrm{E}\big[(P_e(\gamma))^2\big] = &\sum_{i=1}^{p} {A_i}^2 \Phi_\gamma(-2a_i) + \\ &2\sum_{i_1=2}^{p}\sum_{i_2=1}^{i_1-1} A_{i_1} A_{i_2} \Phi_\gamma(-a_{i_1} - a_{i_2}) \end{aligned}$$

$$
\begin{aligned}
\mathrm{E}\left[(P_{\mathrm{e}}(\gamma))^3\right] = & \sum_{i=1}^{p} {A_i}^3 \Phi_\gamma(-3a_i) + \\
& 3\sum_{i_1=2}^{p-1}\sum_{i_2=1}^{p} A_{i_1} {A_{i_2}}^2 \Phi_\gamma(-a_{i_1} - 2a_{i_2}) + \\
& 3\sum_{i=2}^{p} {A_1}^2 A_i \Phi_\gamma(-a_i - 2a_1) + \\
& 3\sum_{i=2}^{p-1} {A_i}^2 A_p \Phi_\gamma(-a_p - 2a_i) + \\
& 6\sum_{j=1}^{\binom{p}{3}} C_j(A_{i_1} A_{i_2} A_{i_3}) \Phi_\gamma(-a_{i_1} - a_{i_2} - a_{i_3})
\end{aligned}
\tag{3.6}
$$

where $\binom{p}{3}$ is the binomial coefficient, C_j is the j-th (i.e., the index j) combinadic of indices i_1, i_2 and i_3; see [95, Sec. 7.2.1.3]. We have used the identity, $\binom{k}{i} = \sum_{\iota=1}^{k-j} \binom{k-\iota}{j}$, to manipulate the combinadic number in (3.6) into a more numerically efficient form that can be readily evaluated even for larger values of p.

3.2.2 Bollinger bands

The Bollinger bands are a frequently used statistical tool for describing the extent of statistical variations of random variables and processes about their mean values [94, 96]. Hence, the Bollinger bands can be used as a performance measure identifying relative highs and lows of random variables and processes above and below their expected values.

Definition 1. *The lower and upper bounds B_1 and B_2, respectively, of the Bollinger band (B_1, B_2) of the conditional BER $P_{\mathrm{e}}(\gamma)$ are defined as,*

$$
\begin{aligned}
B_1 &= -\bar{P}_{\mathrm{e}}(\gamma)\left(\sqrt{M_2}\log(1-\alpha)\right)^{-1} \\
B_2 &= -\bar{P}_{\mathrm{e}}(\gamma)\sqrt{M_2}\log(1-\alpha)
\end{aligned}
$$

so that, $B_1 < \bar{P}_{\mathrm{e}} < B_2$, with a high probability, and a real constant $0 \leq \alpha < 1$ is chosen such that, in a logarithmic scale, the arithmetic average, $(B_1 + B_2)/2 = \bar{P}_{\mathrm{e}}$. ■

Hence, the Bollinger bands characterize the spread of the conditional BER $P_e(\gamma)$ about its expected value $\mathrm{E}[P_e(\gamma)] = \bar{P}_e$. Note that the width of the interval (B_1, B_2) in a logarithmic scale is the scaled version of the second central moment M_2. We can prove the following proposition,

Proposition 1. *The width $\Delta B = B_2 - B_1$ of the Bollinger band (B_1, B_2) is increasing if the value of α is decreasing.* ■

Proof. The width $\Delta B = B_2 - B_1$ of the Bollinger band in a logarithmic scale can be written as, $\Delta B = -2\sqrt{M_2}\log(1-\alpha)$, and thus, ΔB increases if the value of α is decreasing. ■

3.3 Numerical examples

We assume a generalized Ricean distributed channel fading amplitude at the detector input to provide numerical examples, and to study properties of the BER performance metrics defined in the previous section. Consider first the central-moments of the conditional BER. If the channel fading amplitude g is a generalized Ricean distributed, then the PDF of the instantaneous SNR $\gamma = g^2\gamma_b$ can be written as [8],

$$f_\gamma(\gamma|\Omega) = \frac{1}{2\sigma^2\gamma_b}\left(\frac{\gamma}{\gamma_b s^2}\right)^{\frac{n-2}{4}} \mathrm{e}^{-\left(\frac{s^2+\frac{\gamma}{\gamma_b}}{2\sigma^2}\right)} I_{\frac{n}{2}-1}\left(\frac{s}{\sigma^2}\sqrt{\frac{\gamma}{\gamma_b}}\right) \tag{3.7}$$

where $I_n(x)$ is the n-th order modified Bessel function of the first kind, n is the number of degrees-of-freedom, s^2 is the non-centrality parameter, σ^2 is the variance per dimension of the underlying random vector of n independent jointly Gaussian components, and the set $\Omega = \{\gamma_b, \sigma, s, n\}$. The non-central moments, $\mathrm{E}[g^k]$, of the Ricean distributed amplitude g are given by [8, eq. (2-1-146)]; specifically, $\mathrm{E}[g^2] = n\sigma^2 + s^2$. The corresponding MGF of the instantaneous SNR γ is given as [8],

$$\Phi_\gamma(t) = (1 - 2t\gamma_b\sigma^2)^{-\frac{n}{2}} \mathrm{e}^{\left(\frac{s^2 t\gamma_b}{1-2t\gamma_b\sigma^2}\right)}.$$

Assuming $p = 1$ in (3.2) and the PDF (3.7), we can obtain the PDF of $P_e(\gamma)$ as,

$$f_{P_e}(P_e) = \frac{1}{2a_1 A_1 \gamma_b \sigma^2} \left(\frac{\log \frac{A_1}{P_e}}{a_1 \gamma_b s^2} \right)^{\frac{n-2}{4}} \times \\ e^{-\left(\frac{a_1 s^2 \gamma_b + (1 - 2a_1 \gamma_b \sigma^2) \log \frac{A_1}{P_e}}{2a_1 \gamma_b \sigma^2} \right)} I_{\frac{n}{2}-1} \left(\frac{s}{\sigma^2} \sqrt{\frac{\log \frac{A_1}{P_e}}{a_1 \gamma_b}} \right). \tag{3.8}$$

Provided that $p > 1$ in (3.2), since the conditional BER $P_e(\gamma)$ is a monotonically decreasing function of γ, the PDF of $P_e(\gamma)$ can be readily obtained by numerically inverting (3.2) in the PDF expression (3.3). For example, we can use the Newton numerical method [97], and define the inverse solution iteratively, i.e., let,

$$\gamma_{j+1} = \gamma_j + \frac{\sum_{i=1}^{p} A_i e^{-a_i \gamma_j}}{\sum_{i=1}^{p} A_i a_i e^{-a_i \gamma_j}}$$

where, in order to reduce the required number of iterations, the initial value γ_0 is computed as an inverse of the first exponential function in the sum (3.2), i.e.,

$$\gamma_0 = \frac{1}{a_1} \frac{\log A_1}{P_e}.$$

Our numerical experiments indicate that the required number of iterations is dependent on the value of P_e.

3.3.1 Plots

The figures illustrating the properties of the BER performance metrics have been obtained assuming the Ricean distribution with $n = 2$ degrees-of-freedom. Importantly, although $p = 2$ exponentials in (3.2) are sufficient to obtain a highly accurate approximation of the first order non-central moment $\bar{P}_e$, our numerical results show that the value of p must be significantly increased with the moment order k in order to achieve a sufficient accuracy in computing the values of the k-th central moments M_k using (3.5). For example, $p = 150$ exponentials in (3.2) are necessary to evaluate the third central moment M_3 of the conditional BER assuming quadrature amplitude modulations (QAMs) while using the sum-of-exponentials coefficients given in [98].

Consider the PDF of the conditional BER for binary phase shift keying (BPSK) modulation over an AWGN channel. Assuming $p = 1$ and $A_1 = 0.204$ and $a_1 = 1.504$ in (3.2), Fig. 3.1 shows the PDF (3.8) of the conditional BER P_e for different parameters of the channel fading distribution. For comparison, Fig. 3.2 shows the PDF of P_e

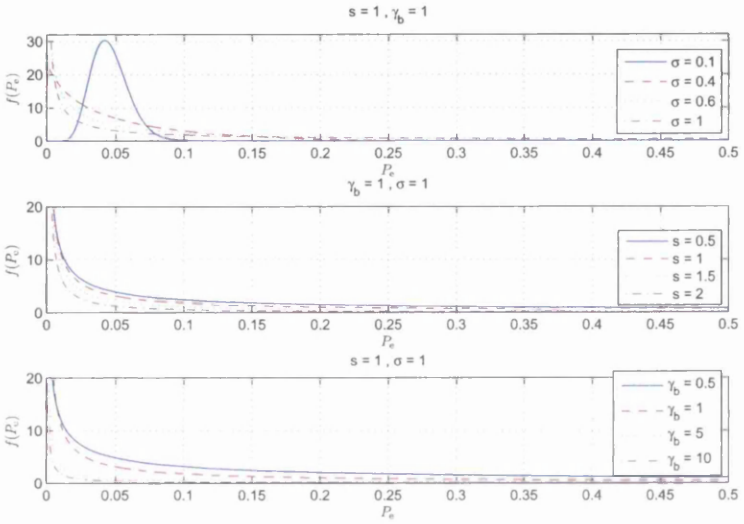

Figure 3.1: The PDF $f_{P_e}(P_e)$ of P_e for BPSK and different channel fading distribution parameters assuming $p = 1$ in (3.2).

assuming $p = 150$ in (3.2) and the same parameters of the channel fading distribution as in Fig. 3.1. As intuitively expected, we observe that the accuracy of the approximation of the conditional BER has significant impact on the accuracy of evaluating the PDF of the conditional BER using the transformation of random variables (3.3).

Examples of the first order non-central and the second and the third central moments of the conditional BER for several linear modulations versus the standard deviation σ per dimension of the Ricean fading distribution having $n = 2$ degrees-of-freedom are shown in Fig. 3.3–Fig. 3.5. We observe that, in all cases considered, the moments of the conditional BER are non-monotonic and reach a maximum for a particular value of σ before decreasing towards zero. In addition, we observe that the maxima of the moments are dependent on all the channel fading distribution parameters, the value of SNR as well as the modulation considered. However, for small values

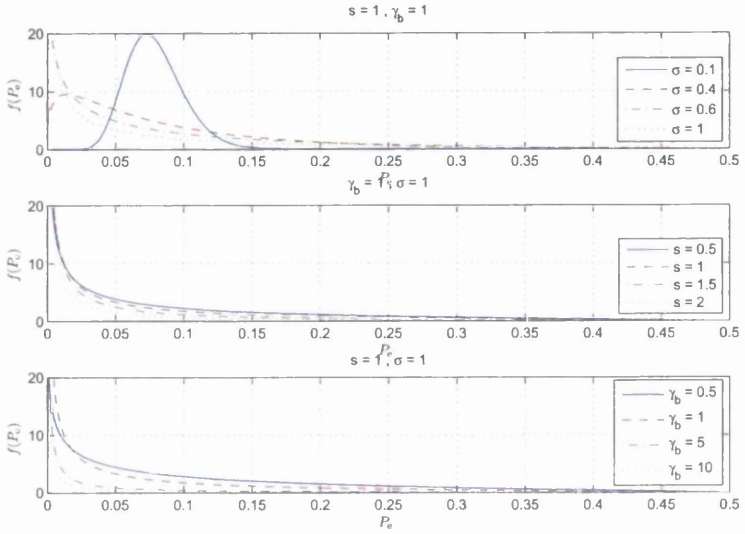

Figure 3.2: The PDF $f_{P_e}(P_e)$ of P_e for BPSK and different channel fading distribution parameters assuming $p = 150$ in (3.2).

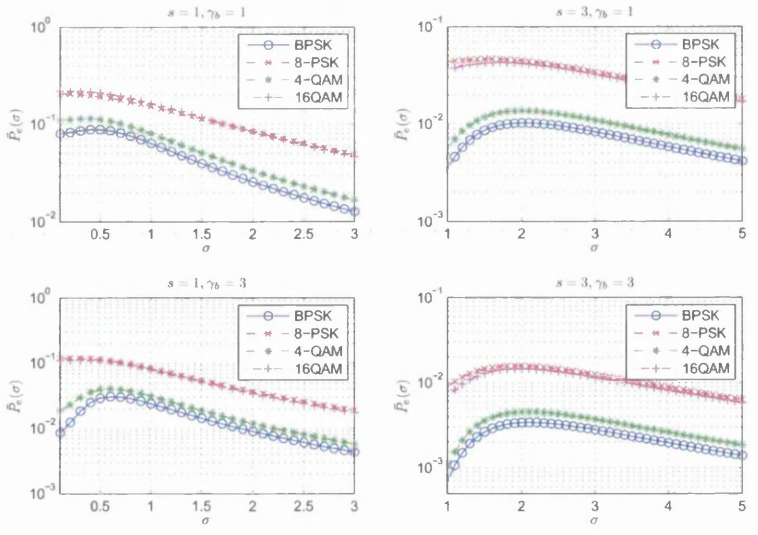

Figure 3.3: The average BER $\bar{P}_e$ versus the standard deviation σ per dimension of the Ricean fading.

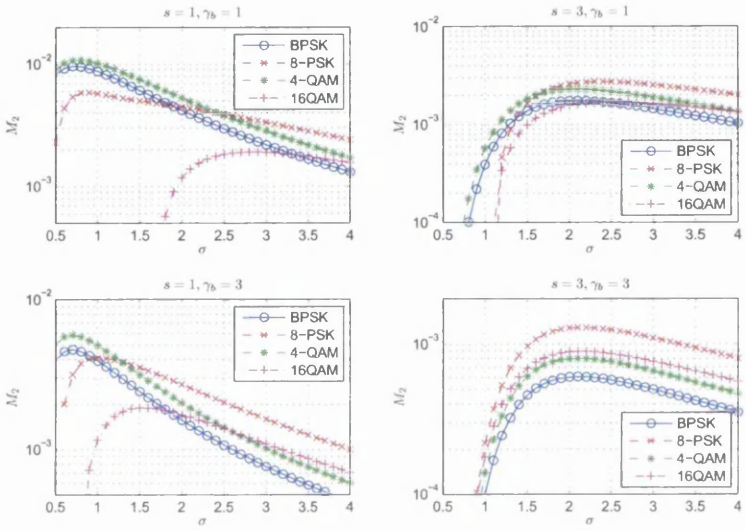

Figure 3.4: The second order central moment M_2 of the conditional BER $P_e(\gamma)$ versus the standard deviation σ per dimension of the Ricean fading.

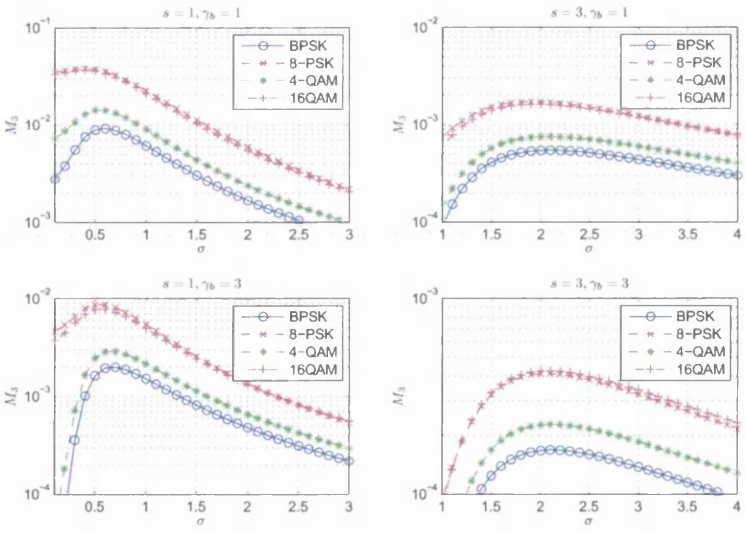

Figure 3.5: The third order central moment M_3 of the conditional BER $P_e(\gamma)$ versus the standard deviation σ per dimension of the Ricean fading.

of the SNR γ_b and for small values of the non-centrality parameter s^2, the maxima become less pronounced. Provided that the non-centrality parameter $s^2 = 0$ corresponding to the Rayleigh distributed fading, the moments of the conditional BER become monotonically decreasing functions of the standard deviation σ. Intuitively, smaller values of the standard deviation σ and non-zero values of the non-centrality parameter s^2 leads to smaller variations of the channel fading amplitude effectively making the transmission channel model to behave more as an AWGN channel. On the other hand, larger values of σ improve the SNR values, so that the average BER decreases. Mathematically, smaller values of σ and $s^2 > 0$ effectively move the single mode of the PDF of the conditional BER to the right, and the BER decreases; cf. Fig. 3.2 and eq. (3.1).

Numerical examples of the Bollinger bands of $P_e(\gamma)$ for several linear modulations are shown in Fig. 3.6. We again observe that the upper and lower boundaries of

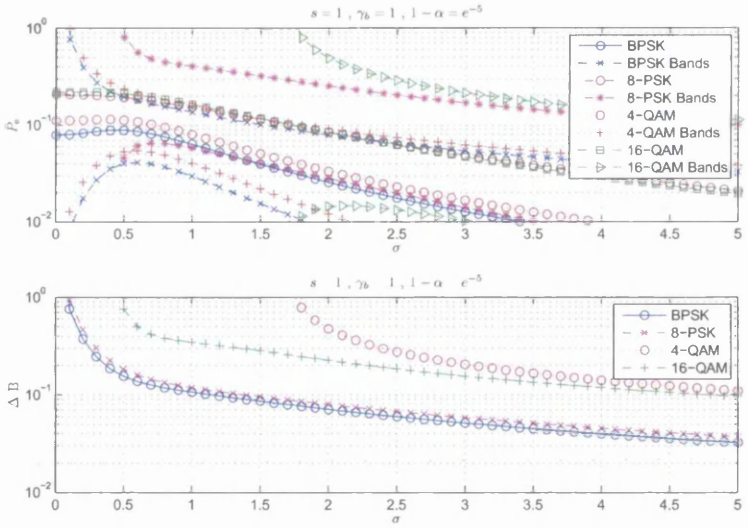

Figure 3.6: The Bollinger bands of the conditional BER $P_e(\gamma)$ versus the standard deviation σ per dimension of the Ricean fading.

the Bollinger band but not the width of the Bollinger band are non-monotonic in the standard deviation σ.

3.4 Discussion

The non-monotonic behavior of the moments of the conditional BER versus the standard deviation per dimension of the Ricean channel fading has the following practical consequences on the design of communication systems. The first order non-central moment corresponding to the average BER (3.1) can be minimized for small values of the standard deviation σ and non-zero values of the non-centrality parameter s^2; this renders the channel to be more benign and to behave as an AWGN channel model. In practice, the smaller values of standard deviation σ can be equivalently achieved by decreasing the transmission power. As shown in Fig. 3.3, the transmission power reduction is particularly feasible for line-of-sight communication links using low-order linear modulations and having larger values of the non-centrality parameter. Furthermore, assuming $p = 2$ in (3.2) and assuming the Ricean fading, we can prove the following proposition,

Proposition 2. *Provided that $s^2 = 0$ corresponding to the Rayleigh fading channel, the average BER $\bar{P}_e$ is a decreasing function of the standard deviation per dimension of the channel fading σ. However, if $s^2 > 0$, then $\bar{P}_e$ is a non-monotonic function of σ reaching a maximum for a particular value of $\sigma = \sigma_*$. The value of $\sigma = \sigma_*$ maximizing $\bar{P}_e$ can be bounded as,*

$$\frac{s^2}{2n} - \frac{1}{C_1} < \sigma_*^2 < \frac{s^2}{2n} - \frac{1}{C_2}$$

where C_1 and C_2 are positive real constants. ■

Proof. Given $\bar{P}_e(\sigma)$, the condition, $\frac{d}{d\sigma}\bar{P}_e(\sigma) = 0$, has to be satisfied for some $\sigma < \infty$ in order to guarantee the existence of the maximum, and in turn, a non-monotonic behavior. This condition is then simplified assuming $p = 2$ exponentials. ■

The second central moment (i.e., the variance) of the conditional BER is a measure of the spread of the random conditional BER values about their mean. The small spread of the conditional BER values corresponds to the small variations of the instantaneous SNR values about their mean; this is desirable when the transmission power control and the receiver automatic gain control are used. The variance of the conditional BER is important in delay limited communications, i.e. voice and multimedia communications, when the receiver is processing received sequences of relatively small length.

When the BER variance is large, the conditional BER values can deviate significantly from their expected value (i.e., their first non-central moment). Hence, as shown in Fig. 3.4, especially for higher-order linear modulations, the variance of the conditional BER can be significantly reduced for line-of-sight communication links by reducing the transmission power. Furthermore, in Fig. 3.3–Fig. 3.5, we have assumed that the channel fading variance per dimension σ^2 varies independently from the number of degrees-of-freedom n. Since the average channel fading power is proportional to $n\sigma^2$, more realistic investigation should consider the case when n and σ^2 do not vary independently. In particular, we have the following proposition,

Proposition 3. *If the variance of the channel fading per dimension σ^2 is directly or inversely proportional to the number of dimensions n, i.e., either $\sigma^2 = Cn$ or $\sigma^2 = C/n$, for some positive real constant C, then the second central moment M_2 is not monotonic in dimension n.* ■

Proof. Provided that the variance of the channel fading per dimension $\sigma^2 = Cn$ or $\sigma^2 = C/n$, one considers the condition, $\frac{\mathrm{d}}{\mathrm{d}n}M_2 = 0$, assuming that $n > 0$ is a real number. However, since n can only be an integer number physically, one can use the sign of the derivative at the integer n values,which indicates the existence of the maximum. ■

Finally, the Bollinger bands can be used to describe the BER of the communication systems operating over time-varying channels. More importantly, the upper bound of the Bollinger band represents the worst case BER performance corresponding to the deep fades, and the lower bound of the Bollinger band indicates more benign channel conditions.

4

Non-ergodic Error Rate Analysis of a Single Finite Length Sequence Over BSC

4.1 Introduction

Conventional communication systems often assume time-unlimited information transmissions. The performance of such systems is evaluated in terms of the ergodic performance measures using expectation over all random system inputs [92]. The ergodic performance measures are also used even when the underlying communication channel may be considered to be non-ergodic. For example, the codewords transmitted over a finite number of fading blocks (so-called a block fading channel model) are designed to approach the capacity versus outage of such non-ergodic channels [99]. The frame error rate (FER) ergodic performance measure is then used and tightly lower-bounded by the probability of outage [45]. The channel models can also become non-ergodic, for example, due to their stochastic construction [100].

In general, the ergodicity property is important, since, in many practical scenarios, measurements and observations are available in the time domain, however, the performance measures as the statistics of interest are defined in the domain of random realizations [8]. Precise mathematical definitions of ergodicity can be found

in books [9] and [10]. In particular, Gardiner [10] defines the mean-ergodicity, the covariance-ergodicity and the distribution-ergodicity of a strict-sense stationary random process using a variance of the time-average statistics. Gardiner also defines mean-square ergodicity of the mean and of the covariance of a random process assuming a mean-square error between the time-averages and the corresponding expected statistics. More importantly, the time-average statistics obtained from finite observations are, in general, random, since some of the channel model parameters cannot be considered as being ergodic (cf. [92]). Then, the mean value of the error rate is less indicative of the system performance, and other statistics are preferred to describe the distribution of the system error rate.

In this chapter, we assume that the received sequence either consists of a finite number of codewords transmitted over a non-ergodic block fading channel, or it is formed by a finite number of uncoded modulation symbols transmitted over an additive white Gaussian noise (AWGN) channel corresponding to one fading block. We assume that the pilot symbols are used in each fading block, so that the receiver can obtain knowledge of the channel fading coefficients. For simplicity, to develop the main ideas of our non-ergodic analysis, we assume binary phase shift keying (BPSK) modulation which leads to an equivalent binary symmetric channel (BSC) model with binary input and binary output. It is straightforward to extend our analysis to more general case of non-binary modulations over memoryless channels.

We study the problem of estimating the instantaneous FER, or equivalently, the instantaneous bit error rate (BER) defined as a fraction of erroneous decisions at the detector or decoder output. We show that the instantaneous FER or BER statistics can be described as a degree of believe using the Bayesian credible intervals [101, 102, 19, 20]; to the authors' best knowledge, the credible intervals of the instantaneous error rates have not been considered previously by others. On the other hand, the confidence intervals as a frequentist interpretation of the system BER and FER performance using computer simulations have been considered extensively in literature; see, for example, [103] and [104]. We introduce a novel degree of ergodicity (DOE) performance measure to quantify the level of ergodicity of the finite length received sequence, and to quantify the transition speed of the detector or decoder from the non-ergodic to ergodic zone of operation with increasing length of the received sequence. We prove several

properties of the proposed DOE measure. In our analysis, we assume that the channel fading is perfectly known at the receiver, however, the effect of channel estimation errors is also considered. Finally, as an application example, the non-ergodic analysis developed in this chapter is exploited by adaptive forward error correction (FEC) coding and by adaptive power control to guarantee, with a certain probability, the worst case instantaneous BER of the data detector and to increase its transition speed from the non-ergodic to ergodic zone of operation. The rest of this chapter is organized as follows. System model is presented in Section 4.2. The credible interval estimators of the instantaneous BER and their properties are obtained in Section 4.3. Applications of the developed non-ergodic analysis are studied in Section 4.4, and chapter conclusions are given in Section 4.5.

4.2 System model

Consider a point-to-point transmission over a frequency non-selective block fading channel, so that the channel coefficients are constant in each fading block, and they are independent between the fading blocks [45]. The transmitted frames can be encoded using a FEC code and span $N \geq 1$ fading blocks. We also assume that a sufficient number of pilots symbols is interleaved across the transmitted codeword in each fading block, and thus, the receiver can accurately estimate all the channel fading coefficients. For asymptotically large (i.e., infinite) number of transmitted frames, the ergodic FER of such communication system can be expanded as,

$$\bar{P}_{\epsilon} = P_{\text{out}} P_{\epsilon,\text{out}} + (1 - P_{\text{out}}) P_{\epsilon,\overline{\text{out}}}$$

where P_{out} is the probability of outage, and $P_{\epsilon,\text{out}}$ and $P_{\epsilon,\overline{\text{out}}}$ are the conditional FERs of the system in and out of the outage conditions, respectively. Note that for $P_{\epsilon,\text{out}} \gg P_{\epsilon,\overline{\text{out}}}$ and small values P_{out} of practical interest, or when $P_{\epsilon,\text{out}} = 1$, the FER is lower-bounded as, $\bar{P}_{\epsilon} > P_{\text{out}}$. Definition of the outage is quite arbitrary, however, it is useful to define the outage to facilitate the FEC coding design [99]. In particular, conditioned on knowledge of the channel fading coefficients at the receiver, the frames are transmitted over the AWGN channels of varying instantaneous channel capacity. Hence, one can design the FEC code of a fixed coding rate to approach the instantaneous channel

capacity of the AWGN channels provided that the chosen coding rate is smaller (with the probability $1 - P_{\text{out}}$) than the instantaneous channel capacity. In the sequel, we assume such AWGN channel capacity approaching FEC code design (described, e.g., in [99]), so that the conditional FER $P_{\epsilon,\overline{\text{out}}}$ can be made arbitrarily small whereas, in the outage, $P_{\epsilon,\text{out}} \to 1$. Consequently and importantly, we can consider an equivalent system model of transmitting N independent and identically distributed (IID) binary symbols (bits) over a BSC with the crossover probability $\tilde{p}_{\text{BSC}} = P_{\text{out}}$. Each transmitted bit then corresponds to one transmitted frame that is decoded correctly at the receiver with the probability $1 - \tilde{p}_{\text{BSC}} = 1 - P_{\text{out}}$, and the system FER performance can be equivalently measured as the BER. Such equivalent system model can be also considered for transmission of frames consisting of pilot symbols for channel estimation and N uncoded BPSK symbols over a block fading channel with hard decision decoding at the receiver. In this case, the crossover probability $\tilde{p}_{\text{BSC}} = Q(\sqrt{2\gamma_b})$ where $Q(\cdot)$ is the Q-function, and γ_b is the signal-to-noise ratio (SNR) per transmitted binary symbol [8].

4.2.1 Instantaneous BER performance measure

Assuming the equivalent system model described above, we analyze the BER properties for a single finite length sequence of N bits transmitted over a BSC. Recall that, in addition to these N binary symbols, pilot symbols are used to perfectly estimate the channel fading at the receiver, i.e., we assume that $\tilde{p}_{\text{BSC}}$ is perfectly known at the receiver. Let e_t be the error indicator, i.e., $e_t = 1$ if the t-th bit is decided erroneously at the detector, and $e_t = 0$ otherwise. The statistics of the error sequence $\mathbf{e} = (e_1, \ldots, e_t, \ldots, e_N)$ corresponding to the N transmitted bits are an important performance indicator that is used to describe the transmission quality. Hence, we define the instantaneous BER as,

$$P_N = \frac{1}{N} \sum_{t=1}^{N} e_t = \frac{1}{N} E_N \tag{4.1}$$

where E_N is the error counter, i.e., the number of errors in the received sequence of N bits. The mean of E_N, i.e., $\mathrm{E}[E_N] = N\tilde{p}_{\text{BSC}}$ where $\mathrm{E}[\cdot]$ denotes expectation, and the variance of P_N, i.e., $\mathrm{E}[(P_N - \mathrm{E}[P_N])^2] = \tilde{p}_{\text{BSC}}(1 - \tilde{p}_{\text{BSC}})/N$, are functions of

N, and thus, for finite values of N, neither the sequence E_N nor the sequence P_N are stationary. In addition, since, for finite N (and the single transmitted sequence), $\mathrm{E}[E_N] \neq E_N$ and $\mathrm{E}[P_N] \neq P_N$, neither E_N nor P_N is the ergodic sequence. However, since the errors are independent, we can use the Slutsky's theorem [105] to show that, in the limit of asymptotically large N, the error sequence, e, is mean-ergodic and variance-ergodic, and the BER (4.1) converges to,

$$\lim_{N\to\infty} P_N = \mathrm{E}[e_t] = \mathrm{Av}[e_t] = \Pr(e_t = 1) = \tilde{p}_{\mathrm{BSC}}$$

where $\mathrm{Av}[e_t] = \lim_{N\to\infty} \frac{1}{N} \sum_{t=1}^{N} e_t$, and $\Pr(e_t = 1)$ is the probability of bit error.

4.3 Estimation of instantaneous BER

For finite observations, any empirical performance measure is random (i.e., non-ergodic), and the interval estimators rather than the point estimators are better suited to describe the system performance. Hence, we obtain interval estimators of the instantaneous BER P_N in (4.1) that can be used in practical receivers rather than in computer simulations.

In general, the interval estimators provide either the confidence intervals or the credible intervals of the parameter estimates depending on the problem formulation [101, 102, 19, 20]. In particular, the confidence interval is calculated from the random observations for some confidence level $(1 - \alpha)$, $0 \leq \alpha \leq 1$, assuming that the a priori distribution of the parameter of interest is not known. It is a random interval having the statistics of the observed samples as its boundary values. The confidence interval has a direct frequentist interpretation of the probability. Thus, if the confidence interval is repeatedly obtained for different measurements or simulation runs for a sufficiently large number of times, the true value of the unknown parameter will be inside the calculated confidence intervals for the fraction of $(1-\alpha)$ trials. For example, the confidence intervals are often obtained for the Monte Carlo BER estimators used computer simulations [103]. The estimation of the crossover probability $\tilde{p}_{\mathrm{BSC}}$ from a finite number of pilot symbols at the receiver is another example of situation where the confidence interval can be obtained.

The Bayesian credible interval, on the other hand, is determined from the a posteriori distribution of the parameter of interest using its known a priori distribution. Unlike the confidence intervals, the confidence level $(1-\alpha)$ of the credible interval computed for a particular sequence of the observed samples is interpreted as the degree of belief (i.e., the probability) that the true value of the unknown parameter is inside the computed credible interval. However, note that neither the confidence interval nor the credible interval is unique unless additional constraints are assumed [101].

In practical receivers, estimation of the instantaneous BER (4.1) from a single received sequence of N bits, and using additional pilot symbols for the channel estimation, yields the Bayesian credible intervals. In particular, for given N, and without any other observations, the a priori probability mass function (PMF) of the instantaneous BER P_N is uniform, i.e., the probability, $\Pr(P_N = E_N/N) = 1/(1+N)$ for $E_N \in \{0, 1, \ldots, N\}$. After observing a sufficient number of pilot symbols, one can obtain an accurate point estimate of the crossover probability $\tilde{p}_{\text{BSC}}$. Then, using the Bayes' theorem [9], the a posteriori PMF of the instantaneous BER is evaluated as,

$$\Pr(P_N|\tilde{p}_{\text{BSC}}) = \frac{f(\tilde{p}_{\text{BSC}}|P_N)\Pr(P_N)}{f(\tilde{p}_{\text{BSC}})}$$

where the probability density function (PDF) $f(\tilde{p}_{\text{BSC}})$ is assumed to be uniform over the interval[1] $\tilde{p}_{\text{BSC}} \in [0, 1]$, $\Pr(P_N) = 1/(N+1)$ is the a priori PMF of P_N, and the conditional PDF $f(\tilde{p}_{\text{BSC}}|P_N)$ is the likelihood of the parameter P_N. For a BSC, the conditional PDF $f(\tilde{p}_{\text{BSC}}|P_N)$ is the beta distribution [103], and thus, for $\tilde{p}_{\text{BSC}} = p$ and $E_N = k$, one has that,

$$f(\tilde{p}_{\text{BSC}}|P_N) = f(\tilde{p}_{\text{BSC}}|E_N) = (N+1)\binom{N}{k}p^k(1-p)^{N-k}$$

where $\binom{N}{k}$ is the binomial coefficient. Consequently, the statistics of the error counter $E_N = k$ are given by the binomial PMF [9, 8],

$$\begin{aligned} b_N(k|p) &= f(p|k)/(N+1) \\ &= \textstyle\sum_{i=0}^{N-k}\binom{N}{k}\binom{N-k}{i}(-p)^{N-i} \end{aligned}$$

[1] It is straightforward to show that any uniform distribution $f(\tilde{p}_{\text{BSC}})$ over an arbitrary interval yields the same credible interval estimate of the instantaneous BER P_N.

for $k = 0, 1, \cdots, N$. The cumulative mass function (CMF) of the binomial distribution is,

$$\begin{aligned} B_N(k|p) &= \sum_{i=0}^{k} b_N(i|p) \\ &= 1 - \frac{\beta(p;k+1,N-k)}{\beta(k+1,N-k)} \\ &= I_{1-p}(N-k, k+1) \end{aligned}$$

where $\beta(p; k+1, N-k)$ is the incomplete beta function, $\beta(k+1, N-k)$ is the beta function, and $I_{1-p}(N-k, k+1)$ is the regularized beta function [106]. Note that $b_N(k|p) = I_{1-p}(N-k, k+1) - I_{1-p}(N-k-1, k)$, $\lim_{N\to\infty} I_{1-p}(N-k, k+1) - I_{1-p}(N-k-1, k) = 0$, and $\lim_{N\to\infty} b_N(k|p) = 0$, for $\forall k, p$. The mean of the binomial distribution $b_N(k|p)$ is exactly equal to Np. Since $b_N(k|p) \leq b_N(k+1|p)$ if and only if $k/N \leq p$, we can show that the binomial distribution is uni-modal for $\forall k, p$.

4.3.1 Credible interval estimators of instantaneous BER

The credible interval of the instantaneous BER P_N with confidence level $(1-\alpha)$ after receiving N bits is denoted as,

$$\mathrm{CI}_N(\alpha) = [P_N^{(\mathrm{l})}(\alpha), P_N^{(\mathrm{u})}(\alpha)] \tag{4.2}$$

so that $P_N^{(\mathrm{l})}(\alpha)$ is a lower bound of P_N *and* $P_N^{(\mathrm{u})}(\alpha)$ is an upper bound of P_N with the probability $(1-\alpha)$. Thus, the credible interval (4.2) is an estimate of the true value of P_N with the confidence (i.e., the degree of belief) $(1-\alpha)$, such that the probability [101],

$$\Pr\left(P_N^{(\mathrm{l})}(\alpha) \leq P_N \leq P_N^{(\mathrm{u})}(\alpha)\right) \geq 1-\alpha. \tag{4.3}$$

We can verify the obtained credible interval (4.2) by computer simulations using the frequentist interpretation of the probability. Particularly, we can evaluate a fraction $(1-\alpha_R)$ of the number of realizations R for which the true value of P_N is inside the calculated credible interval $(P_N^{(\mathrm{l})}(\alpha), P_N^{(\mathrm{u})}(\alpha))$; then, $\lim_{R\to\infty} \alpha_R = \mathrm{E}[\alpha_R] = \alpha$.

More importantly, definition of the credible interval in (4.2) and (4.3) is not unique without any additional constraints assumed. One can use measures of the location and of the spread of the a priori distribution to obtain precise definition of the credible intervals [101]. For instance, for a given confidence level $(1-\alpha)$, it is desirable to obtain the shortest possible interval having the largest credibility. We can show that

the shortest interval is obtained when $\Pr\left(P_N = P_N^{(\mathrm{l})}\right) = \Pr\left(P_N = P_N^{(\mathrm{u})}\right)$. However, in practice, it is often easier to obtain the credible interval having the equal tail areas, i.e., $\Pr\left(P_N < P_N^{(\mathrm{l})}\right) = \Pr\left(P_N > P_N^{(\mathrm{u})}\right)$ [101]. In this chapter, we solve the problem of uniqueness of the credible interval by considering two separate credible intervals, i.e., let,

$$\begin{aligned} \mathrm{CI}_N^{(u)}(\alpha_2) &= [P_N^{(\mathrm{ref})}, P_N^{(\mathrm{u})}(\alpha_2)] \\ \mathrm{CI}_N^{(l)}(\alpha_1) &= [P_N^{(\mathrm{l})}(\alpha_1), P_N^{(\mathrm{ref})}] \end{aligned} \tag{4.4}$$

be the upper and lower credible intervals having the confidence levels $(1-\alpha_2)$ and $(1-\alpha_1)$, respectively. Then, the credible interval $\mathrm{CI}_N(\alpha)$ is a union of the two credible intervals in (4.4). The reference value $P_N^{(\mathrm{ref})}$ is chosen a priori, so that, conditioned on $P_N^{(\mathrm{ref})}$, the credible intervals $\mathrm{CI}_N^{(u)}(\alpha_2)$ and $\mathrm{CI}_N^{(l)}(\alpha_1)$ can be obtained independently from each other. The upper and lower credible intervals that are defined independently are more easily obtained, and, in some applications, it may be more useful to consider either the upper or the lower bound of the instantaneous BER corresponding to the worst case or the best case performance, respectively. By definition, the credible intervals in (4.4) have the probabilities,

$$\begin{aligned} \Pr\left(P_N^{(\mathrm{ref})} \le P_N \le P_N^{(\mathrm{u})}(\alpha_2)\right) &\ge 1-\alpha_2 \\ \Pr\left(P_N^{(\mathrm{l})}(\alpha_1) \le P_N \le P_N^{(\mathrm{ref})}\right) &\ge 1-\alpha_1. \end{aligned} \tag{4.5}$$

Consequently, conditioned on $P_N^{(\mathrm{ref})}$, and given $(1-\alpha_2)$ and $(1-\alpha_1)$, the bounds $P_N^{(\mathrm{u})}(\alpha_2)$ and $P_N^{(\mathrm{l})}(\alpha_1)$ can be uniquely determined as the values minimizing the probabilities in (4.5) under the inequality constraints. Furthermore, with the increasing number of received bits N, we require that, $\lim_{N\to\infty} P_N^{(\mathrm{u})}(\alpha_2) = \lim_{N\to\infty} P_N^{(\mathrm{l})}(\alpha_1) = \tilde{p}_{\mathrm{BSC}}$, and, $P_N^{(\mathrm{l})} \le P_N^{(\mathrm{u})}$ for $\forall N \ge 1$. In the sequel, in order to simplify the development of the credible intervals, we first equivalently obtain the credible intervals for the error counter E_N, and then use $P_N = E_N/N$ to obtain the credible intervals for the instantaneous BER P_N.

Denote as $[a,b]$ the set $\{a, a+1, \cdots, b\}$ of integers, for $b \ge a$. Since $0 \le E_N \le N$, we can define the credible interval of E_N using subsets $\mathcal{E}_1 \subseteq [0,N]$ and $\mathcal{E}_2 \subseteq [0,N]$

such that[1],

$$\begin{aligned} \mathrm{CI}_N^{(u)}(\alpha_2) &= \underset{\mathcal{E}_2}{\operatorname{argmin}} \Pr(\mathcal{E}_2) \text{ s.t. } \Pr(\mathcal{E}_2) \geq 1-\alpha_2 \\ \mathrm{CI}_N^{(l)}(\alpha_1) &= \underset{\mathcal{E}_1}{\operatorname{argmin}} \Pr(\mathcal{E}_1) \text{ s.t. } \Pr(\mathcal{E}_1) \geq 1-\alpha_1 \end{aligned} \tag{4.6}$$

where $\Pr(\mathcal{E}_i) = \sum_{E \in \mathcal{E}_i} \Pr(E_N = E)$ for $i = 1, 2$. Thus, the credible intervals (4.6) are the subsets $\mathcal{E}_1$ and $\mathcal{E}_2$ of all possible number of errors E_N subject to (s.t.) having the probability mass greater than the confidence levels $(1-\alpha_2)$ and $(1-\alpha_2)$, respectively. Since the binomial distribution is always unimodal, we can show that the subsets $\mathcal{E}_1$ and $\mathcal{E}_2$ minimizing (4.6) can be written as,

$$\begin{aligned} \mathcal{E}_2 &= [E_N^{(\mathrm{ref})}, E_N^{(\mathrm{u})}] \\ \mathcal{E}_1 &= [E_N^{(\mathrm{l})}, E_N^{(\mathrm{ref})}] \end{aligned} \tag{4.7}$$

where $E_N^{(\mathrm{ref})}$ is the reference number of errors, and again, the upper and lower bounds $E_N^{(\mathrm{u})}$ and $E_N^{(\mathrm{l})}$ can be obtained independently. Alternatively, we can define the subsets $\mathcal{E}_2$ and $\mathcal{E}_1$ satisfying (4.6) as,

$$\begin{aligned} \mathcal{E}_2 &= [E_N^{(\mathrm{u})}, E_N^{(\mathrm{ref},2)}] \\ \mathcal{E}_1 &= [E_N^{(\mathrm{ref},1)}, E_N^{(\mathrm{l})}]. \end{aligned} \tag{4.8}$$

Note that the subsets $\mathcal{E}_2$ and $\mathcal{E}_1$ defined by (4.7) and (4.8) are unique, and that the condition, $\lim_{N\to\infty} P_N^{(\mathrm{u})} = \lim_{N\to\infty} P_N^{(\mathrm{l})} = \tilde{p}_{\mathrm{BSC}}$, implies the condition, $\lim_{N\to\infty} E_N^{(\mathrm{u})} = \lim_{N\to\infty} E_N^{(\mathrm{l})}$. Finally, the upper and lower bounds of the instantaneous BER P_N in (4.2) are computed as,

$$\begin{aligned} P_N^{(\mathrm{u})} &= E_N^{(\mathrm{u})}/N \\ P_N^{(\mathrm{l})} &= E_N^{(\mathrm{l})}/N. \end{aligned}$$

The above general definitions of the credible intervals of the instantaneous BER can be further elaborated to obtain more practical expressions for their calculation. Hence, we introduce next three practical definitions of the credible intervals that can be used at the receivers having only knowledge of N and $\tilde{p}_{\mathrm{BSC}}$. In the first definition, the probability masses of the upper and lower credible intervals of the number of errors in (4.6) are normalized, so that $(1-\alpha_1) < 1$ and $(1-\alpha_2) < 1$. In the second definition

[1]Note that more than one subset $\mathcal{E}_1$ and $\mathcal{E}_2$ may satisfy (4.6) even though our numerical results indicate that such situation rarely occurs.

of the credible interval, we assume definition (4.8) with the conservative values of the reference number of errors $E_N^{(\text{ref},2)} = N$ and $E_N^{(\text{ref},1)} = 0$ which makes the reference number of errors to be independent of $\tilde{p}_{\text{BSC}}$. In the third definition, the credible interval is computed using a probability threshold to identify the most likely values of the numbers of errors.

Definition 1 of the credible interval (CI1)

The upper and lower credible intervals (4.7) are computed using (4.6). Then, the bounds $E_N^{(\text{l})} \leq E_N^{(\text{ref})} \leq E_N^{(\text{u})}$ for $N \geq 1$, and the intersection, $\text{CI}_N^{(u)}(\alpha_2) \cap \text{CI}_N^{(l)}(\alpha_1) = \{E_N^{(\text{ref})}\}$. We normalize the probabilities $\Pr\left(\text{CI}_N^{(u)}(\alpha_2)\right)$ and $\Pr\left(\text{CI}_N^{(l)}(\alpha_1)\right)$ to ensure that $0 \leq \alpha_1 \leq 1$ and $0 \leq \alpha_2 \leq 1$. Consequently, the upper and lower bounds of the number of errors E_N, respectively, are given as,

$$E_N^{(\text{u})} = \underset{\tilde{E}_N^{(\text{u})}}{\text{argmin}} \frac{\Pr\left(E_N^{(\text{ref})} \leq E_N \leq \tilde{E}_N^{(\text{u})}\right)}{\Pr\left(E_N^{(\text{ref})} \leq E_N \leq N\right)} \quad \text{s.t.} \frac{\Pr\left(E_N^{(\text{ref})} \leq E_N \leq \tilde{E}_N^{(\text{u})}\right)}{\Pr\left(E_N^{(\text{ref})} \leq E_N \leq N\right)} \geq 1 - \alpha_2 \tag{4.9}$$

$$E_N^{(\text{l})} = \underset{\tilde{E}_N^{(\text{l})}}{\text{argmin}} \frac{\Pr\left(\tilde{E}_N^{(\text{l})} \leq E_N \leq E_N^{(\text{ref})}\right)}{\Pr\left(0 \leq E_N \leq E_N^{(\text{ref})}\right)} \quad \text{s.t.} \frac{\Pr\left(\tilde{E}_N^{(\text{l})} \leq E_N \leq E_N^{(\text{ref})}\right)}{\Pr\left(0 \leq E_N \leq E_N^{(\text{ref})}\right)} \geq 1 - \alpha_1. \tag{4.10}$$

The corresponding probabilities of the upper and lower credible intervals are,

$$\Pr\left(\text{CI}_N^{(u)}(\alpha_2)\right) = (1 - \alpha_2) \Pr\left(E_N^{(\text{ref})} \leq E_N \leq E_N^{(\text{u})}\right)$$
$$\Pr\left(\text{CI}_N^{(l)}(\alpha_1)\right) = (1 - \alpha_1) \Pr\left(0 \leq E_N \leq E_N^{(\text{ref})}\right)$$

where $(1 - \alpha_2)$ and $(1 - \alpha_1)$ are the confidence levels of the upper and lower credible intervals $\text{CI}_N^{(u)}(\alpha_2)$ and $\text{CI}_N^{(l)}(\alpha_1)$, respectively. For a BSC, the reference number of errors $E_N^{(\text{ref})}$ in (4.9) and (4.10) is given as,

$$E_N^{(\text{ref})} = \lceil N P_\infty \rfloor \tag{4.11}$$

in order to guarantee that, for any N, α_1 and α_2, the bounds $E_N^{(\mathrm{l})} \leq E_N^{(\mathrm{ref})} \leq E_N^{(\mathrm{u})}$, and $\lim_{N\to\infty} P_N^{(\mathrm{u})} = \lim_{N\to\infty} P_N^{(\mathrm{l})} = \tilde{p}_{\mathrm{BSC}}$. Note also that it is possible to use the mode of the underlying PMF rather than the mean as in (4.11). A relationship between the mode and the mean of the binomial PMF has been established in [107]. However, provided that the mode rather than the mean is considered, it is not straightforward to guarantee that $E_N^{(\mathrm{u})} \geq N\tilde{p}_{\mathrm{BSC}}$ and $E_N^{(\mathrm{l})} \leq N\tilde{p}_{\mathrm{BSC}}$, for all values of N.

Definition 2 of the credible interval (CI2)

The upper and lower credible intervals (4.8) are computed using (4.6), i.e.,

$$\begin{aligned} E_N^{(\mathrm{u})} &= \underset{\tilde{E}_N^{(\mathrm{u})}}{\operatorname{argmin}} \Pr\left(0 \leq E_N \leq \tilde{E}_N^{(\mathrm{u})}\right) \\ &\quad \text{s.t. } \Pr\left(0 \leq E_N \leq \tilde{E}_N^{(\mathrm{u})}\right) \geq 1-\alpha_2 \\ E_N^{(\mathrm{l})} &= \underset{\tilde{E}_N^{(\mathrm{l})}}{\operatorname{argmin}} \Pr\left(\tilde{E}_N^{(\mathrm{l})} \leq E_N \leq N\right) \\ &\quad \text{s.t. } \Pr\left(\tilde{E}_N^{(\mathrm{l})} \leq E_N \leq N\right) \geq 1-\alpha_1. \end{aligned}$$

The probability mass of these credible intervals is given by the confidence levels $(1-\alpha_1)$ and $(1-\alpha_2)$, respectively, i.e.,

$$\begin{aligned} \Pr\left(\mathrm{CI}_N^{(u)}(\alpha_2)\right) &= (1-\alpha_2) \\ \Pr\left(\mathrm{CI}_N^{(l)}(\alpha_1)\right) &= (1-\alpha_1). \end{aligned}$$

However, in order to guarantee that the bounds $E_N^{(\mathrm{u})}$ and $E_N^{(\mathrm{l})}$ converge to the same value in the limit of large N, the values of the confidence levels cannot be chosen arbitrarily. The additional constraints to guarantee that $E_N^{(\mathrm{u})} \geq E_N^{(\mathrm{l})}$ for $N \geq 1$ are,

$$\begin{aligned} (1-\alpha_2) &\geq \Pr\left(0 \leq E_N \leq E_N^{(\mathrm{ref})}\right) \\ (1-\alpha_1) &\geq \Pr\left(E_N^{(\mathrm{ref})} \leq E_N \leq N\right). \end{aligned} \tag{4.12}$$

For simplicity, we can approximates conditions (4.12) as, $(1-\alpha_2) > (1-\tilde{p}_{\mathrm{BSC}})$ and $(1-\alpha_1) > \tilde{p}_{\mathrm{BSC}}(2-\tilde{p}_{\mathrm{BSC}})$. For example, if $\tilde{p}_{\mathrm{BSC}} = 10^{-2}$, then the confidence levels should be chosen to satisfy the inequalities $(1-\alpha_2) > 0.99$ and $(1-\alpha_1) > 0.0199$. For larger values of N, we can further approximate conditions (4.12) as, $(1-\alpha_2) > 0.5$ and $(1-\alpha_1) > 0.5$.

Definition 3 of the credible interval (CI3)

In this definition, a probability threshold is used to select the most likely numbers of errors to form the credible interval. The probability threshold is obtained using the probability of the reference number of errors, i.e., let $P_N^{(\mathrm{ref})} = \Pr\left(E_N = E_N^{(\mathrm{ref})}\right)$. Then, the upper and lower bounds $E_N^{(\mathrm{u})}$ and $E_N^{(\mathrm{l})}$ of E_N are calculated as,

$$E_N^{(\mathrm{u})} = \underset{E_N^{(\mathrm{u})} \geq E_N^{(\mathrm{ref})}}{\operatorname{argmin}} \Pr\left(E_N = E_N^{(\mathrm{u})}\right) \quad \text{s.t. } \Pr\left(E_N = E_N^{(\mathrm{u})}\right) \geq \alpha_2 P_N^{(\mathrm{ref})} \tag{4.13}$$

$$E_N^{(\mathrm{l})} = \underset{E_N^{(\mathrm{l})} \leq E_N^{(\mathrm{ref})}}{\operatorname{argmin}} \Pr\left(E_N = E_N^{(\mathrm{l})}\right) \quad \text{s.t. } \Pr\left(E_N = E_N^{(\mathrm{l})}\right) \geq \alpha_1 P_N^{(\mathrm{ref})} \tag{4.14}$$

where $\alpha_1 P_N^{(\mathrm{ref})}$ and $\alpha_2 P_N^{(\mathrm{ref})}$ are the probability thresholds, and the coefficients $0 \leq \alpha_2 \leq 1$ and $0 \leq \alpha_1 \leq 1$ are equivalent to the confidence levels $(1-\alpha_2)$ and $(1-\alpha_1)$ for the credible intervals CI1 and CI2, respectively. We can show that definitions (4.13) and (4.14) satisfy, $\lim_{N\to\infty} E_N^{(\mathrm{l})} = \lim_{N\to\infty} E_N^{(\mathrm{u})} = \lim_{N\to\infty} E_N^{(\mathrm{ref})}$, and $E_N^{(\mathrm{l})} \leq E_N^{(\mathrm{ref})} \leq E_N^{(\mathrm{u})} \quad \forall N \geq 1$.

More interestingly, we can show that all three credible intervals introduced above for a BSC can be rewritten in a unified form as,

$$E_N^{(\mathrm{u})} = \underset{\tilde{E}_N^{(\mathrm{u})}}{\operatorname{argmin}} \left\{ T_{\tilde{p}_{\mathrm{BSC}}}^{(\mathrm{u})}(\tilde{E}_N^{(\mathrm{u})}) \geq (1-\alpha_2) \right\} \tag{4.15}$$

$$E_N^{(\mathrm{l})} = \underset{\tilde{E}_N^{(\mathrm{l})}}{\operatorname{argmin}} \left\{ T_{\tilde{p}_{\mathrm{BSC}}}^{(\mathrm{l})}(\tilde{E}_N^{(\mathrm{l})}) \geq (1-\alpha_1) \right\} \tag{4.16}$$

where for the credible interval CI1,

$$T_{\tilde{p}_{\mathrm{BSC}}}^{(\mathrm{u})}(E_N^{(\mathrm{u})}) = \frac{I_{1-\tilde{p}_{\mathrm{BSC}}}(N-E_N^{(\mathrm{u})}, E_N^{(\mathrm{u})}+1) - I_{1-\tilde{p}_{\mathrm{BSC}}}(N-E_N^{(\mathrm{ref})}-1, E_N^{(\mathrm{ref})})}{I_{1-\tilde{p}_{\mathrm{BSC}}}(0, N+1) - I_{1-\tilde{p}_{\mathrm{BSC}}}(N-E_N^{(\mathrm{ref})}-1, E_N^{(\mathrm{ref})})}$$

$$T_{\tilde{p}_{\mathrm{BSC}}}^{(\mathrm{l})}(E_N^{(\mathrm{l})}) = \frac{I_{1-\tilde{p}_{\mathrm{BSC}}}(N-E_N^{(\mathrm{ref})}, E_N^{(\mathrm{ref})}+1) - I_{1-\tilde{p}_{\mathrm{BSC}}}(N-E_N^{(\mathrm{l})}-1, E_N^{(\mathrm{l})})}{I_{1-\tilde{p}_{\mathrm{BSC}}}(N-E_N^{(\mathrm{ref})}, E_N^{(\mathrm{ref})}+1) - I_{1-\tilde{p}_{\mathrm{BSC}}}(N-1, 0)}$$

for the credible interval CI2,

$$\begin{aligned} T^{(\mathrm{u})}_{\tilde{p}_{\mathrm{BSC}}}(E_N^{(\mathrm{u})}) &= I_{1-\tilde{p}_{\mathrm{BSC}}}(N - E_N^{(\mathrm{u})}, E_N^{(\mathrm{u})} + 1) \\ T^{(\mathrm{l})}_{\tilde{p}_{\mathrm{BSC}}}(E_N^{(\mathrm{l})}) &= I_{\tilde{p}_{\mathrm{BSC}}}(E_N^{(\mathrm{l})}, N - E_N^{(\mathrm{l})} - 1) \end{aligned}$$

and for the credible interval CI3,

$$\begin{aligned} &T^{(\mathrm{u})}_{\tilde{p}_{\mathrm{BSC}}}(E_N^{(\mathrm{u})}) = \\ &\quad I_{1-\tilde{p}_{\mathrm{BSC}}}(N - E_N^{(\mathrm{u})}, E_N^{(\mathrm{u})} + 1) - \\ &\quad I_{1-\tilde{p}_{\mathrm{BSC}}}(N - E_N^{(\mathrm{u})} - 1, E_N^{(\mathrm{u})}) \\ &\qquad\qquad \text{s.t. } E_N^{(\mathrm{u})} \geq E_N^{(\mathrm{ref})} \\ &T^{(\mathrm{l})}_{\tilde{p}_{\mathrm{BSC}}}(E_N^{(\mathrm{l})}) = \\ &\quad I_{1-\tilde{p}_{\mathrm{BSC}}}(N - E_N^{(\mathrm{l})}, E_N^{(\mathrm{l})} + 1) - \\ &\quad I_{1-\tilde{p}_{\mathrm{BSC}}}(N - E_N^{(\mathrm{l})} - 1, E_N^{(\mathrm{l})}) \\ &\qquad\qquad \text{s.t. } E_N^{(\mathrm{l})} \leq E_N^{(\mathrm{ref})}. \end{aligned}$$

4.3.2 Degree of ergodicity

The estimation error of the credible interval estimate of P_N is related to the width of this interval. For the properly constructed (i.e., consistent) credible interval, the estimation error becomes negligible with the length of the received sequence. The PMF of P_N then converges to its expected value, and the performance is given by the expected BER value. Hence, the width of the credible interval can indicate the level of ergodicity of the received sequence with respect to the instantaneous BER P_N. In other words, the estimation interval width $P_N^{(\mathrm{u})}(\alpha_2) - P_N^{(\mathrm{l})}(\alpha_1)$ of the obtained credible intervals describes the spread of P_N about its expected value $P_\infty = \tilde{p}_{\mathrm{BSC}}$. Correspondingly, we can define the DOE measure of the received sequence of N bits for the instantaneous BER using its estimation interval width. It is desirable that the DOE measure has the following properties.

- For any realization of the random channel parameters, the DOE measure is a non-decreasing and non-negative function of N.
- The DOE definition (i.e., not the DOE value) should be independent from a particular data detector employed in order to facilitate comparison of different

data detectors using the DOE (i.e., a given DOE value is reached for smaller or larger values of N depending on the particular detector considered).

These DOE requirements are satisfied by the following definition.[1]

Definition 1. *The degree of ergodicity of the received sequence of N bits for the instantaneous BER (4.1) is defined as,*

$$\mathrm{DOE}_N(\alpha_2, \alpha_1) = \frac{1}{P_N^{(\mathrm{u})}(\alpha_2) - P_N^{(\mathrm{l})}(\alpha_1)} \tag{4.17}$$

where $\left[P_N^{(\mathrm{l})}(\alpha_1), P_N^{(\mathrm{u})}(\alpha_2)\right]$ is the credible interval estimate of P_N. The normalized DOE measure is defined as,

$$\begin{aligned} \mathrm{NDOE}_N(\alpha_2, \alpha_1) &= \mathrm{E}[P_N]\ \mathrm{DOE}_N(\alpha_2, \alpha_1) \\ &= \frac{\mathrm{E}[P_N]}{P_N^{(\mathrm{u})}(\alpha_2) - P_N^{(\mathrm{l})}(\alpha_1)} \end{aligned}$$

where, for a BSC, $\mathrm{E}[P_N] = P_\infty = \tilde{p}_{\mathrm{BSC}}$.

For any values α_2 and α_1, and for all definitions of the credible interval, we have that, $P_1^{(\mathrm{l})}(\alpha_1) = 0$, $P_1^{(\mathrm{u})}(\alpha_2) = 1$, and $\lim_{N\to\infty} P_N^{(\mathrm{u})}(\alpha_2) - P_N^{(\mathrm{l})}(\alpha_1) = 0$, and thus, $\mathrm{DOE}_N(\alpha_2, \alpha_1) \geq 1$, $\mathrm{NDOE}_N(\alpha_2, \alpha_1) \geq \tilde{p}_{\mathrm{BSC}}$, and $\lim_{N\to\infty} \mathrm{DOE}_N(\alpha_2, \alpha_1) = \lim_{N\to\infty} \mathrm{NDOE}_N(\alpha_2, \alpha_1) = \infty$. Note that we can also consider the mean-square error (MSE) [10, 103], i.e., $\mathrm{MSE}_N = \mathrm{E}[(P_N - \mathrm{E}[P_N])^2] = \mathrm{E}[(P_N - P_\infty)^2]$, to define the DOE measure of a finite length received sequence for the instantaneous BER P_N. In this case, the DOE measure satisfying the above properties is defined as,

$$\mathrm{DOE}_N = \frac{1}{\mathrm{MSE}_N} \geq 0.$$

Finally, another possibility is to define the DOE measure using the Chernoff upper and lower bounds [108].

In practical receivers, the DOE measure is computed from the credible interval estimate of the instantaneous BER which, in turn, requires knowledge of N and $\tilde{p}_{\mathrm{BSC}}$.

[1]Note that the normalized DOE in Definition 1 is an inverse of the difference of the peak values (with a given probability) to the expected value of the instantaneous BER. Such definition is similar to the peak-to-average power ratio (PAPR) measure that is often used to describe the spread of the instantaneous signal power.

In general, the DOE measure can be used to quantify the transition of the detector operating on a finite length received sequence described by the instantaneous BER to an asymptotically large received sequence described by the expected BER. Thus, assuming Definition 1, we can define a minimum length $N^*_{\min}$ of the received sequence to have approximately ergodic[1] properties, so that the time average in (4.1) can be replaced by expectation to describe the detector error rate properties. Particularly, for the received sequence of $N \gg N^*_{\min}$ bits, the BER properties are well described using expectation, and we say that the detector operates in the ergodic zone. On the other hand, for $N \ll N^*_{\min}$, the BER properties of the detector are more accurately described using the interval estimates of the instantaneous BER, and we say that the detector operates in the non-ergodic zone. The DOE can be used to determine the value of $N^*_{\min}$ as follows.

Definition 2. *The detector operates in the ergodic zone if the length of the received sequence* $N \gg N^*_{\min}$ *where*

$$N^*_{\min} = \underset{N}{\operatorname{argmin}} \{\mathrm{DOE}_N \geq \mathrm{DOE}^*\}$$

for a given threshold of ergodicity DOE^* *depending on the particular application requirements and the detector used. On the other hand, if* $N \ll N^*_{\min}$, *the detector operates in the non-ergodic zone.*

4.3.3 DOE measure properties

We investigate properties of the DOE measure assuming three definitions of the credible intervals given above. Propositions here are proved for the case of a BSC, however, we conjecture that all propositions hold for a more general case of memoryless channels. The proposition proofs assume unified expressions of the instantaneous BER bounds (4.15) and (4.16), and exploit the fact that the incomplete beta function $I_{1-p}(\alpha, \beta)$ is a decreasing function of p and α and an increasing function of β.

Proposition 1. *For given* N *and values of the confidence levels* $(1-\alpha_1)$ *and* $(1-\alpha_2)$, *the upper bound* $E_N^{(\mathrm{u})}$ *is a non-decreasing function of* $\tilde{p}_{\mathrm{BSC}}$, *and the lower bound* $E_N^{(\mathrm{l})}$ *is non-increasing if* $\tilde{p}_{\mathrm{BSC}}$ *is decreasing.* ■

[1]Note that the received sequence is exactly ergodic only if its length is approaching infinity.

Proof. Let $E_N^{(\mathrm{u})}$ and $E_N^{(\mathrm{l})}$ be the bounds computed for some value of $\tilde{p}_{\mathrm{BSC}}$. Consider another value of the crossover probability $\tilde{p}^*_{\mathrm{BSC}} \neq \tilde{p}_{\mathrm{BSC}}$ and the corresponding bounds $E_N^{(\mathrm{u}*)}$ and $E_N^{(\mathrm{l}*)}$. In order to obtain approximately the same confidence levels $(1-\alpha_1)$ and $(1-\alpha_2)$ in both cases corresponding to $\tilde{p}_{\mathrm{BSC}}$ and $\tilde{p}^*_{\mathrm{BSC}}$, respectively, we assume the following additional constraints to compute the bounds $E_N^{(\mathrm{u}*)}$ and $E_N^{(\mathrm{l}*)}$, i.e.,

$$\begin{aligned} &\min_{E_N^{(\mathrm{u}*)}} \left| T^{(\mathrm{u})}_{\tilde{p}_{\mathrm{BSC}}}(E_N^{(\mathrm{u})}) - T^{(\mathrm{u})}_{\tilde{p}^*_{\mathrm{BSC}}}(E_N^{(\mathrm{u}*)}) \right| \\ &\min_{E_N^{(\mathrm{l}*)}} \left| T^{(\mathrm{l})}_{\tilde{p}_{\mathrm{BSC}}}(E_N^{(\mathrm{l})}) - T^{(\mathrm{l})}_{\tilde{p}^*_{\mathrm{BSC}}}(E_N^{(\mathrm{l}*)}) \right| \end{aligned} \tag{4.18}$$

where $|\cdot|$ denotes the absolute value. We exploit monotonicity of the function $I_{1-p}(\alpha, \beta)$ to show that the minimization of $E_N^{(\mathrm{u}*)}$ in (4.18) for $\tilde{p}^*_{\mathrm{BSC}} > \tilde{p}_{\mathrm{BSC}}$ is achieved for $E_N^{(\mathrm{u}*)} \geq E_N^{(\mathrm{u})}$. Similarly, we can show that the minimization of $E_N^{(\mathrm{l}*)}$ in (4.18) for $\tilde{p}^*_{\mathrm{BSC}} < \tilde{p}_{\mathrm{BSC}}$ is achieved for $E_N^{(\mathrm{l}*)} \leq E_N^{(\mathrm{l})}$ which completes the proof. ■

We note that the proof of Proposition 1 for the case of the credible interval CI2 is straightforward. However, even though the proof for the case of the credible intervals CI1 and CI3 follows along the same lines, it is much more evolved. The limiting values of the DOE measure for $\tilde{p}_{\mathrm{BSC}} = 1$, $\tilde{p}_{\mathrm{BSC}} = 0$ and $\tilde{p}_{\mathrm{BSC}} = 1/2$ are exploited in the following proposition.

Proposition 2. *For given values of the confidence levels* $(1-\alpha_1)$ *and* $(1-\alpha_2)$*, the DOE measure is a convex function in the crossover probability* $\tilde{p}_{\mathrm{BSC}}$*, such that, for* $\forall N \geq 1$*, the limits,* $\lim_{\tilde{p}_{\mathrm{BSC}} \to 0} \mathrm{DOE}_N = \lim_{\tilde{p}_{\mathrm{BSC}} \to 1} \mathrm{DOE}_N = \infty$*, and* DOE_N *reaches a minimum value for* $\tilde{p}_{\mathrm{BSC}} = 1/2$*.* ■

Proof. As in the proof of Proposition 1, assume again the bounds $E_N^{(\mathrm{u})}$ and $E_N^{(\mathrm{l})}$ computed for some $\tilde{p}_{\mathrm{BSC}}$, and the bounds $E_N^{(\mathrm{u}*)}$ and $E_N^{(\mathrm{l}*)}$ computed for $\tilde{p}^*_{\mathrm{BSC}} = 0.5$ with the additional constraints,

$$\begin{aligned} &\min_{E_N^{(\mathrm{u}*)}} \left| T^{(\mathrm{u})}_{\tilde{p}_{\mathrm{BSC}}}(E_N^{(\mathrm{u})}) - T^{(\mathrm{u})}_{0.5}(E_N^{(\mathrm{u}*)}) \right| \\ &\min_{E_N^{(\mathrm{l}*)}} \left| T^{(\mathrm{l})}_{\tilde{p}_{\mathrm{BSC}}}(E_N^{(\mathrm{l})}) - T^{(\mathrm{l})}_{0.5}(E_N^{(\mathrm{l}*)}) \right| \end{aligned}$$

in order to guarantee approximately the same confidence levels $(1-\alpha_1)$ and $(1-\alpha_2)$ in both cases corresponding to $\tilde{p}_{\mathrm{BSC}}$ and $\tilde{p}^*_{\mathrm{BSC}} = 0.5$, respectively.

Consider first the case when $\tilde{p}_{\text{BSC}} < 0.5$. Recall that the CMF of a binomial random variable X is $B_N(k;\tilde{p}_{\text{BSC}}) = \Pr(X \leq k;\tilde{p}_{\text{BSC}}) = I_{1-\tilde{p}_{\text{BSC}}}(N-k, k+1)$. Then, for $0 \leq k \leq N$, we have that the probability difference $\Pr(X \leq k; 0.5) - \Pr(X \leq k;\tilde{p}_{\text{BSC}})$ is a non-negative increasing function of k, and more importantly, also a non-negative increasing function of $(1-\tilde{p}_{\text{BSC}})$. If $\tilde{p}_{\text{BSC}} = 0.5$, then $0 \leq E_N^{(\text{u})} - E_N^{(\text{l})} \leq 1$ for $\forall N \geq 1$. Since, always, $E_N^{(\text{u}*)} - E_N^{(\text{l}*)} \geq 1$, we can use Proposition 1 to show that, for all three definitions of the credible interval, $E_N^{(\text{u}*)} - E_N^{(\text{l}*)} \geq E_N^{(\text{u})} - E_N^{(\text{l})}$, and thus, $\text{DOE}_N^* > \text{DOE}_N$ for $\forall N \geq 1$; see (4.17). The second part of the proof, for $\tilde{p}_{\text{BSC}} > 0.5$, is obtained using the symmetry of the binomial distribution $B_N(k;\tilde{p}_{\text{BSC}})$ and $B_N(k; 1 - \tilde{p}_{\text{BSC}})$. Particularly, $\Pr(X \leq k;\tilde{p}_{\text{BSC}}) - \Pr(X \leq k; 0.5)$ is a non-negative increasing function of k as well as of $(1 - \tilde{p}_{\text{BSC}})$. The rest of the proof then follows along the same lines as for $\tilde{p}_{\text{BSC}} < 0.5$. Finally, since the DOE measure is a non-decreasing function of $\tilde{p}_{\text{BSC}} > 0.5$ as well as of $\tilde{p}_{\text{BSC}} < 0.5$, the DOE reaches a minimum for $\tilde{p}_{\text{BSC}} = 0.5$. ■

Assume now that the value of the channel crossover probability $\tilde{p}_{\text{BSC}}$ is estimated at the receiver from known pilot symbols. For a finite number of pilot symbols, the estimate $\hat{p}_{\text{BSC}}$ of $\tilde{p}_{\text{BSC}}$ corresponds to the confidence interval $[\hat{p}_{\text{BSC}}^{(l)}, \hat{p}_{\text{BSC}}^{(u)}]$ at some confidence level $(1 - \alpha')$. Consequently, in case of the channel uncertainty at the receiver, we can use Proposition 1 and replace the true value of $\tilde{p}_{\text{BSC}}$ in definitions of the credible intervals CI1, CI2 and CI3 with the boundary confidence interval values $\hat{p}_{\text{BSC}}^{(u)}$ and $\hat{p}_{\text{BSC}}^{(l)}$, respectively. We then obtain a modified credible interval $\tilde{\text{CI}}_N = [\tilde{E}_N^{(\text{l})}, \tilde{E}_N^{(\text{u})}]$ as an estimate of E_N that accounts for the channel uncertainty. We have the following proposition.

Proposition 3. *The channel uncertainty corresponding to the channel estimation error at the receiver reduces the DOE value, and thus, reduces the transition speed of the detector from the non-ergodic to ergodic zone of operation with the number of received bits N.* ■

Proof. The proof readily follows by assuming that $\tilde{p}_{\text{BSC}} \in [\hat{p}_{\text{BSC}}^{(l)}, \hat{p}_{\text{BSC}}^{(u)}]$ with 100% confidence level (i.e., with certainty), and by using Proposition 2 for $\tilde{p}_{\text{BSC}} = \hat{p}_{\text{BSC}}^{(l)}$ and $\tilde{p}_{\text{BSC}} = \hat{p}_{\text{BSC}}^{(u)}$, respectively. ■

Proposition 4. *The optimum (maximum-likelihood) detector achieves the largest DOE value.* ■

Proof. Since, in practice, communication systems operate over a BSC with the crossover probability $\tilde{p}_{\text{BSC}} < 0.5$, and among all data detectors, the output of the maximum-likelihood detector corresponds to an equivalent BSC with the smallest crossover probability $\tilde{p}^{*}_{\text{BSC}} \leq \tilde{p}_{\text{BSC}}$, we can use Proposition 2 to complete the proof. ■

Proposition 4 indicates that the maximum-likelihood detector has the fastest transition from the non-ergodic to ergodic zone of operation during processing of the incoming sequence of received bits.

4.3.4 Numerical examples

We compare three definitions of the credible intervals for the instantaneous BER introduced above using numerical examples. The curves in figures are labeled as $(1 - \alpha_2)/(1 - \alpha_1)$ to denote the chosen confidence levels expressed in percents.

Fig. 4.1 compares the credible intervals CI1, CI2 and CI3 of the instantaneous BER for a BSC with the crossover probability, $\tilde{p}_{\text{BSC}} = P_{\infty} = 10^{-2}$. The discrete sequences of the upper and lower bounds of P_N are shown as continuous functions of N for better clarity. More importantly, we observe that both the upper and lower bounds contain discontinuities. These discontinuities are an artifact of the optimization problem solutions over a finite set of possible instantaneous BER values in our definitions of the credible intervals. Furthermore, the discrete nature of the instantaneous BER also causes the lower bounds $P_N^{(\text{l})}$ to be exactly zero for small-to-medium values of N in all three definitions of the credible intervals considered. However, the credible interval CI2 is more useful than the credible intervals CI1 and CI3 to lower-bound the instantaneous BER for small-to-medium values of N. We also observe from Fig. 4.1 that the width of the credible intervals is increasing with their confidence levels as expected. For the same confidence levels, the credible interval CI2 is the most narrow whereas the credible interval CI3 is the widest. However, since the upper and lower bounds $P_N^{(\text{u})} = E_N^{(\text{u})}/N$ and $P_N^{(\text{l})} = E_N^{(\text{l})}/N$ are defined, so that they converge to $P_{\infty} = \tilde{p}_{\text{BSC}}$ in the limit of large N, the differences between definitions of the credible intervals are diminishing with increasing N.

The proposed DOE measure is studied in Fig. 4.2 and Fig. 4.3. In Fig. 4.2, the

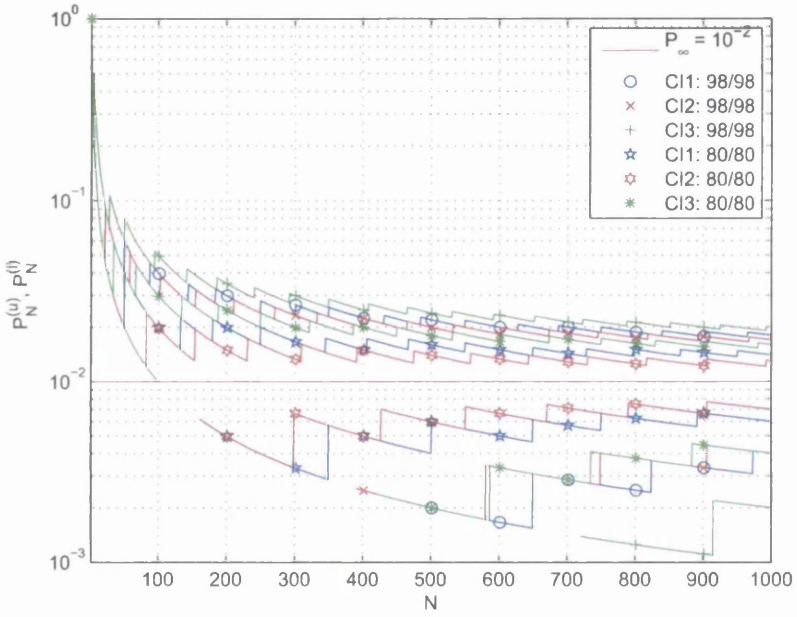

Figure 4.1: The upper and lower bounds of the credible intervals CI1, CI2 and CI3 for the instantaneous BER P_N versus the received sequence length N assuming $P_\infty = \tilde{p}_{\mathrm{BSC}} = 10^{-2}$.

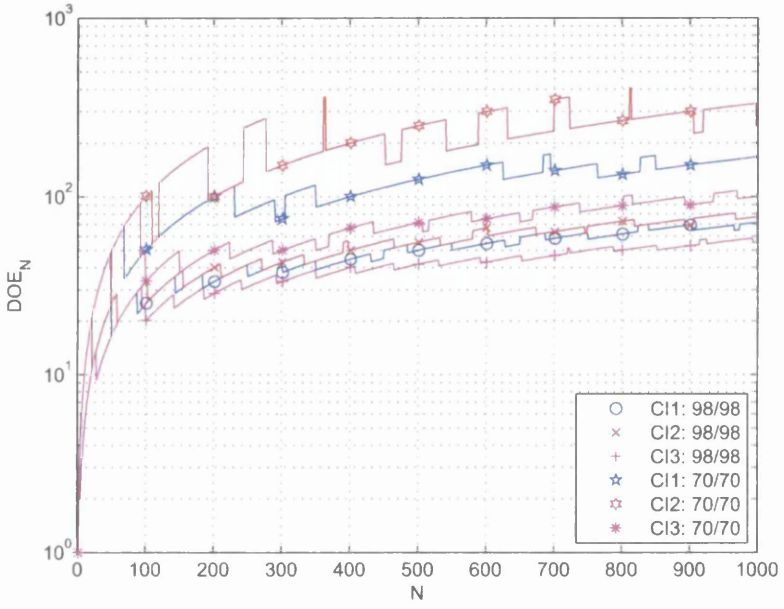

Figure 4.2: The DOE measures corresponding to the credible intervals CI1, CI2 and CI3 versus the received sequence length N assuming $P_\infty = \tilde{p}_{\mathrm{BSC}} = 10^{-2}$.

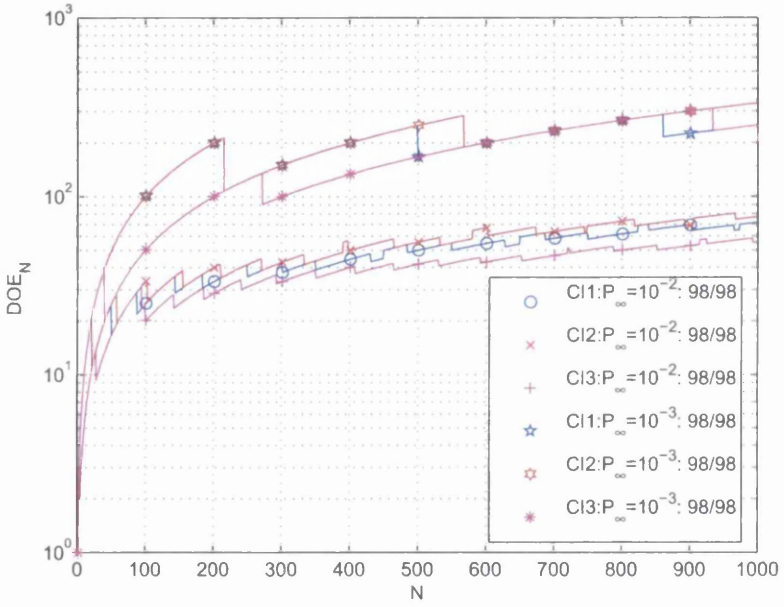

Figure 4.3: The DOE measures corresponding to the credible intervals CI1, CI2 and CI3 versus the received sequence length N assuming the confidence levels $(1-\alpha_1) = (1-\alpha_2) = 98\%$.

DOE curves are shown for $\tilde{p}_{\text{BSC}} = 10^{-2}$ and several values of the confidence levels $(1-\alpha_1) = (1-\alpha_2)$, whereas Fig. 4.3 compares the DOE curves for $P_\infty = \tilde{p}_{\text{BSC}} = 10^{-2}$ and $P_\infty = \tilde{p}_{\text{BSC}} = 10^{-3}$ and the constant values of the confidence levels $(1-\alpha_1) = (1-\alpha_2) = 98\%$. We observe that the DOE curves again contain discontinuities due to the discrete nature of the instantaneous BER. In general, the DOE curves are increasing with N in a sense that, for any integer $N_1 \geq 1$, there exists an integer $N_2 > N_1$ such that, for $\forall N \geq N_2$, $\text{DOE}_N > \text{DOE}_{N_2}$. For given value of $\tilde{p}_{\text{BSC}}$, the DOE values are larger for smaller values of $(1-\alpha_1) = (1-\alpha_2)$. For any $(1-\alpha_1) = (1-\alpha_2)$ and all three definitions of the credible intervals, the DOE values are increasing if the $\tilde{p}_{\text{BSC}}$ value is reduced as proved in Proposition 2. We also observe that the DOE values are larger for the credible interval CI2 than for the credible interval CI1, and the DOE values are larger for the credible interval CI1 than for the credible interval CI3.

We now use the frequentist approach to verify the obtained credible intervals. In particular, for the R simulation trials, we measure the fractions $(1-\alpha_{2R})$ and $(1-\alpha_{1R})$ of the number of cases when the actual instantaneous BER P_N is inside the computed upper and lower credible intervals $(P_N^{(\text{ref})}, P_N^{(\text{u})})$ and $(P_N^{(\text{l})}, P_N^{(\text{ref})})$, respectively. Fig. 4.4 and Fig. 4.5 show the maximum and minimum measured values of $(1-\alpha_{2R})$ and $(1-\alpha_{1R})$ versus the number of simulation trials R for the credible intervals CI1, CI2 and CI3 (from top) assuming the received sequence of $N = 108$ bits and assuming the designed values of the confidence levels $(1-\alpha_1) = (1-\alpha_2) = 90\%$ for computing the credible intervals $(P_N^{(\text{ref})}, P_N^{(\text{u})})$ and $(P_N^{(\text{l})}, P_N^{(\text{ref})})$. We observe that, for $R > 100$, the values of $(1-\alpha_{2R})$ are, in general, larger than $(1-\alpha_2)$ for the credible intervals CI1 and CI3, and smaller than $(1-\alpha_2)$ for the credible interval CI2. On the other hand, the values $(1-\alpha_{1R})$ are larger than $(1-\alpha_1)$ for the credible intervals CI1 and CI3 and smaller than $(1-\alpha_1)$ for the credible interval CI2. Thus and importantly, Fig. 4.4 and Fig. 4.5 indicate that the computed credible intervals of the instantaneous BER have larger (smaller) measured confidence levels than the designed values $(1-\alpha_1)$ and $(1-\alpha_2)$ for the credible intervals CI1 and CI3 (the credible interval CI2). However, the observed differences between $(1-\alpha_{2R})$ and $(1-\alpha_2)$, and $(1-\alpha_{1R})$ and $(1-\alpha_2)$ are small, especially, for the credible intervals CI1 and CI2.

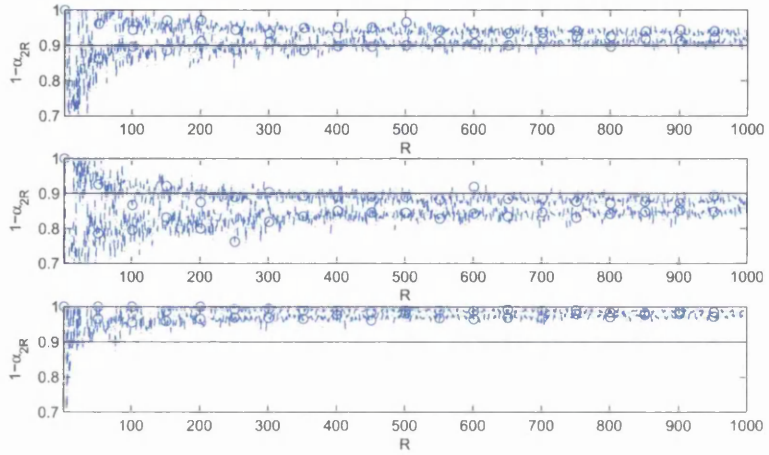

Figure 4.4: The measured upper confidence levels $(1 - \alpha_{2R})$ versus the number of realization R assuming $N = 108$ and $(1 - \alpha_2) = 90\%$.

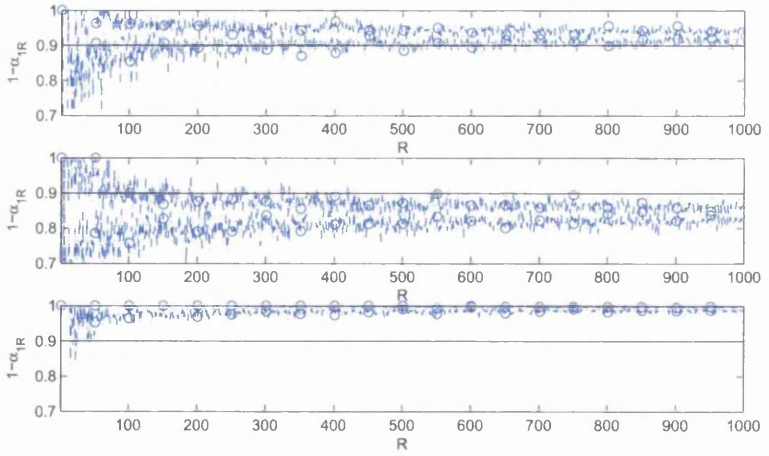

Figure 4.5: The measured lower confidence levels $(1 - \alpha_{1R})$ versus the number of realization R assuming $N = 108$ and $(1 - \alpha_1) = 90\%$.

4.4 Applications of DOE measure

We utilize the credible interval estimators of the instantaneous BER and the proposed DOE measure to control the instantaneous BER performance of the communication link operating in the non-ergodic zone. We assume BPSK signaling over an AWGN channel with hard decisions at the receiver[1]. Assuming knowledge of $\tilde{p}_{\text{BSC}}$ at the transmitter as well as at the receiver, we employ a hypothetical adaptive FEC coding, and then, also the adaptive power control in order to guarantee, with a given probability, and for all transmitted packets, the worst case instantaneous BER performance.

4.4.1 Case I: Adaptive linear block coding

We denote as $(N, K, d_{\min})$ a linear binary block code of length N, dimension K, rate K/N, and the minimum Hamming distance between any two codewords $d_{\min}$. We assume that each transmitted packet corresponds to one codeword of an adaptive linear binary block code. The received packets are decoded, and the instantaneous BER is computed as a fraction of bits in error in the total number of bits received so far in all packets. We consider the following two code design strategies to guarantee the worst case instantaneous BER specified as the error-free transmission with the probability $(1 - \alpha_2)$ after the decoding. In particular, the first strategy varies the code parameters K and $d_{\min}$ for a fixed packet length N. In the second strategy, the code parameters K and N are chosen for a fixed value of $d_{\min}$.

Consider the case of the fixed code block-length first. For a given FEC code, denote as $\tilde{p}^1_{\text{BSC}}$ the expected BER after the decoding corresponding to an infinite number of transmitted packets. Our design goal is to achieve the error-free transmission corresponding to $\tilde{p}^1_{\text{BSC}} = 0$ with the probability $(1 - \alpha_2)$ for *all* the received packets; this guarantees the worst case packet error rate PER $= 1 - \alpha_2$. Hence, for given $\tilde{p}_{\text{BSC}}$ and the chosen confidence level $(1 - \alpha_2)$, and the packet index $i = 1, 2, \ldots$, we compute

[1]Note that the frequency non-selective block fading channel with perfect knowledge of the fading is perceived as an AWGN channel at the receiver, however, for simplicity, here, we assume that the SNR is constant during the whole transmission.

the upper bound $E_{N,i}^{(u)}(\alpha_2)$ of the number of errors $E_{N,i}$ we can expect in the i-th received packet before its decoding. Provided that we set $d_{\min,i} \geq 2(E_{N,i}^{(u)} - E_{N,(i-1)}^{(u)}) + 1$, the FEC code $(N, K_i, d_{\min,i})$ guarantees to correct $(E_{N,i}^{(u)} - E_{N,(i-1)}^{(u)})$ errors in the i-th received packet. Then, given the values of N and $d_{\min,i}$, we choose the code dimension K_i. However, particularly for larger values of $\tilde{p}_{\text{BSC}}$ and N and small desired values of $\tilde{p}_{\text{BSC}}^1$, no such code $(N, K_i, d_{\min,i})$ to correct at least $(E_{N,i}^{(u)} - E_{N,(i-1)}^{(u)})$ errors may exist. In this case, we can reduce $(1 - \alpha_2)$ in order to reduce $(E_{N,i}^{(u)} - E_{N,(i-1)}^{(u)})$, and thus, to reduce the required $d_{\min,i}$ and to relax the constraint on K_i. As a numerical example, assume the upper bound $E_{N,i}^{(u)}$ for the credible interval CI1 with the confidence level $(1 - \alpha_2) = 98\%$, and let the BSC crossover probability be $\tilde{p}_{\text{BSC}} = 10^{-2}$. Table 4.1 shows the required minimum Hamming distances $d_{\min,i} = 2(E_{N,i}^{(u)} - E_{(N,i-1)}^{(u)}) + 1$ for the first 8 received packets. We observe that, for sufficiently large packet index i, the

Table 4.1: Required $d_{\min,i}$ for $\tilde{p}_{\text{BSC}} = 10^{-2}$ and Error-Free Transmission with 98% Probability

Packet i	1	2	3	4	5	6	7	8
$N = 100$	9	5	3	5	5	3	5	3
$N = 200$	13	7	7	7	7	1	5	5
$N = 500$	23	15	1	11	11	11	11	11
$N = 1000$	37	5	21	21	21	21	21	21

required $d_{\min,i}$ converges to a constant. Note also that, in general, larger values of $d_{\min}$ reduce more the channel crossover probability $\tilde{p}_{\text{BSC}}^1$ after the decoding; in turn, the decoder transition from the non-ergodic to ergodic zone of operation is faster as indicated by the increased DOE values.

Alternatively, we can design a linear binary block code $(N_i, K_i, d_{\min})$ with varying values of N_i and K_i and a fixed fixed value of $d_{\min}$ in order to again guarantee the worst case BER performance with a given probability. Thus, given $d_{\min}$ and the packet index $i = 1, 2, \ldots$, we use the upper bound $E_{\sum_i N_i}^{(u)}(\alpha_2)$ to obtain the minimum value of N_i that guarantees the error-free transmission for the i-th received packet with the desired probability $(1 - \alpha_2)$ corresponding to the overall packet error rate $\text{PER} = 1 - \alpha_2$. As a numerical example, Table 4.2 shows the required packet length N_i to obtain the error-free transmission with the probability $(1 - \alpha_2) = 98\%$. We observe that, for

Table 4.2: Required N_i for $\tilde{p}_{\text{BSC}} = 10^{-2}$ and Error-Free Transmission with 98% Probability

Packet i	1	2	3	4	5	6	7	8	9	10
$d_{min} = 5$	22	66	96	117	130	120	136	153	125	985
$d_{min} = 7$	50	134	166	201	199	215	1085	300	300	301
$d_{min} = 11$	144	287	319	1200	501	500	499	500	500	501
$d_{min} = 21$	431	1519	1001	999	1001	1000	999	1000	1000	1000

sufficiently large packet index i, the required value of N_i becomes a constant.

In both code design strategies discussed above, we can also consider a non-zero target crossover probability after the decoding $\tilde{p}^1_{\text{BSC}} > 0$. For example, assuming at most one error in the decoded packet with the probability $(1-\alpha_2)$, the minimum packet length is $N \geq 1/\tilde{p}^1_{\text{BSC}}$ corresponding to PER $\leq \tilde{p}^1_{\text{BSC}}$.

4.4.2 Case II: Transmission power control

We can show that the communication system operating at a certain DOE value over a BSC with the crossover probability $\tilde{p}_{\text{BSC}}$ has, with a certain confidence level (i.e., with a certain probability), the instantaneous BER smaller than $\tilde{p}_{\text{BSC}} + 1/\text{DOE}_N$. Thus, the DOE measure can be used to control the values of the instantaneous BER. In particular, assume transmission of uncoded packets of N_i bits with the transmitter power control of the instantaneous BER. After receiving the packet $i = 1, 2, \ldots$, the transmitter power for the next packet is minimized assuming the received sequence of $\sum_i N_i$ bits to achieve the minimum required value of the DOE. Then, the transmitter powers are decreased for each new transmitted packet until the target transmitted power is reached. However, note that more than one pair of the i-packet length and the transmitter power values can achieve the minimum required DOE.

As a numerical example, assume the credible interval CI1 with the confidence levels $(1 - \alpha_1) = (1 - \alpha_2) = 98\%$, and the target channel crossover probability $\tilde{p}_{\text{BSC}} = 10^{-2}$. Recall that the BSC crossover probability $\tilde{p}_{\text{BSC}} = Q(\sqrt{2\gamma_b})$. Let $N_1 = 100$ bits be the first packet length, and let the target minimum required DOE

be 10^4. Then, we need to obtain the i-th packet length N_i and the packet SNR per bit γ_{bi} to guarantee the worst case instantaneous BER equal to $\tilde{p}_{\text{BSC}} + \frac{1}{10^4}$ with the probability 98%. The minimum required SNR of the first packet to achieve $\text{DOE}_{N_1} \geq 10^4$ is $\gamma_{b1} = 6.1895$dB corresponding to $\tilde{p}_{\text{BSC}} = 10^{-3}$. For the second packet, we set $\gamma_{b2} = 5.6895$ dB and $N_2 = 42$ in order to achieve $\text{DOE}_{142} \geq 10^4$. The minimum required values of γ_{bi} and the corresponding packet length N_i for $i = 1, 2, \ldots, 7$ are summarized in Table 4.3. After the 7-th packet has been received corresponding to 256

Table 4.3: Required γ_{bi} and Packet Length N_i for $\text{DOE}_{\sum_i N_i} \geq 10^4$

Packet i	N_i	γ_{bi} [dB]
1	100	6.1895
2	42	5.6895
3	32	5.2895
4	26	4.7895
5	24	4.6895
6	21	4.3895
7	20	4.2895

received bits in total, an arbitrary packet length and the constant SNR $\gamma_b = 4.2985$dB corresponding to the target $\tilde{p}_{\text{BSC}} = 10^{-2}$ can be used to guarantee that the DOE remains greater than 10^4 for all other received packets.

4.5 Conclusions

Error rate performance measures were investigated for communication systems with non-ergodic transmissions. An equivalent system model for transmission of a single finite length sequence of bits over a BSC was adopted. Such system model was shown to represent the transmission of a finite number of frames employing a properly designed FEC coding over a block fading channel. The instantaneous BER measure was defined for the equivalent system model as a ratio of bits in error to the total number of bits received so far. Since the actual number of bits in error is not known in practical receivers, the credible interval estimators of the instantaneous BER for a single

received sequence of finite length were investigated. The DOE measure was introduced to quantify the level of ergodicity for the instantaneous BER. A threshold value of the DOE was then used to define the non-ergodic and ergodic zones of operation of the data detector processing the sequence of received bits. For the case of a BSC and assuming perfect knowledge of its crossover probability at the receiver, three credible interval estimators of the instantaneous BER were obtained. Several properties of the DOE measure were proved. In particular, it was shown that the channel uncertainty at the receiver reduces ergodicity of the received sequence, so that a longer received sequence is required before the instantaneous BER converges to its expected value. In addition, it was proved that the optimum maximum-likelihood detector has the fastest transition from the non-ergodic to ergodic zone among all data detectors.

The system design implications of the non-ergodic BER analysis presented in this chapter were illustrated using several examples. The design goal was to guarantee a worst case instantaneous BER performance with a given probability. In particular, the parameters of a hypothetical adaptive binary linear block code were obtained for each transmitted packet using an upper bound of the instantaneous BER rather than using the expected BER that is only meaningful for asymptotically large number of transmitted packets. In addition, the adaptive transmitter power was used to control the crossover probability of an equivalent BSC to guarantee the worst case instantaneous BER with a given probability. Consequently, by varying the parameters of a FEC coding, and by varying the transmitter power, it is possible to achieve the transmission ergodicity for a smaller number of transmitted packets.

5

Improving Link Reliability Complexity Trade-off by Exploiting Reliable Feedback Signaling

5.1 Introduction

The reliability of information transmission over unreliable communication links can be achieved by exploiting the transmission diversity. The transmission diversity can be obtained in the time, frequency and spatial domains. For example, the time domain diversity is exploited by by the forward error correction (FEC) coding and the automatic repeat request (ARQ) retransmissions. In the spatial domain, multiple antennas can be deployed at the receiver as well as at the transmitter. More importantly, the diversity signaling requires that the degrees-of-freedom of the communication link are used jointly which may significantly increase the computational as well as implementation complexity of the associated signal processing, particularly at the receiver side.

It is well-known that the feedback link does not improve the information theoretic capacity of the memoryless channels. However, the feedback signaling can greatly simplify the encoding and the decoding complexity [109]. A good example of a scheme with the reduced implementation complexity exploiting the feedback signaling are the ARQ retransmission schemes [8, 110]. On the other hand, the feedback

signaling does increase capacity of the channels with memory [111].

In general, the transmission schemes are optimized to trade-off their reliability (i.e., the error rate), throughput and implementation complexity. For instance, the go-back-N ARQ retransmission scheme is optimized in [112]. A hybrid FEC and ARQ scheme for reliable delivery of control messages is designed in [113]. The type-II hybrid ARQ scheme using a finite receiver buffer and a rate $1/2$ convolutional code over a two state Markov channel is investigated in [114]. The type-II hybrid ARQ scheme with one retransmission and the binary block codes assuming a ideally interleaved Nakagami fading channel is analyzed in [115]. A time diversity scheme utilizing the ARQ with a finite number of retransmissions is considered in [116]. Assuming noisy feedback, a truncated type II hybrid ARQ over block fading channels is considered in [117]. The permutations of bits in the retransmitted packets are used in [118] to improve the transmission reliability of the ARQ schemes assuming a bit-to-symbol mapping for multilevel linear modulations, and in [119] assuming a symbol-to-subcarrier mapping for orthogonal frequency division multiplexing (OFDM). Furthermore, MacKay [120, Ch. 50] notes that: *"The best solution to the communication problem is to combine a simple, pseudo-random code with a message-passing decoder."*

In this chapter, we improve the bit error rate (BER) performance of a point-to-point transmission link by designing a novel retransmission scheme that exploits a finite number of packet retransmissions with the reliable feedback signaling. Unlike the most frequently used conventional ARQ schemes [121], the proposed retransmission scheme does not use any forward error correction (FEC) coding nor it uses the cyclic redundancy check (CRC) bits for error detection. The proposed scheme uses random permutations at the receiver to decide on the particular group of bits to be retransmitted. We note that the proposed scheme resembles a random coding approach described in [120] in that the proposed scheme employs a random selection of bits for the retransmission that are agreed between the transmitter and the receiver. Furthermore, the proposed scheme is designed for a predefined finite number of retransmissions, and thus, achieving the fixed transmission delay, whereas the conventional ARQ schemes typically assume a finite random number of retransmissions until either the CRC in the received packet is satisfied or the maximum number of retransmissions is exhausted.

The proposed scheme also benefits from using more than one bit of feedback per transmitted packet unlike the conventional ARQ schemes that typically use only one bit of feedback per retransmission. Lastly, in our retransmission scheme design, we assume that there exists a reliable reverse link that can deliver feedback error-free messages from the receiver to the transmitter.

The rest of this chapter is organized as follows. System model is presented in Section 5.2. The mathematical theoretic analysis of the proposed scheme is developed in Section 5.3. Practical design examples as well as numerical examples are provided in Section 5.4. Conclusions are given in Section 5.5. Section 5.6 is an appendix for this chapter.

5.2 System model

Consider a point-to-point transmission between a source and a destination that consists of the forward and reverse links as shown in Fig. 5.1. We assume that the communication channel corresponding to the forward link has much larger information theoretic capacity (i.e, the achievable transmission rate) than the communication channel corresponding to the reverse link. More importantly, the transmission rate in the reverse link is assumed to be sufficiently small, so that the feedback signaling from the destination to the source over the reverse link can be considered to be free of the transmission errors. For simplicity, the forward link is modeled as an additive white Gaussian noise

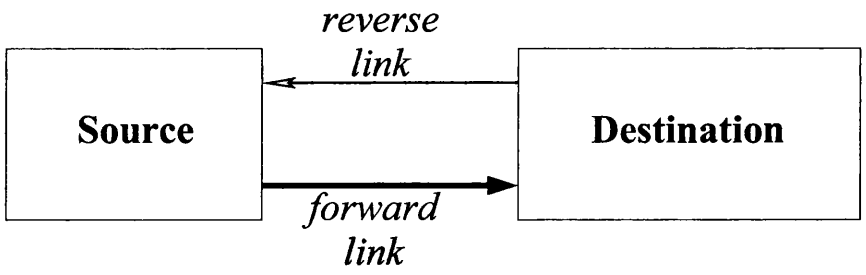

Figure 5.1: A point-to-point communication system.

(AWGN) channel, and the source uses binary phase shift keying (BPSK) modulation for all transmissions. Thus, in this case, the reliabilities (i.e., the log-likelihood ratios) of the bits received at the destination are proportional to the absolute value of the

received BPSK symbols [122]. The signal-to-noise ratio (SNR) per bit is denoted as $\gamma_b = E_b/N_0$ where E_b is the average energy of the transmitted BPSK symbols normalized by the forward (information) rate R_f defined as a fraction of the information bits in the sequence of all transmitted bits, and $N_0 = 2\sigma_w^2$ is the one-sided power spectral density of the AWGN with the variance σ_w^2. Assuming the BPSK symbols '+1' and '-1', the variance, $\sigma_w^2 = (2R_f\gamma_b)^{-1}$. Hence and importantly, note that the bits transmitted over the reverse link are not considered in the normalization of the SNR since the source does not expend any energy on transmitting these feedback bits.

We assume that the source generates packets of N information bits to be transmitted to the destination. After receiving the last of the N BPSK symbols in the packet, the destination receiver uses the received reliabilities to decide which of the W_d binary symbols among the N received, $0 \leq W_d < N$, should be retransmitted, where $d = 0, 1, 2, \ldots, D$ is the retransmission number. Thus, after the first transmission of the packet of N information bits from the source to the destination, $d = 0$.

The retransmission request is a feedback message of $C_d \geq 1$ bits sent to the source from the destination via the reverse (feedback) link. Consequently, after D retransmissions, the total number of bits sent over the forward link to the destination is,

$$N + \sum_{d=0}^{D} W_d = N + P$$

and the total number of bits sent from the destination to the source over the reverse link is,

$$\sum_{d=0}^{D} C_d = Q$$

we assume that $W_0 = C_0 = 0$ bits. For simplicity, we assume $W_1 = W_2 = \ldots = W_D = W$, and, $C_1 = C_2 = \ldots = C_D = C$, and thus, $P = DW$, and $Q = DC$. For example, the conventional stop-and-wait ARQ scheme is described by the parameters, $W = N$ and $C = 1$. The received signals of the retransmitted bits are combined using, for example, maximum ratio combining (MRC) in order to improve their reliabilities. Fig. 5.2 shows the timing (scheduling) of the first transmission and the subsequent retransmissions. In Fig. 5.2, $T_d = K2^{-C_d}$ represents the delay at the destination receiver to evaluate the K random permutations where the integer $K \geq 1$ itself is a random

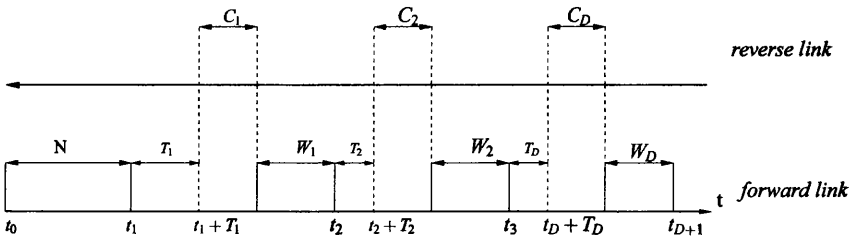

Figure 5.2: The timing of the first transmission and the subsequent retransmissions in the proposed scheme.

variable. We then define the system information rate over the forward link from the source to the destination, and refer to it as the information forward rate, i.e.,

$$R_{\mathrm{f}} = \frac{N}{N+P} = \frac{N}{N+DW}. \tag{5.1}$$

Similarly, we define the reverse information rate,

$$R_{\mathrm{r}} = \frac{DC}{N+P}.$$

Hence, for asymptotically large packets and finite values of D, C and W, the forward rate, $\lim_{N\to\infty} R_{\mathrm{f}} = 1$, and, $\lim_{N\to\infty} R_{\mathrm{r}} = 0$. More importantly, note that the forward rate R_{f} does not include the delays T_d and C_d, and that the the source does not transmit during times T_d and C_d.

Recall that neither FEC coding nor CRC bits are used in the proposed retransmission scheme. Hence, the total number of retransmissions D as well as the retransmission window size W, and thus, also the forward rate R_{f} are assumed to be fixed (i.e., set a priory). It is also possible to terminate the retransmissions, for example, when the reliabilities of all N bits in the packet at the destination are above a specified threshold which requires knowledge of the SNR at the receiver, however, this scenario is not considered in this chapter. Hence, the main design criterion of the proposed retransmission scheme is the average BER that is achieved for given values of N, W and D. Furthermore, the proposed retransmission scheme requires that the source and the destination can generate an identical pseudo-random sequence that is used to obtain the identical random permutations of N bits at the source and at the destination. This can be achieved, for example, if the source and the destination share the same initial

random seed. Furthermore, the source and the destination are assumed to be symbol-time synchronized, so that they can generate the same number of permutations every symbol period. The feedback message is the permutation number within one symbol period, and the proposed retransmission scheme operates as follows.

As soon as the last of the N information bits is transmitted by the source, the destination starts to generate 2^C random permutations of the received N bits during each consecutive symbol period. The purpose of these random permutations is to place the bits with the smallest reliabilities into a predefined window of length W bits; for example, it is convenient to choose the first W bit positions to be such a window. In general, many stopping criteria can be devised to stop the generation of the random permutations, and to request the retransmission of bits corresponding to the permutation that placed most of the low reliability bits into the predefined window. It is straightforward to show that this strategy minimizes the overall BER. However, and importantly, evaluation of the stopping condition to determine whether sufficiently many bits of small reliabilities are located in the predetermined window is non-trivial, and it represents a significant proportion of the implementation (and also simulation) complexity. One possible solution to efficiently evaluate the stopping condition is to order the received bits according to their reliabilities, and then test cardinality of the intersection of the integer sets of the bit indices. Once the desired permutation is found (i.e., the stopping condition is satisfied), the feedback message is the permutation number modulo the number of permutations tested during one symbol period, i.e., modulo 2^C. The choice of the value of C is a design trade-off. On one hand, the larger the value of C the more permutations are tested during one symbol period and the smaller the delay before the feedback message is sent. On the other hand, the smaller values of C reduce the number of the feedback message bits transmitted to the source. The maximum value of C is also practically limited by the real-time computation processing capability available at the destination. Finally, the source counts the number of elapsed symbol periods until the feedback message arrives, and thus, it can deduce the total number of permutations tested at the destination. Knowledge of the permutation number is used to select the W bits from the original N bits to be retransmitted to the destination. At the destination, the retransmitted bits are combined using the MRC, and the combined received values

are scaled, so that the average energy of the BPSK symbols in the received samples is unchanged.

In the next section, we consider three possible choices of the retransmitted window sizes W. We also optimize the number of feedback message bits C to maximize the system throughput assuming $D = 1$ retransmission, and compare the proposed retransmission scheme with the stop-and-wait ARQ.

5.3 Performance analysis

We first obtain the BER of the proposed scheme assuming $D = 1$ and $D = 2$ retransmissions, respectively. We then generalize the obtained BER expressions for the case of $D > 2$ retransmissions.

Denote the transmitted BPSK symbols as $S_1 = \sqrt{E_b}$ and $S_2 = -\sqrt{E_b}$. For the AWGN channel, and omitting the bit indices, the reliability of the received bits is equal to $|\bar{r}|$ where $\bar{r} = r/\sigma_{\mathrm{w}}^2$, r is the received sample, and $|\cdot|$ is the absolute value. With no retransmissions, i.e., for $D = 0$, the conditional probability density function (PDF) of $\bar{r}$ is,

$$\begin{aligned} \mathrm{f}_{\bar{\mathrm{r}}}(\bar{\mathrm{r}}|\mathrm{S}_1, \mathrm{D}=0) &= \frac{1}{2}\sqrt{\frac{N_o}{\pi}}\mathrm{e}^{-\frac{(\bar{r}N_o - 2\sqrt{E_b})^2}{4N_o}} \\ \mathrm{f}_{\bar{\mathrm{r}}}(\bar{\mathrm{r}}|\mathrm{S}_2, \mathrm{D}=0) &= \frac{1}{2}\sqrt{\frac{N_o}{\pi}}\mathrm{e}^{-\frac{(\bar{r}N_o + 2\sqrt{E_b})^2}{4N_o}}. \end{aligned}$$

It is useful to compute the BER of the received bit provided that this received bit has the reliability in the interval, $L_D\sqrt{E_b} \leq |\bar{r}| \leq U_D\sqrt{E_b}$, for some positive constants $U_D \geq L_D \geq 0$. Then, the symbol error event 'e' that S_1 was transmitted, however, S_2 is decided at the receiver occurs provided that, $-U_D\sqrt{E_b} \leq \bar{r} \leq -L_D\sqrt{E_b}$. Assuming no retransmissions, i.e., $D = 0$, the probability of such error event is equal to,

$$\begin{aligned} \Pr(e|S_1, D=0) &= \Pr\left(-U_0\sqrt{E_b} \leq \bar{r} \leq -L_0\sqrt{E_b}\,|S_1\right) \\ &= \int_{-U_0\sqrt{E_b}}^{-L_0\sqrt{E_b}} \mathrm{f}_{\bar{\mathrm{r}}}(\bar{\mathrm{r}}|\mathrm{S}_1, \mathrm{D}=0)\,\mathrm{d}\bar{r} \\ &= \mathrm{Q}\left(\sqrt{2\gamma_{\mathrm{b}}}\left(\frac{L_0N_o}{2}+1\right)\right) - \mathrm{Q}\left(\sqrt{2\gamma_{\mathrm{b}}}\left(\frac{U_0N_o}{2}+1\right)\right) \end{aligned}$$

and due to the symmetry, we have that $\Pr(e|S_1, D=0) = \Pr(e|S_2, D=0)$. Assuming that the a priori probabilities, $\Pr(S_1) = \Pr(S_2) = 1/2$, the overall average BER, $\Pr(e) = \Pr(e|S_1) = \Pr(e|S_2)$. In our proposed retransmission scheme, we assume $L_0 = 0$, so that the average BER after $D = 0$ retransmissions is,

$$\mathrm{BER}_0 = \mathrm{Q}\left(\sqrt{2\gamma_\mathrm{b}}\right) - \mathrm{Q}\left(\sqrt{2\gamma_\mathrm{b}}\left(\frac{U_0 N_o}{2} + 1\right)\right). \tag{5.2}$$

Note that, for $U_0 \to \infty$, the BER expression (5.2) corresponds to the BER of uncoded BPSK over an AWGN channel, i.e., $\mathrm{BER} = \mathrm{Q}\left(\sqrt{2\gamma_\mathrm{b}}\right)$. The probability that the reliability of the received bit is in the interval, $L_D\sqrt{E_b} \le |\bar{r}| \le U_D\sqrt{E_b}$, conditioned on S_1 being transmitted, and for $D = 0$ retransmissions, is computed as,

$$\begin{aligned}
\mathrm{P}_{0|S_1} &= \Pr\left(L_0\sqrt{E_b} \le |\bar{r}| \le U_0\sqrt{E_b}\,\middle|\,S_1\right) \\
&= \int_{-U_0\sqrt{E_b}}^{-L_0\sqrt{E_b}} \mathrm{f}_{\bar{\mathrm{r}}}(\bar{\mathrm{r}}|\mathrm{S}_1, \mathrm{D}=0)\,\mathrm{d}\bar{r} + \int_{L_0\sqrt{E_b}}^{U_0\sqrt{E_b}} \mathrm{f}_{\bar{\mathrm{r}}}(\bar{\mathrm{r}}|\mathrm{S}_1, \mathrm{D}=0)\,\mathrm{d}\bar{r} \\
&= \mathrm{Q}\left(\sqrt{2\gamma_\mathrm{b}}\left(\frac{L_0 N_o}{2} + 1\right)\right) - \mathrm{Q}\left(\sqrt{2\gamma_\mathrm{b}}\left(\frac{U_0 N_o}{2} + 1\right)\right) + \\
&\quad \mathrm{Q}\left(\sqrt{2\gamma_\mathrm{b}}\left(\frac{L_0 N_o}{2} - 1\right)\right) - \mathrm{Q}\left(\sqrt{2\gamma_\mathrm{b}}\left(\frac{U_0 N_o}{2} - 1\right)\right).
\end{aligned}$$

For $L_0 = 0$, this probability is equal to,

$$\mathrm{P}_0 = 1 - \mathrm{Q}\left(\sqrt{2\gamma_\mathrm{b}}\left(\frac{U_0 N_o}{2} + 1\right)\right) - \mathrm{Q}\left(\sqrt{2\gamma_\mathrm{b}}\left(\frac{U_0 N_o}{2} - 1\right)\right) \tag{5.3}$$

and $\mathrm{P}_0 \to 1$ for $U_0 \to \infty$. The probability P_0 also represents a fraction of bits among the N received bits that have the reliabilities in the interval, $0 \le |\bar{r}| \le U_0\sqrt{E_b}$, and thus, we can write, $\mathrm{P}_0 = \mathrm{E}[Z/N] = \bar{Z}/N$ where Z is the random number of such bits in the packet of N received bits having the expected value $\bar{Z} = \mathrm{E}[Z]$. In our proposed retransmission scheme, we use the expected value $\mathrm{E}[Z]$ to obtain the retransmission window size W. Consequently, the probability P_0 is equal to the normalized expected window size $\mathrm{E}[Z]/N$.

In general, for $D \ge 1$ retransmissions, the MRC output signal of any received sample within the packet of N bits can be written as,

$$\bar{r}_{\mathrm{MRC}} = \frac{1}{D+1}\sum_{d=0}^{D} \bar{r}_d$$

where we denoted as $\bar{r}_d$ the received sample in the d-th retransmission. Recall also, that we assume $L_d = 0$ for $\forall d \geq 0$, and, without loss of generality, we assume that the sequences of N symbols S_1 is transmitted.

5.3.1 BER for one retransmission

After the first transmission of N bits, only those bits that have the reliabilities in the interval $0 \leq |\bar{r}| \leq U_0\sqrt{E_b}$ are requested for retransmission. The retransmitted window size is assumed to be $W_1 = \lceil N\mathrm{P}_0 \rfloor$ where $\lceil \cdot \rfloor$ denotes the round function, and the probability P_0 is computed in (5.3). After this retransmission, the samples of the retransmitted bits are combined using the MRC, i.e.,

$$\bar{r}_{\mathrm{MRC}} = \begin{cases} \frac{1}{2}(\bar{r}_0 + \bar{r}_1) & \text{for} \quad |\bar{r}_0| \leq U_0\sqrt{E_b} \\ \bar{r}_0 & \text{for} \quad |\bar{r}_0| > U_0\sqrt{E_b}. \end{cases}$$

Note that $\bar{r}_0$ is a truncated random variable corresponding to the PDF, $\mathrm{f}_{\bar{\mathrm{r}}}(\bar{\mathrm{r}}|\mathrm{S}_1, \mathrm{D} = 0)$, with the support limited to $|\bar{r}| \leq U_0\sqrt{E_b}$, whereas $\bar{r}_1$ has the PDF, $\mathrm{f}_{\bar{\mathrm{r}}}(\bar{\mathrm{r}}|\mathrm{S}_1, \mathrm{d} = 0)$. Since the random received samples $\bar{r}_0$ and $\bar{r}_1$ are statistically independent, the PDF of $\bar{r}_{\mathrm{MRC}}$ is given by the convolution (denoted as $\otimes$), i.e.,

$$\mathrm{f}_{\bar{\mathrm{r}}_{\mathrm{MRC}}}(\bar{\mathrm{r}}|\mathrm{S}_1, \mathrm{D} = 1) = \frac{\mathrm{f}_{\bar{\mathrm{r}}}(\bar{\mathrm{r}}|\mathrm{S}_1, \mathrm{d} = 0)\phi_1(\bar{r}, U_0\sqrt{E_b})}{\Pr\left(|\bar{r}_0| \leq U_0\sqrt{E_b}\,|S_1, D = 0\right)} \otimes \mathrm{f}_{\bar{\mathrm{r}}}(\bar{\mathrm{r}}|\mathrm{S}_1, \mathrm{d} = 0)$$

where

$$\phi_1(\bar{r}, U_0\sqrt{E_b}) = \eta(\bar{r} + U_0\sqrt{E_b})\left(1 - \eta(\bar{r} - U_0\sqrt{E_b})\right)$$

and $\eta(\bar{r})$ is the unit-step function, i.e., $\eta(\bar{r}) = 1$ if $\bar{r} \geq 0$, and 0 otherwise. After some manipulations, the PDF of $\bar{r}_{\mathrm{MRC}}$ can be written as,

$$\mathrm{f}_{\bar{\mathrm{r}}_{\mathrm{MRC}}}(\bar{\mathrm{r}}|\mathrm{S}_1, \mathrm{D} = 1) = \frac{\chi_1(\bar{r}, U_0\sqrt{E_b})}{\Pr\left(|\bar{r}_0| \leq U_0\sqrt{E_b}\,|S_1, D = 0\right)}$$

where we defined the function,

$$\begin{aligned} \chi_d(\bar{r}, U_0\sqrt{E_b}) \;=\; & \frac{1}{4}\sqrt{\frac{(d+1)N_o}{\pi}}\mathrm{e}^{-\frac{\left(\bar{r}-2\sqrt{\frac{E_b}{N_o}}\right)^2}{\frac{4}{(d+1)N_o}}} \\ & \times \left\{ \mathrm{erf}\left(\sqrt{\frac{(d+1)N_o}{4d}}(U_0\sqrt{E_b} - \bar{r})\right) \right. \\ & \left. +\mathrm{erf}\left(\sqrt{\frac{(d+1)N_o}{4d}}(U_0\sqrt{E_b} + \bar{r})\right) \right\} \end{aligned}$$

and $\mathrm{erf}(\cdot)$ is the error function [8].

The overall BER_1 for case of $D = 1$ retransmission, assuming that all the bits with the reliabilities $|\bar{r}_0| \leq U_0\sqrt{E_b}$ are retransmitted, and then combined using the MRC, is computed as [8],

$$\begin{aligned}\mathrm{BER}_1 &= \Pr(e|d=0,S_1)\Pr(d=0|S_1) + \Pr(e|d=1,S_1)\Pr(d=1|S_1) \\ &= \int_{-\infty}^{-U_0\sqrt{E_b}} \mathrm{f}_{\bar{\mathrm{r}}}(\bar{\mathrm{r}}|\mathrm{S}_1,\mathrm{d}=0)\,\mathrm{d}\bar{r} + \int_{-\infty}^{0} \chi_1(\bar{r}, U_0\sqrt{E_b})\,\mathrm{d}\bar{r}\end{aligned}$$

since for no-retransmissions, $\Pr(d=0|S_1) = 1$, and
$\Pr(d=1|S_1) = \Pr\left(|\bar{r}_0| \leq U_0\sqrt{E_b}\,|S_1, d=0\right)$ where $\Pr(D|S_1)$ are the conditional probabilities that a particular bit is retransmitted D times. In the appendix 5.6, we show that BER_1 can be evaluated using the approximation,

$$\begin{aligned}\mathrm{BER}_1 \approx\ & \mathrm{Q}\left(\sqrt{2\gamma_\mathrm{b}}\left(\frac{U_0\sqrt{E_b}}{2}+1\right)\right) + \mathrm{Q}\left(\sqrt{4\gamma_\mathrm{b}}\right) - \sum_{k=1}^{t}\frac{A_k}{\sqrt{1+2B_k}} \times \\ & \times\left\{\mathrm{e}^{-\alpha^-_{k,1}(U_0)\gamma_\mathrm{b}}\mathrm{Q}\left(\beta^+_{k,1}(U_0)\sqrt{\gamma_\mathrm{b}}\right) + \mathrm{e}^{-\alpha^+_{k,1}(U_0)\gamma_\mathrm{b}}\mathrm{Q}\left(\beta^-_{k,1}(U_0)\sqrt{\gamma_\mathrm{b}}\right)\right\}\end{aligned}$$

where the coefficients A_k and B_k, for $t = 2$, are given in the appendix 5.6, and the functions,

$$\alpha^-_{k,d}(U) = \frac{B_k(d+1)(2-UN_o)^2}{2d(1+\frac{2B_k}{d})} \qquad \alpha^+_{k,d}(U) = \frac{B_k(d+1)(2+UN_o)^2}{2d(1+\frac{2B_k}{d})}$$

$$\beta^-_{k,d}(U) = \frac{1-\frac{B_kUN_o}{d}}{\sqrt{\frac{1+\frac{2B_k}{d}}{2(d+1)}}} \qquad \beta^+_{k,d}(U) = \frac{1+\frac{B_kUN_o}{d}}{\sqrt{\frac{1+\frac{2B_k}{d}}{2(d+1)}}}.$$

5.3.2 BER for two retransmissions

Consider now the case of two retransmissions. After the second retransmission, the received bits having the reliabilities $|\bar{r}| \leq U_1\sqrt{E_b}$ are combined with the retransmitted samples $\bar{r}_2$. The threshold value U_1 can be chosen to be greater than U_0 due to improvement of the bits reliabilities after the first retransmission. More generally, we can assume that,

$$U_{D-1} \geq U_{D-2} \ldots \geq U_0.$$

Thus, the received bits having the reliabilities $|\bar{r}_0| \leq U_0\sqrt{E_b}$ are combined with two other retransmissions whereas the received bits with the reliabilities in the interval $U_0\sqrt{E_b} < |\bar{r}_0| \leq U_1\sqrt{E_b}$ are combined with one retransmission only. The received signals after two retransmissions can be then written as,

$$\bar{r}_{\mathrm{MRC}} = \begin{cases} \frac{1}{3}(\bar{r}_0 + \bar{r}_1 + \bar{r}_2) & \text{for} \quad |\bar{r}_0| \leq U_0\sqrt{E_b} \\ \frac{1}{2}(\bar{r}_0 + \bar{r}_2) & \text{for} \quad U_0\sqrt{E_b} < |\bar{r}_0| \leq U_1\sqrt{E_b} \\ \bar{r}_0 & \text{for} \quad |\bar{r}_0| > U_1\sqrt{E_b}. \end{cases}$$

The PDF $\mathrm{f}_{\bar{\mathrm{r}}_{\mathrm{MRC}}}(\bar{\mathrm{r}}|\mathrm{S}_1, \mathrm{D} = 2)$ of $\bar{r}_{\mathrm{MRC}}$, for $|\bar{r}| \leq U_0\sqrt{E_b}$, is given as,

$$\mathrm{f}_{\bar{\mathrm{r}}_{\mathrm{MRC}}}(\bar{\mathrm{r}}|\mathrm{S}_1, \mathrm{d} = 2) = \frac{\chi_2(\bar{r}, U_0\sqrt{E_b})}{\Pr\left(|\bar{r}_0| \leq U_0\sqrt{E_b}\,|S_1, d = 0\right)}$$

for $U_0\sqrt{E_b} < |\bar{r}_0| \leq U_1\sqrt{E_b}$, it is given as,

$$\mathrm{f}_{\bar{\mathrm{r}}_{\mathrm{MRC}}}(\bar{\mathrm{r}}|\mathrm{S}_1, \mathrm{d} = 2) = \frac{\lambda_1(\bar{r}, U_1\sqrt{E_b}, U_0\sqrt{E_b})}{\Pr\left(U_0\sqrt{E_b} < |\bar{r}_0| \leq U_1\sqrt{E_b}\,|S_1, d = 0\right)}$$

where

$$\lambda_d(\bar{r}, U_d\sqrt{E_b}, U_{d-1}\sqrt{E_b}) = \tfrac{1}{4}\sqrt{\tfrac{(d+1)N_o}{\pi}}\mathrm{e}^{-\frac{\left(\bar{r}-2\sqrt{\frac{\gamma_b}{N_o}}\right)^2}{\frac{4}{(d+1)N_o}}}\left\{\mathrm{erf}\left(\sqrt{\tfrac{(d+1)N_o}{4d}}(U_d\sqrt{E_b} + \bar{r})\right)\right.$$
$$+\mathrm{erf}\left(\sqrt{\tfrac{(d+1)N_o}{4d}}(U_d\sqrt{E_b} - \bar{r})\right) - \mathrm{erf}\left(\sqrt{\tfrac{(d+1)N_o}{4d}}(U_{d-1}\sqrt{E_b} + \bar{r})\right)$$
$$\left.-\mathrm{erf}\left(\sqrt{\tfrac{(d+1)N_o}{4d}}(U_{d-1}\sqrt{E_b} - \bar{r})\right)\right\}$$

and, finally, for $|\bar{r}_0| > U_1\sqrt{E_b}$, the PDF $\mathrm{f}_{\bar{\mathrm{r}}_{\mathrm{MRC}}}(\bar{\mathrm{r}}|\mathrm{S}_1, \mathrm{d} = 2)$ is given by the PDF $\mathrm{f}_{\bar{\mathrm{r}}}(\bar{\mathrm{r}}|\mathrm{S}_1, \mathrm{d} = 0)$.

The overall BER_2 is obtained using a law of the total probability, i.e.,

$$\begin{aligned} \mathrm{BER}_2 &= \sum_{d=0}^{2} \Pr(e|d, S_1)\Pr(d|S_1) \\ &= \int_{-\infty}^{-U_1\sqrt{E_b}} \mathrm{f}_{\bar{\mathrm{r}}}(\bar{\mathrm{r}}|\mathrm{S}_1, \mathrm{D} = 0)\,\mathrm{d}\bar{r} + \int_{-\infty}^{0} \lambda_1(\bar{r}, U_1\sqrt{E_b}, U_0\sqrt{E_b})\,\mathrm{d}\bar{r} \\ &\quad + \int_{-\infty}^{0} \chi_2(\bar{r}, U_0\sqrt{E_b})\,\mathrm{d}\bar{r} \end{aligned}$$

where the probability of the second retransmission of a bit is, $\Pr(d=2|S_1) = \Pr\left(\bar{r} \leq -U_1\sqrt{E_b}\,|S_1, d=1\right)$. Similarly to the one retransmission case, BER_2 can be approximated as,

$$\begin{aligned}
\mathrm{BER}_2 \approx\ & \mathrm{Q}\left(\sqrt{2\gamma_\mathrm{b}}(\frac{U_1N_o}{2}+1)\right) + \mathrm{Q}\left(\sqrt{6\gamma_\mathrm{b}}\right) - \sum_{k=1}^{t}\frac{A_k}{\sqrt{1+B_k}} \times \\
& \times\left\{\mathrm{e}^{-\alpha^-_{k,2}(U_0)\gamma_\mathrm{b}}\mathrm{Q}\left(\beta^+_{k,2}(U_0)\sqrt{\gamma_\mathrm{b}}\right) + \mathrm{e}^{-\alpha^+_{k,2}(U_0)\gamma_\mathrm{b}}\mathrm{Q}\left(\beta^-_{k,2}(U_0)\sqrt{\gamma_\mathrm{b}}\right)\right\} \\
& + \sum_{t=1}^{t}\frac{A_k}{\sqrt{1+2B_k}}\Bigg\{\mathrm{e}^{-\alpha^-_{k,1}(U_0)\gamma_\mathrm{b}}\mathrm{Q}\left(\beta^+_{k,1}(U_0)\sqrt{\gamma_\mathrm{b}}\right) \\
& + \mathrm{e}^{-\alpha^+_{k,1}(U_0)\gamma_\mathrm{b}}\mathrm{Q}\left(\beta^-_{k,1}(U_0)\sqrt{\gamma_\mathrm{b}}\right) - \mathrm{e}^{-\alpha^-_{k,1}(U_1)\gamma_\mathrm{b}}\mathrm{Q}\left(\beta^+_{k,1}(U_1)\sqrt{\gamma_\mathrm{b}}\right) \\
& - \mathrm{e}^{-\alpha^+_{k,1}(U_1)\gamma_\mathrm{b}}\mathrm{Q}\left(\beta^-_{k,1}(U_1)\sqrt{\gamma_\mathrm{b}}\right)\Bigg\}.
\end{aligned}$$

The retransmission window size after the first retransmission is determined as, $W_2 = \lceil N\mathrm{P}_1\rfloor$, where the probability,

$$\begin{aligned}
\mathrm{P}_1 =\ & \Pr\left(|\bar{r}| \leq U_1\sqrt{E_b}\,|S_1, d=0\right)\Pr(d=0|S_1) \\
& + \Pr\left(|\bar{r}| \leq U_1\sqrt{E_b}\,|S_1, d=1\right)\Pr(d=1|S_1) \\
=\ & \int_{-U_1\sqrt{E_b}}^{U_1\sqrt{E_b}} \mathrm{f}_{\bar{\mathrm{r}}}(\bar{\mathrm{r}}|\mathrm{S}_1, \mathrm{D}=0)\,\mathrm{d}\bar{r} - \int_{-U_0\sqrt{E_b}}^{U_0\sqrt{E_b}} \mathrm{f}_{\bar{\mathrm{r}}}(\bar{\mathrm{r}}|\mathrm{S}_1, \mathrm{D}=0)\,\mathrm{d}\bar{r} + \int_{-U_1\sqrt{E_b}}^{U_1\sqrt{E_b}} \chi_1(\bar{r}, U_0)\,\mathrm{d}\bar{r}
\end{aligned}$$

can be efficiently computed using the approximation,

$$\begin{aligned}
\mathrm{P}_1 \approx\ & \mathrm{Q}\left(\sqrt{2\gamma_\mathrm{b}}(\frac{U_0N_o}{2}+1)\right) + \mathrm{Q}\left(\sqrt{2\gamma_\mathrm{b}}(\frac{U_0N_o}{2}-1)\right) - \mathrm{Q}\left(\sqrt{2\gamma_\mathrm{b}}(\frac{U_1N_o}{2}+1)\right) \\
& - \mathrm{Q}\left(\sqrt{2\gamma_\mathrm{b}}(\frac{U_1N_o}{2}-1)\right) + \mathrm{Q}((2-U_1N_o)\sqrt{\gamma_\mathrm{b}}) - \mathrm{Q}((2+U_1N_o)\sqrt{\gamma_\mathrm{b}}) \\
& - \sum_{k=1}^{t}\frac{A_k}{2\sqrt{1+2B_k}}\Bigg\{\mathrm{e}^{-\alpha^+_{k,1}(U_0)\gamma_\mathrm{b}}\left\{\mathrm{erf}\left(\theta^{+-}_{k,1}(U_0)\sqrt{\gamma_\mathrm{b}}\right) + \mathrm{erf}\left(\theta^{-+}_{k,1}(U_0)\sqrt{\gamma_\mathrm{b}}\right)\right\} \\
& + \mathrm{e}^{-\alpha^-_{k,1}(U_0)\gamma_\mathrm{b}}\left\{\mathrm{erf}\left(\theta^{++}_{k,1}(U_0)\sqrt{\gamma_\mathrm{b}}\right) + \mathrm{sign}(\mu(U_0)\sqrt{\gamma_\mathrm{b}})\,\mathrm{erf}\left(\theta^{--}_{k,1}(U_0)\sqrt{\gamma_\mathrm{b}}\right)\right\}\Bigg\}
\end{aligned}$$

where

$$\theta^{+-}_{k,d}(U) = \frac{\frac{U_d\sqrt{N_o}}{2} + \frac{1}{\sqrt{N_o}} + \frac{B_k\sqrt{N_o}(U_d-U)}{d}}{\frac{1+\frac{2B_k}{d}}{(d+1)N_o}} \qquad \theta^{-+}_{k,d}(U) = \frac{\frac{U_d\sqrt{N_o}}{2} - \frac{1}{\sqrt{N_o}} + \frac{B_k\sqrt{N_o}(U_d+U)}{d}}{\frac{1+\frac{2B_k}{d}}{(d+1)N_o}}$$

$$\theta_{k,d}^{++}(U) = \frac{\frac{U_d\sqrt{N_o}}{2} + \frac{1}{\sqrt{N_o}} + \frac{B_k\sqrt{N_o}(U_d+U)}{d}}{\frac{1+\frac{2B_k}{d}}{(d+1)N_o}} \qquad \theta_{k,d}^{--}(U) = \frac{|\mu(U)|}{2}\sqrt{(d+1)N_o(1+\frac{2B_k}{d})}$$

$$\mu(U) = U_D\sqrt{N_o} - \frac{\frac{2}{\sqrt{N_o}} + 2B_kU\sqrt{N_o}}{1+2B_k}$$

and $\mathrm{sign}(\cdot)$ is the sign function.

5.3.3 BER for D retransmissions

For the $D \geq 1$ retransmissions, the overall BER is calculated as,

$$\mathrm{BER}_D = \sum_{d=0}^{D} \Pr(e|d, S_1) \Pr(d|S_1).$$

In the proposed retransmission scheme, the received bits with the reliabilities in the interval $|\bar{r}| \leq U_0\sqrt{E_b}$ will be retransmitted D times, the bits with the reliabilities in the interval $U_0\sqrt{E_b} < |\bar{r}| \leq U_1\sqrt{E_b}$ will be retransmitted $D-1$ times and so on. The number of received copies for each reliability range after the D retransmissions is shown in Fig. 5.3. Consequently, the overall BER can be expressed using the functions

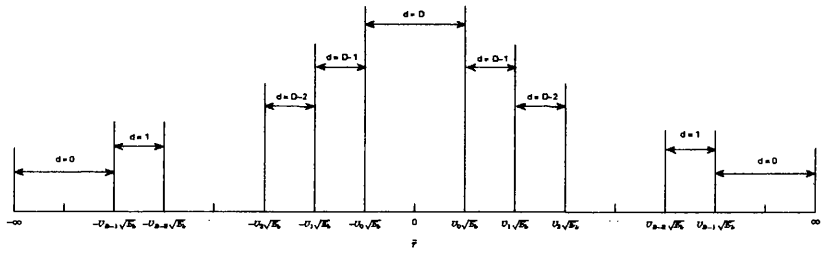

Figure 5.3: The number of the received packet copies after D retransmissions for each reliability range.

$\chi_D(\bar{r}, U_{D-1}\sqrt{E_b})$ and $\lambda_D(\bar{r}, U_D\sqrt{E_b}, U_{D-1}\sqrt{E_b})$ as,

$$\begin{aligned}\mathrm{BER}_D = &\int_{-\infty}^{-U_{D-1}\sqrt{E_b}} \mathrm{f}_{\bar{\mathrm{r}}}(\bar{\mathrm{r}}|\mathrm{S}_1, \mathrm{D}=0)\,\mathrm{d}\bar{r} + \sum_{i=1}^{D-1}\int_{-\infty}^{0} \lambda_i(\bar{r}, U_{D-i}\sqrt{E_b}, U_{D-i-1}\sqrt{E_b})\,\mathrm{d}\bar{r} \\ &+ \int_{-\infty}^{0} \chi_D(\bar{r}, U_0\sqrt{E_b})\,\mathrm{d}\bar{r} \end{aligned} \tag{5.4}$$

where the middle term is zero for $D = 1$ retransmission. The BER (5.4) can be approximated as,

$$\begin{aligned}\mathrm{BER}_D \approx & \mathrm{Q}\left(\sqrt{2\gamma_\mathrm{b}}\left(\frac{U_{D-1}N_o}{2}+1\right)\right)+\mathrm{Q}\left(\sqrt{2\gamma_\mathrm{b}(D+1)}\right)-\sum_{k=1}^{t}\frac{A_k}{\sqrt{1+\frac{2B_k}{D}}}\times \\ & \times\left\{\mathrm{e}^{-\alpha^-_{k,D}(U_0)\gamma_\mathrm{b}}\mathrm{Q}\left(\beta^+_{k,D}\left(U_0\right)\sqrt{\gamma_\mathrm{b}}\right)+\mathrm{e}^{-\alpha^+_{k,D}(U_0)\gamma_\mathrm{b}}\mathrm{Q}\left(\beta^-_{k,D}\left(U_0\right)\sqrt{\gamma_\mathrm{b}}\right)\right\} \\ & +\sum_{i=1}^{D-1}\sum_{k=1}^{t}\frac{A_k}{\sqrt{1+\frac{2B_k}{i}}}\Big\{\mathrm{e}^{-\alpha^-_{k,i}(U_{D-i-1})\gamma_\mathrm{b}}\mathrm{Q}\left(\beta^+_{k,i}\left(U_{D-i-1}\right)\sqrt{\gamma_\mathrm{b}}\right) \\ & +\mathrm{e}^{-\alpha^+_{k,i}(U_{D-i-1})\gamma_\mathrm{b}}\mathrm{Q}\left(\beta^-_{k,i}\left(U_{D-i-1}\right)\sqrt{\gamma_\mathrm{b}}\right)-\mathrm{e}^{-\alpha^-_{k,i}(U_{D-i})\gamma_\mathrm{b}}\mathrm{Q}\left(\beta^+_{k,i}\left(U_{D-i}\right)\sqrt{\gamma_\mathrm{b}}\right) \\ & -\mathrm{e}^{-\alpha^+_{k,i}(U_{D-i})\gamma_\mathrm{b}}\mathrm{Q}\left(\beta^-_{k,i}\left(U_{D-i}\right)\sqrt{\gamma_\mathrm{b}}\right)\Big\}.\end{aligned}$$

The probability P_D to calculate the retransmission window size $W_D = \lceil N\mathrm{P}_D \rfloor$ is computed as,

$$\begin{aligned}\mathrm{P}_D = & \int_{-U_D\sqrt{E_b}}^{U_D\sqrt{E_b}}\mathrm{f}_{\bar{\mathrm{r}}}(\bar{\mathrm{r}}|\mathrm{S}_1,\mathrm{D}=0)\,\mathrm{d}\bar{r}-\int_{-U_0\sqrt{E_b}}^{U_0\sqrt{E_b}}\mathrm{f}_{\bar{\mathrm{r}}}(\bar{\mathrm{r}}|\mathrm{S}_1,\mathrm{D}=0)\,\mathrm{d}\bar{r} \\ & +\sum_{i=1}^{D-1}\int_{-U_D\sqrt{E_b}}^{U_D\sqrt{E_b}}\lambda_i(\bar{r},U_{D-i}\sqrt{E_b},U_{D-i-1}\sqrt{E_b})\,\mathrm{d}\bar{r}+\int_{-U_D\sqrt{E_b}}^{U_D\sqrt{E_b}}\chi_D(\bar{r},U_0\sqrt{E_b})\,\mathrm{d}\bar{r}\end{aligned}$$

where the third term is zero for $D = 1$ retransmission. In order to calculate P_D, we

can use the approximation,

$$
\begin{aligned}
\mathrm{P}_D \approx & \mathrm{Q}\Big(\sqrt{2\gamma_\mathrm{b}}(\frac{U_0N_o}{2}+1)\Big)+\mathrm{Q}\Big(\sqrt{2\gamma_\mathrm{b}}(\frac{U_0N_o}{2}-1)\Big)-\mathrm{Q}\Big(\sqrt{2\gamma_\mathrm{b}}(\frac{U_DN_o}{2}+1)\Big) \\
& -\mathrm{Q}\Big(\sqrt{2\gamma_\mathrm{b}}(\frac{U_DN_o}{2}-1)\Big)+\mathrm{Q}\left(\frac{(2-U_DN_o)\sqrt{\gamma_\mathrm{b}}}{\sqrt{\frac{2}{(D+1)}}}\right)-\mathrm{Q}\left(\frac{(2+U_DN_o)\sqrt{\gamma_\mathrm{b}}}{\sqrt{\frac{2}{(D+1)}}}\right) \\
& -\sum_{k=1}^{t}\frac{A_k}{2\sqrt{1+\frac{2B_k}{D}}}\Big\{\mathrm{e}^{-\alpha_{k,D}^{+}(U_0)\gamma_\mathrm{b}}\big\{\mathrm{erf}\big(\theta_{k,D}^{+-}(U_0)\sqrt{\gamma_\mathrm{b}}\big)+\mathrm{erf}\big(\theta_{k,D}^{-+}(U_0)\sqrt{\gamma_\mathrm{b}}\big)\big\} \\
& +\mathrm{e}^{-\alpha_{k,D}^{-}(U_0)\gamma_\mathrm{b}}\Bigg\{\mathrm{erf}\big(\theta_{k,D}^{++}(U_0)\sqrt{\gamma_\mathrm{b}}\big)+\mathrm{sign}(\mu(U_0)\sqrt{\gamma_\mathrm{b}})\times \\
& \times\mathrm{erf}\left(\frac{|\mu(U_0)\sqrt{\gamma_\mathrm{b}}|}{2}\sqrt{(D+1)N_o(1+\frac{2B_k}{D})}\right)\Bigg\}\Big\}+\sum_{i=1}^{D-1}\sum_{k=1}^{t}\frac{A_k}{2\sqrt{1+\frac{2B_k}{i}}}\times \\
& \times\Big\{\mathrm{e}^{-\alpha_{k,i}^{+}(U_{D-i-1})\gamma_\mathrm{b}}\big\{\mathrm{erf}\big(\theta_{k,i}^{+-}(U_{D-i-1})\sqrt{\gamma_\mathrm{b}}\big)+\mathrm{erf}\big(\theta_{k,i}^{-+}(U_{D-i-1})\sqrt{\gamma_\mathrm{b}}\big)\big\} \\
& +\mathrm{e}^{-\alpha_{k,i}^{-}(U_{D-i-1})\gamma_\mathrm{b}}\big\{\mathrm{erf}\big(\theta_{k,i}^{++}(U_{D-i-1})\sqrt{\gamma_\mathrm{b}}\big)+\mathrm{sign}(\mu(U_{D-i-1})\sqrt{\gamma_\mathrm{b}})\times \\
& \times\mathrm{erf}\big(\theta_{k,i}^{--}(U_{D-i-1})\sqrt{\gamma_\mathrm{b}}\big)\big\}-\mathrm{e}^{-\alpha_{k,i}^{+}(U_{D-i})\gamma_\mathrm{b}}\big\{\mathrm{erf}\big(\theta_{k,i}^{+-}(U_{D-i})\sqrt{\gamma_\mathrm{b}}\big) \\
& +\mathrm{erf}\big(\theta_{k,i}^{-+}(U_{D-i})\sqrt{\gamma_\mathrm{b}}\big)\big\}-\mathrm{e}^{-\alpha_{k,i}^{-}(U_{D-i})\gamma_\mathrm{b}}\big\{\mathrm{erf}\big(\theta_{k,i}^{++}(U_{D-i})\sqrt{\gamma_\mathrm{b}}\big) \\
& +\mathrm{sign}(\mu(U_{D-i})\sqrt{\gamma_\mathrm{b}})\,\mathrm{erf}\big(\theta_{k,i}^{--}(U_{D-i-1})\sqrt{\gamma_\mathrm{b}}\big)\big\}.
\end{aligned}
$$

5.3.4 BER analysis for slow Rayleigh fading

We extend our analysis to the case of a slow block fading channel with the Rayleigh distributed fading amplitude. Then, the SNR is a random variable having the PDF, $f_{\gamma_\mathrm{b}}(\gamma_\mathrm{b})=\frac{1}{\bar{\gamma}_\mathrm{b}}\mathrm{e}^{-\frac{\gamma_\mathrm{b}}{\bar{\gamma}_\mathrm{b}}}$, and $\bar{\gamma}_\mathrm{b}=\mathrm{E}[\gamma_\mathrm{b}]$ is the average SNR. We assume that the fading is constant during the first transmission and the subsequent D retransmissions, and then, the fading amplitude changes independently during transmission of the next packet of N bits. The average BER is evaluated using the single integration, i.e.,

$$\overline{\mathrm{BER}}_D=\int_0^\infty \mathrm{BER}_D(\gamma_\mathrm{b})\,f_{\gamma_\mathrm{b}}(\gamma_\mathrm{b})\,\mathrm{d}\gamma_\mathrm{b}$$

and its computationally efficient form is given as,

$$\overline{\mathrm{BER}}_D \approx 1-\tfrac{1}{2}\left(\tfrac{4}{\bar{\gamma}_\mathrm{b}(U_{D-1}N_o+2)^2}+1\right)^{-1/2}-\tfrac{1}{2}\left(1+\tfrac{1}{\bar{\gamma}_\mathrm{b}(D+1)}\right)^{-1/2}+\sum_{k=1}^{t}\tfrac{A_k}{\sqrt{1+\frac{2B_k}{D}}}\times$$
$$\times\Bigg\{\left(1+\bar{\gamma}_\mathrm{b}\Big(\alpha^{-}_{k,D}(U_0)+\tfrac{\beta^{+}_{k,D}(U_0)}{\sqrt{2}}\Big(\tfrac{\beta^{+}_{k,D}(U_0)}{\sqrt{2}}+\sqrt{\tfrac{1}{\bar{\gamma}_\mathrm{b}}+\alpha^{-}_{k,D}(U_0)+\tfrac{\beta^{+}_{k,D}(U_0)^2}{2}}\Big)\Big)\right)^{-1}$$
$$+\left(1+\bar{\gamma}_\mathrm{b}\Big(\alpha^{+}_{k,D}(U_0)+\tfrac{\beta^{-}_{k,D}(U_0)}{\sqrt{2}}\Big(\tfrac{\beta^{-}_{k,D}(U_0)}{\sqrt{2}}+\sqrt{\tfrac{1}{\bar{\gamma}_\mathrm{b}}+\alpha^{+}_{k,D}(U_0)+\tfrac{\beta^{-}_{k,D}(U_0)^2}{2}}\Big)\Big)\right)^{-1}\Bigg\}$$
$$+\sum_{i=1}^{D-1}\sum_{k=1}^{t}\tfrac{A_k}{\sqrt{1+\frac{2B_k}{i}}}\Bigg\{\left(1+\bar{\gamma}_\mathrm{b}\Big(\alpha^{-}_{k,i}(U_{D-i-1})+\tfrac{\beta^{+}_{k,i}(U_{D-i-1})}{\sqrt{2}}\Big(\tfrac{\beta^{+}_{k,i}(U_{D-i-1})}{\sqrt{2}}+\right.$$
$$\left.+\sqrt{\tfrac{1}{\bar{\gamma}_\mathrm{b}}+\alpha^{-}_{k,i}(U_{D-i-1})+\tfrac{\beta^{+}_{k,i}(U_{D-i-1})^2}{2}}\Big)\Big)\right)^{-1}+\left(1+\bar{\gamma}_\mathrm{b}\Big(\alpha^{+}_{k,i}(U_{D-i-1})+\right.$$
$$\left.+\tfrac{\beta^{-}_{k,i}(U_{D-i-1})}{\sqrt{2}}\Big(\tfrac{\beta^{-}_{k,i}(U_{D-i-1})}{\sqrt{2}}+\sqrt{\tfrac{1}{\bar{\gamma}_\mathrm{b}}+\alpha^{+}_{k,i}(U_{D-i-1})+\tfrac{\beta^{-}_{k,i}(U_{D-i-1})^2}{2}}\Big)\Big)\right)^{-1}$$
$$-\left(1+\bar{\gamma}_\mathrm{b}\Big(\alpha^{-}_{k,i}(U_{D-i})+\tfrac{\beta^{+}_{k,i}(U_{D-i})}{\sqrt{2}}\Big(\tfrac{\beta^{+}_{k,i}(U_{D-i})}{\sqrt{2}}+\right.$$
$$\left.+\sqrt{\tfrac{1}{\bar{\gamma}_\mathrm{b}}+\alpha^{-}_{k,i}(U_{D-i})+\tfrac{\beta^{+}_{k,i}(U_{D-i})^2}{2}}\Big)\Big)\right)^{-1}-\left(1+\bar{\gamma}_\mathrm{b}\Big(\alpha^{+}_{k,i}(U_{D-i})+\right.$$
$$\left.+\tfrac{\beta^{-}_{k,i}(U_{D-i})}{\sqrt{2}}\Big(\tfrac{\beta^{-}_{k,i}(U_{D-i})}{\sqrt{2}}+\sqrt{\tfrac{1}{\bar{\gamma}_\mathrm{b}}+\alpha^{+}_{k,i}(U_{D-i})+\tfrac{\beta^{-}_{k,i}(U_{D-i})^2}{2}}\Big)\Big)\right)^{-1}\Bigg\}.$$

The probability $\bar{\mathrm{P}}_D$ to compute the retransmission window size $W_D=\lceil N\bar{\mathrm{P}}_D\rfloor$ is efficiently computed as,

$$\bar{\mathrm{P}}_D \approx \frac{1}{2}\Big\{-\Lambda\Big(\frac{U_0N_o}{2}+1\Big)-\Lambda\Big(\frac{U_0N_o}{2}-1\Big)+\Lambda\Big(\frac{U_DN_o}{2}+1\Big)+\Lambda\Big(\frac{U_DN_o}{2}-1\Big)$$
$$-\Lambda\Big(\frac{2-U_DN_o}{\frac{2}{\sqrt{D+1}}}\Big)+\Lambda\Big(\frac{2+U_DN_o}{\frac{2}{\sqrt{D+1}}}\Big)\Big\}-\sum_{k=1}^{t}\frac{A_k}{2\sqrt{1+\frac{2B_k}{D}}}\times$$
$$\times\Big\{\Omega\big[\theta^{-+}_{k,D}(U_0)\big]+\Omega\big[\theta^{+-}_{k,D}(U_0)\big]+\Omega\big[\theta^{++}_{k,D}(U_0)\big]+\mathrm{sign}(\mu(U_0))\,\Omega\big[\theta^{--}_{k,D}(U_0)\big]\Big\}$$
$$+\sum_{i=1}^{D-1}\sum_{k=1}^{t}\frac{A_k}{2\sqrt{1+\frac{2B_k}{i}}}\Big\{\Omega\big[\theta^{-+}_{k,i}(U_{D-i-1})\big]+\Omega\big[\theta^{+-}_{k,i}(U_{D-i-1})\big]+\Omega\big[\theta^{++}_{k,i}(U_{D-i-1})\big]$$
$$+\mathrm{sign}(\mu(U_{D-i-1}))\,\Omega\big[\theta^{--}_{k,i}(U_{D-i-1})\big]-\Omega\big[\theta^{-+}_{k,i}(U_{D-i})\big]+\Omega\big[\theta^{+-}_{k,i}(U_{D-i})\big]$$
$$+\Omega\big[\theta^{++}_{k,i}(U_{D-i})\big]+\mathrm{sign}(\mu(U_{D-i}))\,\Omega\big[\theta^{--}_{k,i}(U_{D-i})\big]\Big\}$$

where

$$\Lambda(x) = \frac{x}{\sqrt{\frac{1}{\bar{\gamma}_b} + x^2}}$$

$$\Omega\left[\theta^{\mathrm{x}}_{k,d}(U)\right] = \begin{cases} \frac{\theta^{\mathrm{x}}_{k,d}(U)}{(1+\bar{\gamma}_b\alpha^{-}_{k,d}(U))(\sqrt{\frac{1}{\bar{\gamma}_b}+\alpha^{-}_{k,d}(U)+(\theta^{\mathrm{x}}_{k,d}(U))^2})} & \mathrm{x} \in \{++,--\} \\ \frac{\theta^{\mathrm{x}}_{k,d}(U)}{(1+\bar{\gamma}_b\alpha^{+}_{k,d}(U))(\sqrt{\frac{1}{\bar{\gamma}_b}+\alpha^{+}_{k,d}(U)+(\theta^{\mathrm{x}}_{k,d}(U))^2})} & \text{elsewhere.} \end{cases}$$

5.4 Design and numerical examples

In this section, we consider three strategies how to choose parameters of the proposed retransmission scheme.

5.4.1 Fixed rate technique

In this design, we assume the equal window size for each retransmission, i.e., $W_1 = W_2 = \ldots = W_D = W$, and the fixed forward rate R_{f}. Then, the window size is determined as,

$$W = \left\lceil \frac{N}{D}\left(\frac{1}{R_{\mathrm{f}}} - 1\right) \right\rceil .$$

Thus, for given parameters D, R_{f} and N, the number of retransmitted bits is fixed. However, the window size W is assumed to be in the range, $1 \leq W \leq N$, which restricts the possible forward rates that can be considered to the interval, $\frac{1}{D+1} < R_{\mathrm{f}} \leq \frac{N}{D+N}$. Note also that, for $W = N$, the rate $R_{\mathrm{f}} = \frac{1}{1+D}$, and the proposed retransmission scheme corresponds to a repetition code with D repetitions of the original packet. We denote such block repetition code as $r(1,1)$. We have the following proposition.

Proposition 1. *For given SNR, the fixed rate technique achieves the minimum value of the BER for a specific value of the rate R_{f} and this value of R_{f} increases with the SNR.* ■

Proposition 1 can be proved by forcing the derivative $\frac{\mathrm{d}}{\mathrm{d}R_{\mathrm{f}}}\mathrm{BER}_D$ to be equal to zero. Furthermore, for large values of N, the forward rate approaches unity and the retransmissions can be neglected. More importantly, in such case, when N is large,

or when $W = N$, the BER of the retransmission scheme approaches the BER of the block repetition code $r(1, 1)$.

Fig. 5.4 and Fig. 5.5 show the system BER versus the forward rate R_f for different number of retransmissions D and the SNR values $\gamma_b = 0$dB and $\gamma_b = 5$dB, respectively. The BER curves in Fig. 5.4 and Fig. 5.5 also compare the simulations with

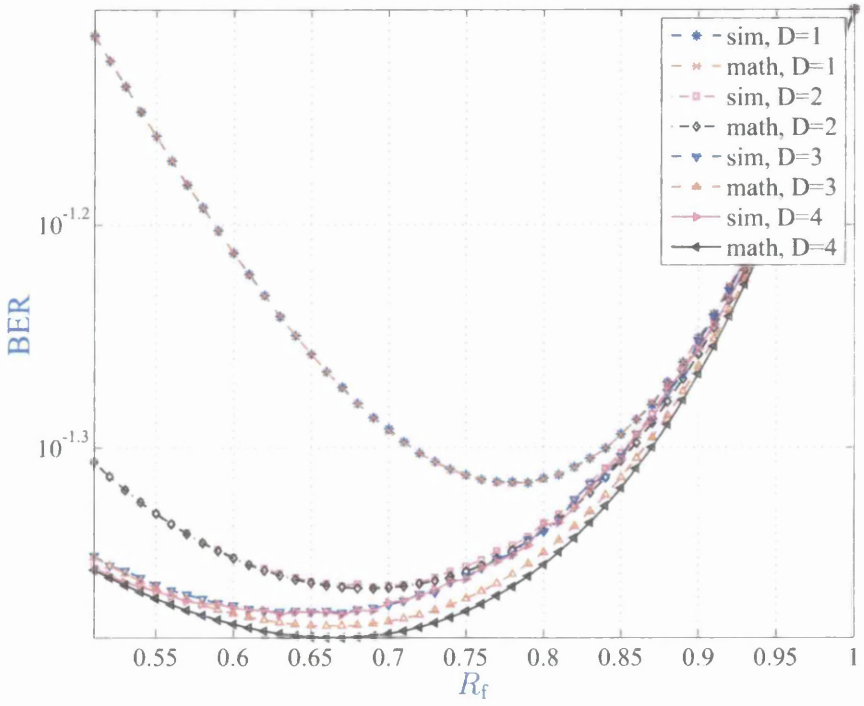

Figure 5.4: The BER versus the rate R_f for $SNR = 0$ dB and different number of retransmissions D.

the approximate expressions provided above; we observe that, for larger values of D, the difference between the approximate expressions and the simulations becomes negligible. Also, note that the minimum BER value is more apparent for larger values of SNR. The forward rates R_f corresponding to the minimum BER are shown in Fig. 5.6 for the different number of retransmissions D. Finally, Fig. 5.7 shows the system BER versus the SNR γ_b for the different number of retransmissions D assuming that R_f is optimized for each value of the SNR γ_b in order to minimize the achieved BER. Note that such optimization becomes more effective if the SNR is increased.

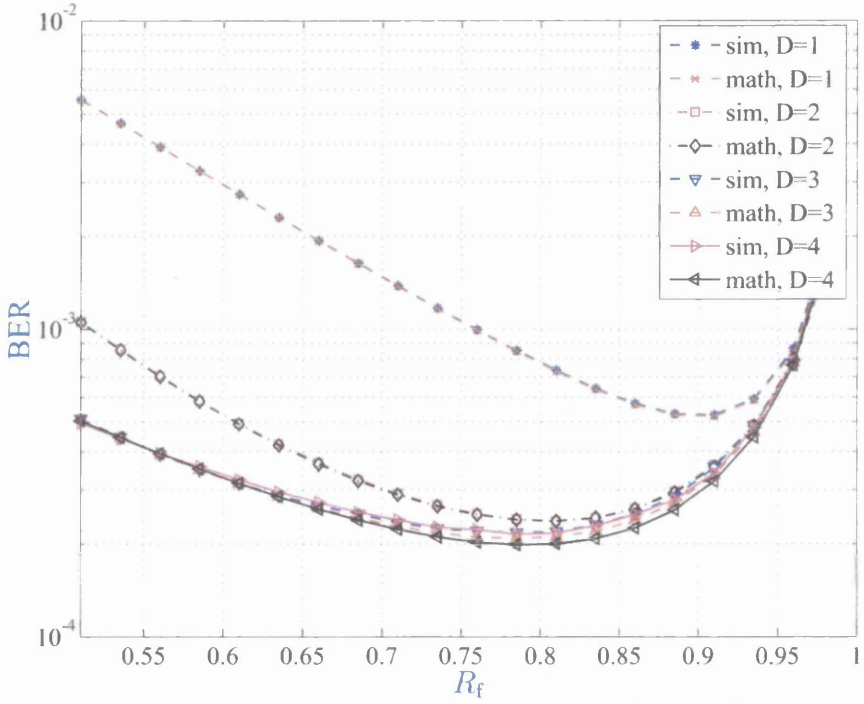

Figure 5.5: The BER versus the rate R_f for $SNR = 5$ dB and different number of retransmissions D.

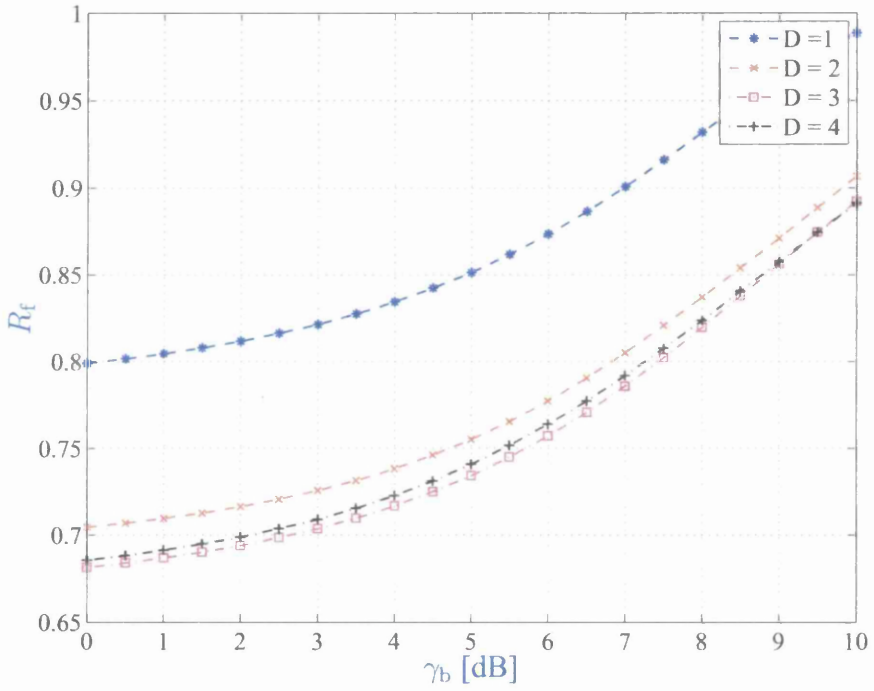

Figure 5.6: The rate R_f corresponding to the minimum BER versus the SNR γ_b for the different number of retransmissions D.

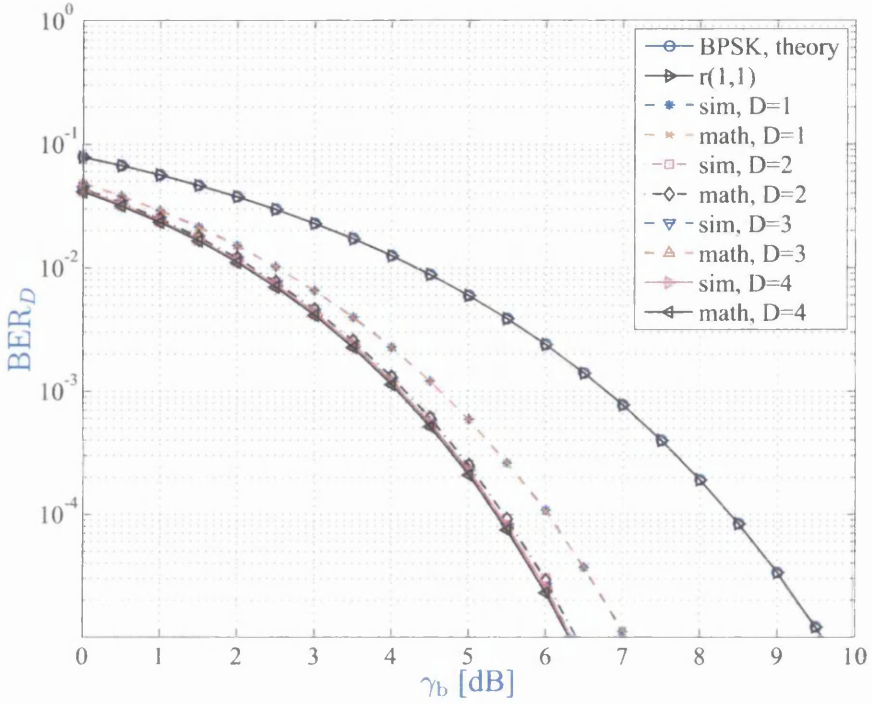

Figure 5.7: The BER_D versus the SNR γ_b for the different number of retransmissions D.

5.4.2 Fixed window technique

We assume that the normalized expected window size is the same for all retransmissions, i.e., $\mathrm{P}_0 = \mathrm{P}_1 = \mathrm{P}_2 = \ldots = \mathrm{P}_D - 1 = P$. Consequently, the retransmission window size for each retransmission is fixed, i.e., $W_1 = W_2 = \ldots = W_D = W = \lceil N\,P \rfloor$. The forward rate is then computed as,

$$R_\mathrm{f} = \frac{1}{1 + D\,W/N}$$

and thus, for a given fixed ratio W/N, the forward rate is dependent on the total number of retransmissions D. For this design, we have the following proposition.

Proposition 2. *For a given SNR, the fixed window technique achieves the minimum BER for some value of the retransmission window size. This window size value decreases with the increasing SNR.* ■

Proposition 2 can be again proved by forcing the derivative, $\frac{\mathrm{d}}{\mathrm{d}\left(\frac{W}{N}\right)}\mathrm{BER}_D$ to be equal to zero. Furthermore, for large values of W, the ratio W/N approaches unity

and and the proposed retransmission scheme approaches the BER performance of a repetition code. On the other hand, when the ratio W/N approaches zero, the overhead of retransmissions can be neglected.

Fig. 5.8 and Fig. 5.9 show the BER versus the normalized window size W/N for the different number of retransmissions D and the SNR values $\gamma_b = 0$dB and $\gamma_b = 5$dB, respectively. We again observe a negligible difference between the obtained approxi-

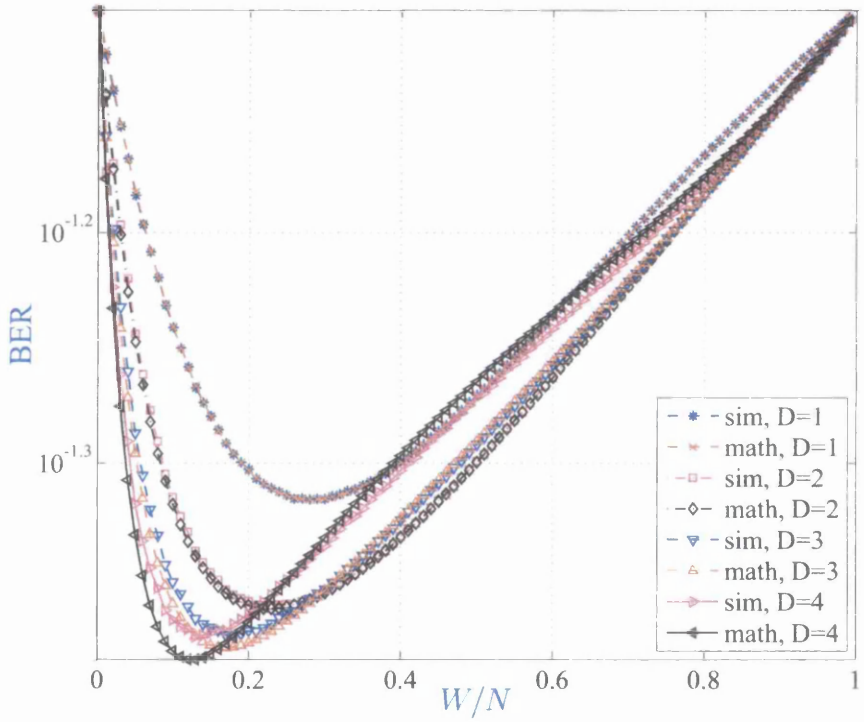

Figure 5.8: The BER versus the normalized window size W/N for the $\gamma_b = 0$ dB and the different number of retransmissions D.

mate BER expressions and the simulation results, especially for larger values of D. In addition, we observe that the minimum BER values are more apparent when the SNR is increased. Fig. 5.10 then shows the normalized window size W/N corresponding to the minimum BER for the different number of retransmissions D. Finally, Fig. 5.11 shows the BER versus the SNR γ_b for the different number of retransmissions D assuming the optimum value of W/N for each γ_b that minimizes the BER. Note again that such minimization of the BER is more effective when the SNR is increased.

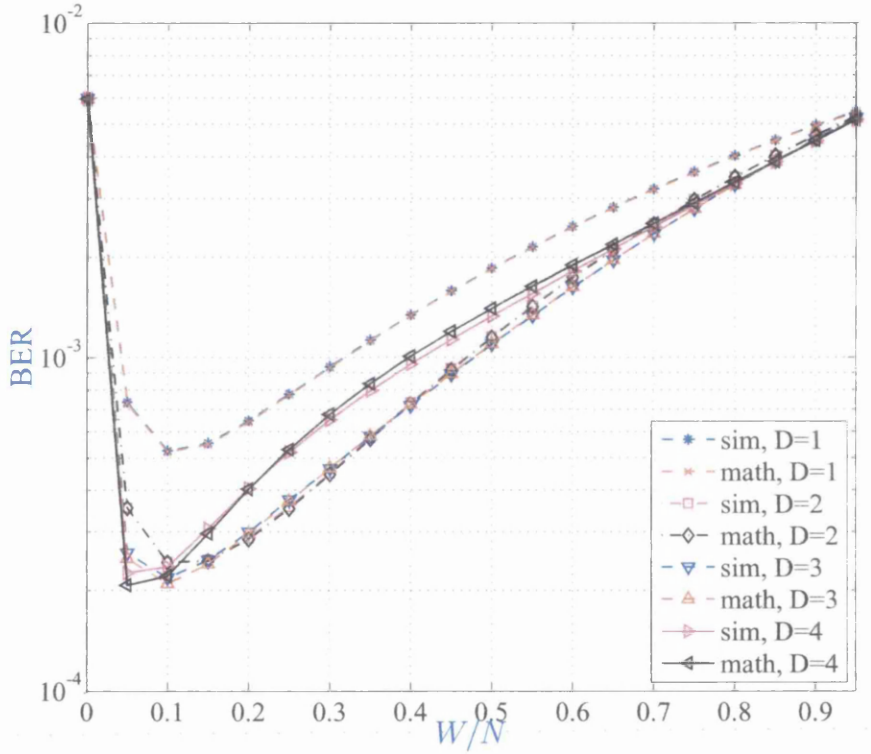

Figure 5.9: The BER versus the normalized window size W/N for the $\gamma_b = 5$ dB and the different number of retransmissions D.

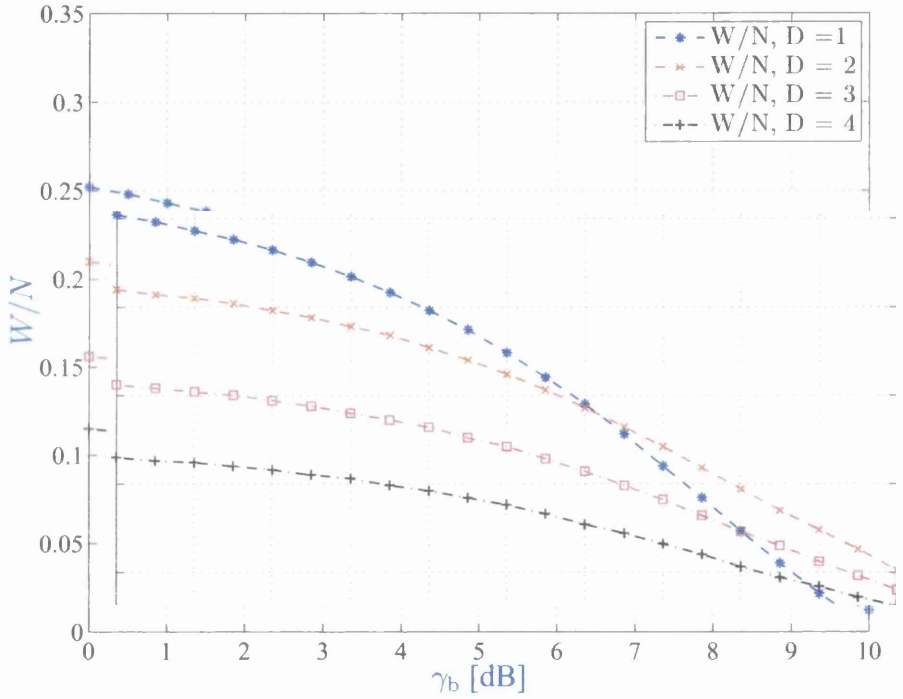

Figure 5.10: The normalized window size W/N versus the SNR γ_b having the minimum BER for the different number of retransmissions D.

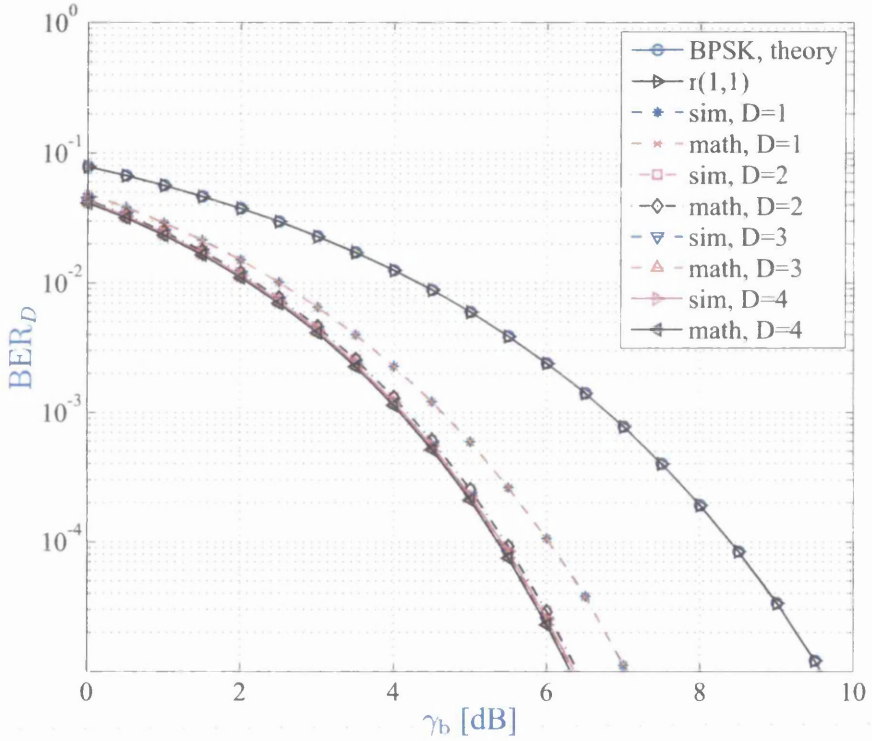

Figure 5.11: The BER_D versus the SNR γ_b for the different number of retransmissions D.

5.4.3 Fixed threshold technique

In this technique, we assume the constant thresholds, $U_0 = U_1 = \ldots = U_{D-1} = \frac{U}{E_b}$, for each retransmission, so that the reliabilities to select bits for retransmissions are constrained to the interval, $|\bar{r}| \leq \frac{U}{\sqrt{E_b}}$. However, the different window size W_d is selected for each retransmission, i.e., for $d = 1, 2, \ldots, D$, let,

$$W_d = \lceil N\mathrm{P}_d \rfloor .$$

The forward rate is then given as,

$$R_{\mathrm{f}} = \frac{1}{1 + \sum_{d=1}^{D} W_d}.$$

We have the following proposition.

Proposition 3. *For a given SNR, the fixed threshold technique achieves a minimum BER value for some specific threshold $\frac{U}{E_b}$. This specific threshold value is increasing with the SNR.*

Proposition 3 can be proved by letting the derivative, $\frac{\mathrm{d}}{\mathrm{d}U}\mathrm{BER}_D$ to be equal to zero. Furthermore, for $U = 0$, the BER performance of the proposed scheme can be approximated by theoretical BPSK. More importantly, when U is asymptotically large, the BER performance of the proposed scheme approaches the BER of the block repetition code $r(1, 1)$.

Fig. 5.12 and Fig. 5.13 show the BER versus the normalized threshold U/E_b for the different number of retransmissions D and the SNR values $\gamma_{\mathrm{b}} = 0\mathrm{dB}$ and $\gamma_{\mathrm{b}} = 5\mathrm{dB}$, respectively. Since the obtained BER expressions were verified for the other two techniques considered, the BER curves in Fig. 5.12 and Fig. 5.13 are shown only using these theoretical expressions. We again observe that the minimum BER values are more apparent when the SNR is increased. Fig. 5.14 shows the thresholds U/E_b that have the minimum BER for the different number of retransmissions D. Finally, Fig. 5.15 shows the BER versus the SNR γ_{b} for different D assuming the optimum thresholds U/E_b for each SNR γ_{b} that have the minimum BER. Again, one has that the minimization of the BER by optimizing the value of the threshold U/E_b is more effective when the SNR is increased.

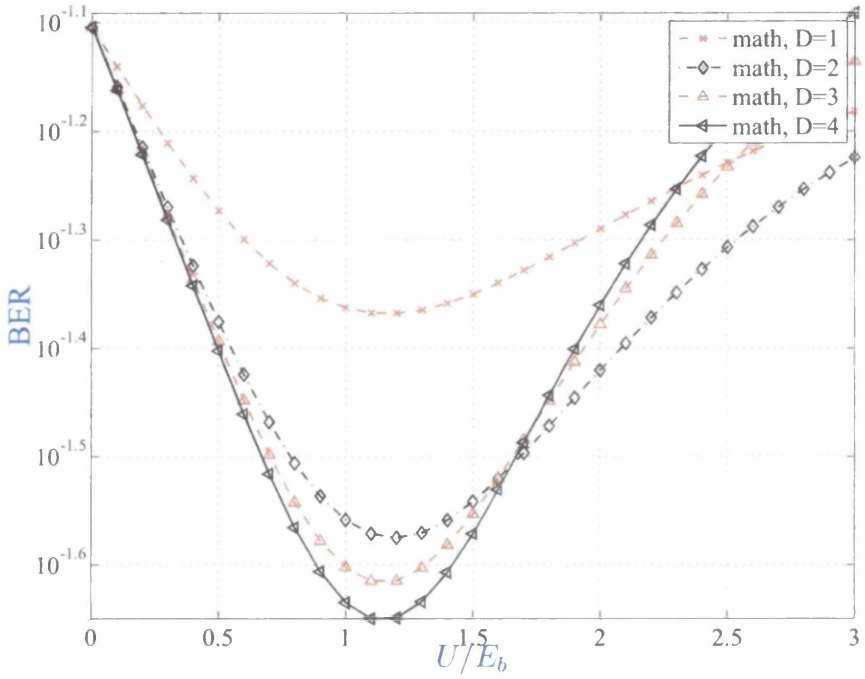

Figure 5.12: The BER versus the normalized threshold U/E_b for the SNR $\gamma_b = 0$ dB and the different number of retransmissions D.

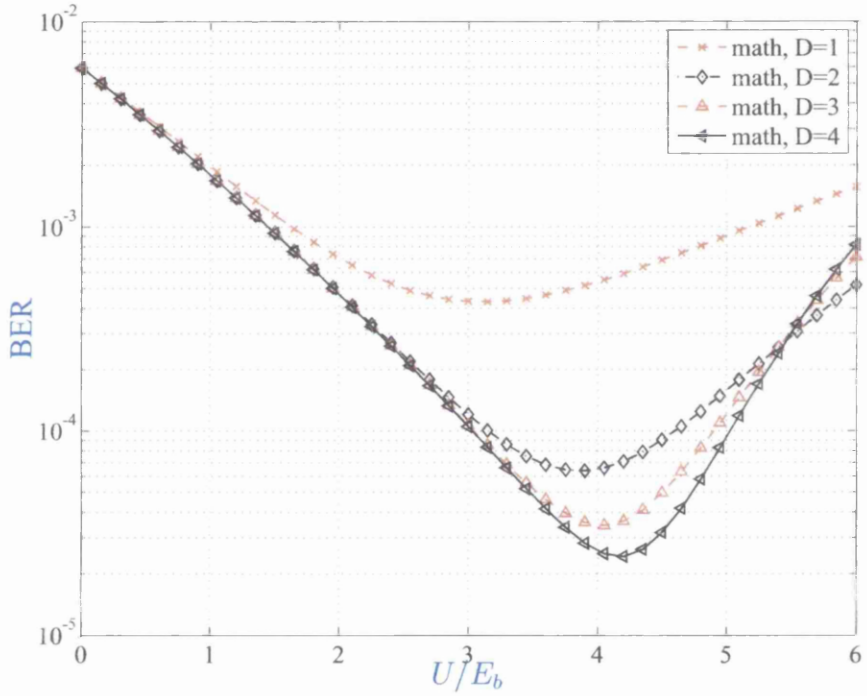

Figure 5.13: The BER versus the normalized threshold U/E_b for the SNR $\gamma_b = 5$ dB and the different number of retransmissions D.

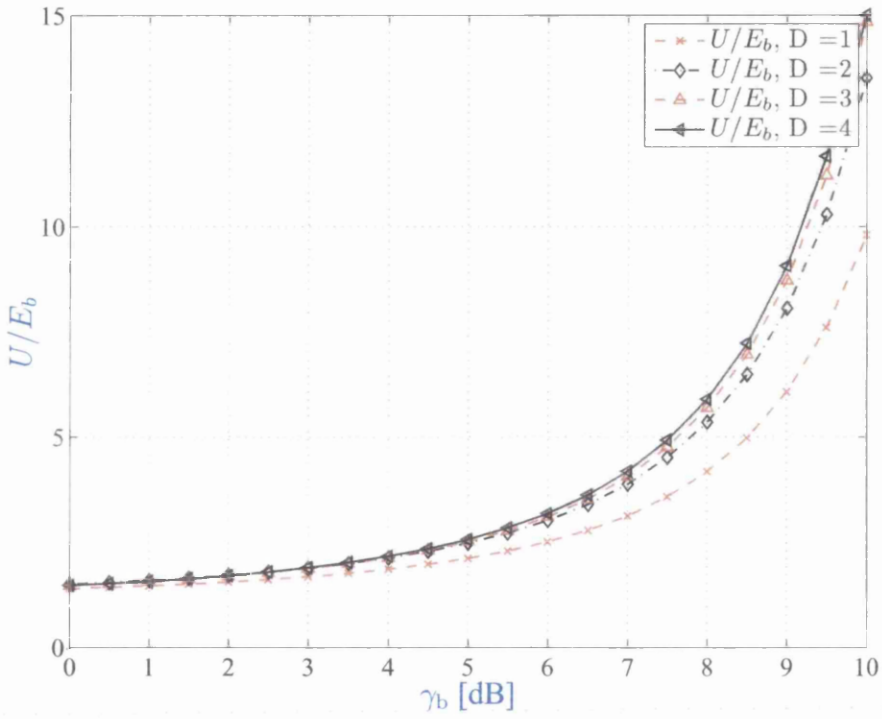

Figure 5.14: The values of the normalized threshold U/E_b corresponding to the minimum BER versus the SNR γ_b for the different number of retransmissions D.

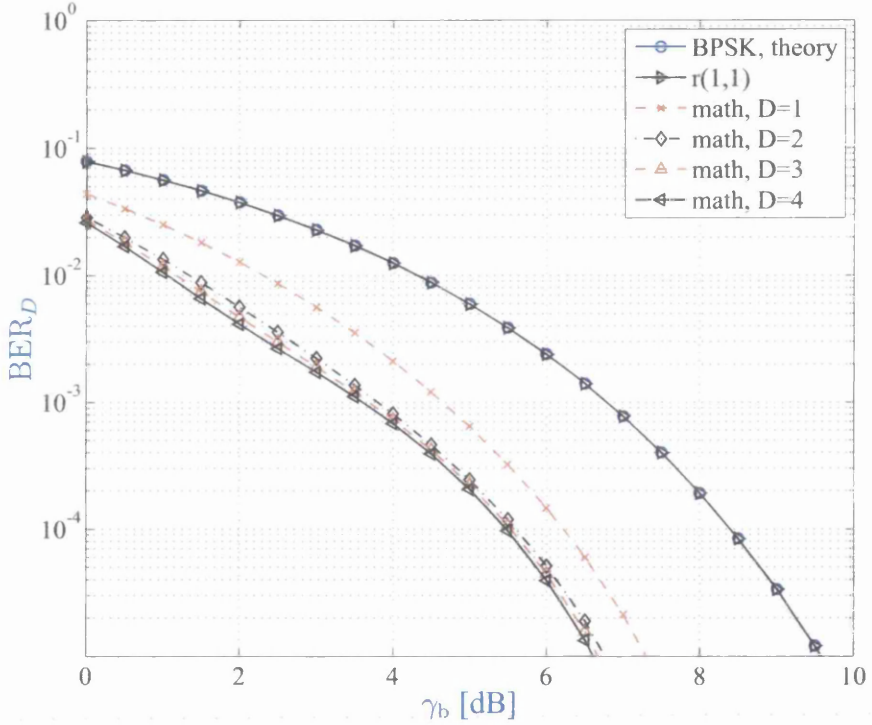

Figure 5.15: The BER_D versus the SNR γ_b for the different number of retransmissions D.

5.4.4 Other numerical results

Recall our discussion on the trade-offs in selecting the value of the number of feedback bits per retransmission C_d. The probability that the random permutation of N bits in the received packet places a given number of W bits into a predefined window of the same length W is,

$$P_s = \frac{1}{\binom{N}{W}}$$

where $\binom{N}{W}$ is the binomial coefficient. Hence, the stopping condition that exactly W bits with the smallest reliabilities are placed into the predefined window of length W has a geometric distribution with the probability of success P_s. The expected number of the random permutations required to achieve the stopping condition is,

$$\mathrm{E}[K] = \frac{1}{P_s}.$$

Fig. 5.16 shows this expected number of the required random permutations versus the packet length N for different window sizes W. More importantly, note that the expectation $\mathrm{E}[K]$ is proportional to the transmission delay with the proportionality constant 2^{-C_D}, and that the expected number of random permutations is reduced for smaller values of W, however, it is increased for larger values of N. Fig. 5.17 shows the expected number of random permutations $\mathrm{E}[K]$ versus the SNR γ_b for different packet length N assuming the fixed window technique.

For the retransmission systems considered, denote as T to the time to deliver N information bits from the source to the destination with D retransmission attempts. We can then define the average throughput as,

$$\zeta = \frac{N}{T_{\mathrm{av}}} = \frac{N}{\mathrm{E}[T]}.$$

Assuming the fixed window technique with $D = 1$ retransmission, we can show that,

$$T_{\mathrm{av}} = \mathrm{E}[T] = (N + W + C_1 + \mathrm{E}[K]\, 2^{-C_1})T_s$$

where T_s is the duration of one symbol. We can show that there exists an optimum value of C_1 minimizing the expected delay T_{av}. This optimum value can be computed as,

$$C_1 = \lceil \log_2(\mathrm{E}[K] \ln 2) \rfloor$$

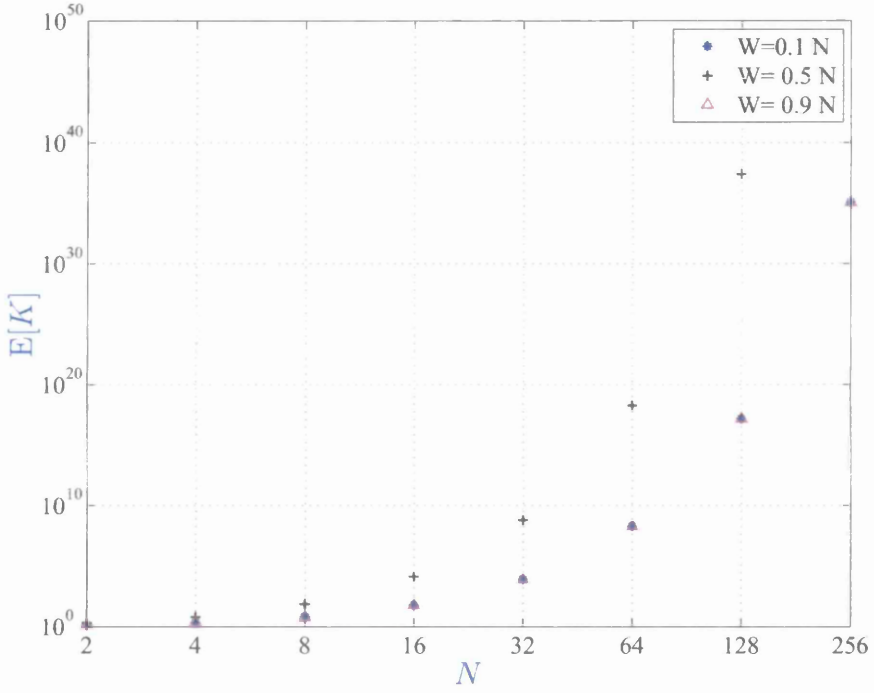

Figure 5.16: The expected number of required random permutations $\mathrm{E}[K]$ versus the packet length N for the different retransmission window sizes W.

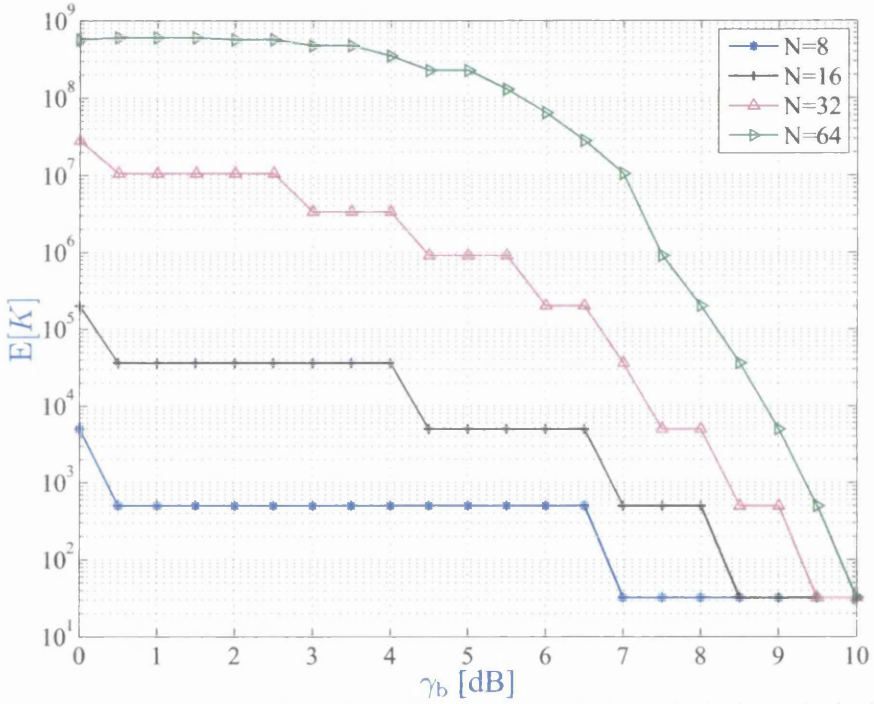

Figure 5.17: The expected number of required random permutations $\mathrm{E}[K]$ versus the SNR γ_b for different packet length N.

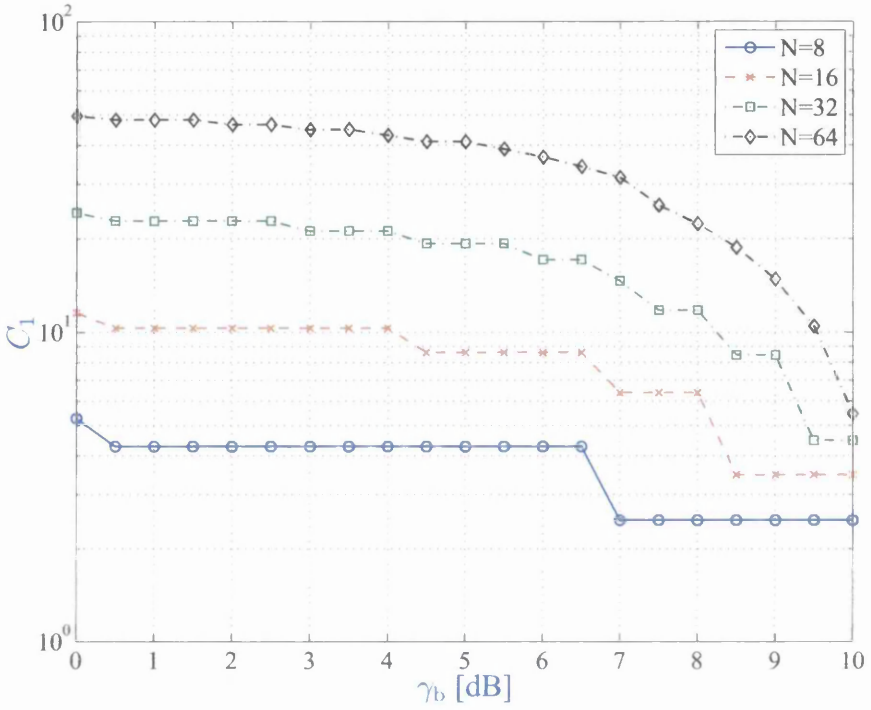

Figure 5.18: The values C_1 versus the SNR γ_b for different packet length N.

and it is shown in Fig. 5.18 assuming different values of the packet length N.

The throughput ζ of the proposed retransmission scheme assuming the fixed window technique for different packet length N is shown in Fig. 5.19. For comparison, the throughput $1/2$ of the repetition code corresponding to the conventional stop-and-wait ARQ with one retransmission is also shown in Fig. 5.19. More importantly, we observe that the proposed scheme can achieve better throughput than the repetition code for the same number of retransmissions D, especially at medium to large values of the SNR. In addition, we can show that, for the fixed window technique, in the limit of large SNR, the throughput,

$$\lim_{\gamma_b \to \infty} \zeta \approx \frac{N}{N+1}$$

since $\lim_{\gamma_b \to \infty} W/N = 0$. Finally, for the different number of retransmission D, Fig. 5.20 shows the BER that is achieved over a slowly Rayleigh fading channel with the unit fading power provided that the system parameters are optimized in order to minimize the BER.

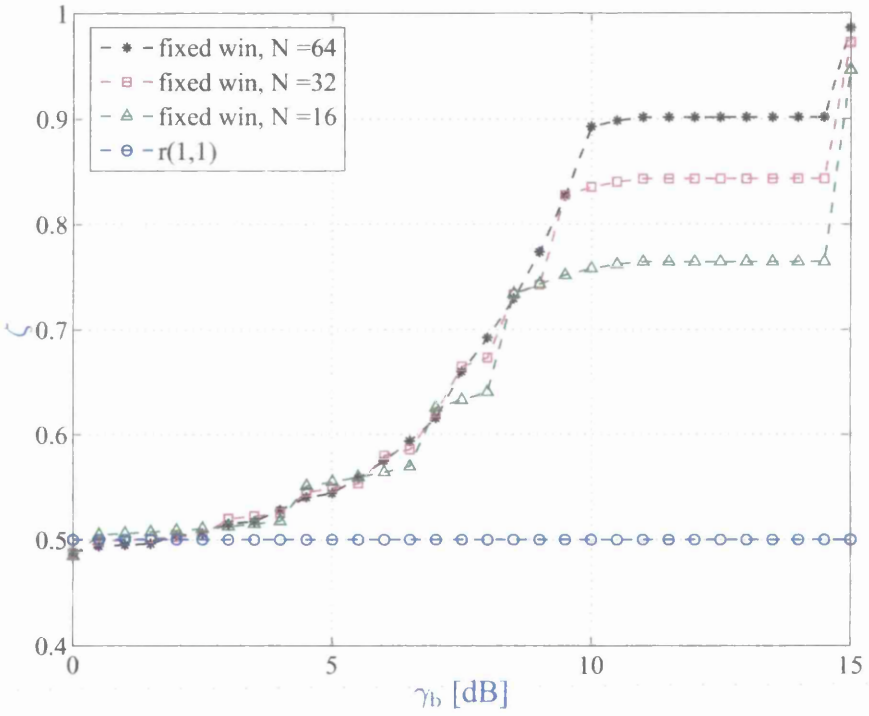

Figure 5.19: The throughput ζ versus the SNR γ_b for different packet length N.

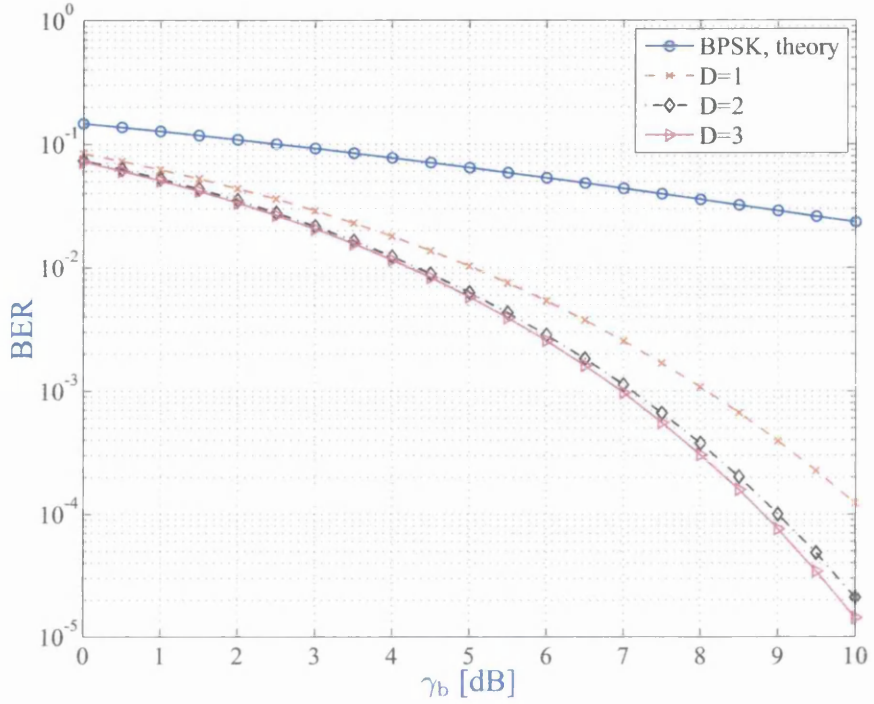

Figure 5.20: The average BER versus the SNR γ_b over a slowly Rayleigh fading channel.

5.5 Conclusions

A novel retransmission scheme using random permutations at the receiver to decide which bits in the packet should be retransmitted was proposed and its BER performance as well as the throughput have been analyzed. The proposed scheme does not employ the FEC coding, nor does not relay on the CRC bits to detect the transmission errors. However, the proposed scheme assumes a predefined finite number of retransmissions, and in this chapter, it was designed assuming a reliable reverse link to deliver error-free feedback messages from the destination to the source. Thus, using the random permutations, it is guaranteed that only the bits within the received packet having small reliabilities are selected for retransmission. The retransmitted bits are combined at the destination receiver using a low complexity diversity combining. This has an overall benign effect on the implementation complexity and the transmission efficiency of the proposed scheme. The comparison of the proposed scheme and the usage of conventional ARQ shows that the proposed scheme can provide higher BER

and throughput gains on the expense of additional complexity to the system design. However, the added complexity is reasonable in comparison with the FEC techniques decoding complexity.

Three strategies to select the parameters of the proposed retransmission scheme were considered. These parameters were optimized to achieve the minimum BER. The performance of the proposed retransmission scheme was compared to the block repetition code corresponding to a conventional ARQ retransmission strategy. It was shown that, for the same number of retransmissions, and the same packet length, the proposed scheme always outperforms such repetition coding, and, in some scenarios, the performance improvement is found to be significant. Numerical examples were used to verify the derived mathematical expressions and approximations by computer simulations. Most of our analysis has been done for the case of AWGN channel, however, the case of a slow Rayleigh block fading channel was also investigated. However, critically, the proposed scheme appears to provide the throughput and the BER reduction gains only for the medium to large SNR values.

5.6 Appendix

We obtain several approximations that can be used to efficiently evaluate the integrals in the BER expressions. These approximations are based on the so-called Prony approximation of the $\mathrm{Q}(x)$ function [92], i.e.,

$$\mathrm{Q}(x) = \sum_{k=1}^{t} A_k \mathrm{e}^{-B_k x^2}$$

where $t = 2$ is sufficient, as shown by our numerical examples, to obtain a good approximation accuracy. For $t = 2$, the coefficients, $A_1 = 0.208$, $A_2 = 0.147$, $B_1 = 0.971$, and $B_2 = 0.525$.

Assuming positive constants $H > 0$, and $h_i > 0$, $i = 1, 2, 3, 4, 5$, since $\mathrm{erf}(x) = 1 - 2\mathrm{Q}(\sqrt{2}x)$, the expressions for BER_D and P_D can be approximated using the following approximations. These approximation are verified numerically in Fig. 5.21 assuming the BER of the proposed retransmission scheme designed with the fixed window technique.

$$\int_{-\infty}^{0} h_1 e^{-\frac{(\bar{r}-h_2)^2}{h_3}} Q(h_4(h_5-\bar{r}))\,d\bar{r} \approx \sum_{k=1}^{t} \int_{-\infty}^{0} h_1 e^{-\frac{(\bar{r}-h_2)^2}{h_3}} A_k e^{-B_k(h_4(h_5-\bar{r}))^2}\,d\bar{r}$$
$$\approx \sum_{k=1}^{t} \frac{h_1 A_k}{2\sqrt{\frac{1}{h_3}+{h_4}^2 B_k}} e^{-\frac{B_k {h_4}^2 (h_2-h_5)^2}{1+h_3 {h_4}^2 B_k}} \sqrt{\pi}\,\mathrm{erfc}\left(\frac{h_2+h_3{h_4}^2 h_5 B_k}{\sqrt{h_3(1+h_3{h_4}^2 B_k)}}\right)$$

$$\int_{-\infty}^{0} h_1 e^{-\frac{(\bar{r}-h_2)^2}{h_3}} Q(h_4(h_5+\bar{r}))\,d\bar{r} \approx \sum_{k=1}^{t} \int_{-\infty}^{0} h_1 e^{-\frac{(\bar{r}-h_2)^2}{h_3}} A_k e^{-B_k(h_4(h_5+\bar{r}))^2}\,d\bar{r}$$
$$\approx \sum_{k=1}^{t} \frac{h_1 h_3 A_k}{2\sqrt{h_3(1+h_3{h_4}^2 B_k)}} e^{-\frac{B_k {h_4}^2 (h_2+h_5)^2}{1+h_3 {h_4}^2 B_k}} \sqrt{\pi}\,\mathrm{erfc}\left(\frac{h_2-h_3{h_4}^2 h_5 B_k}{\sqrt{h_3(1+h_3{h_4}^2 B_k)}}\right)$$

$$\int_{-H}^{H} h_1 e^{-\frac{(\bar{r}-h_2)^2}{h_3}} Q(h_4(h_5-\bar{r}))\,d\bar{r} \approx \sum_{k=1}^{t} \int_{-H}^{H} h_1 e^{-\frac{(\bar{r}-h_2)^2}{h_3}} A_k e^{-B_k(h_4(h_5-\bar{r}))^2}\,d\bar{r}$$
$$\approx \sum_{k=1}^{t} \frac{h_1 A_k \sqrt{h_3}}{2\sqrt{1+h_3{h_4}^2 B_k}} e^{-\frac{B_k {h_4}^2 (h_2-h_5)^2}{1+h_3 {h_4}^2 B_k}} \sqrt{\pi}\left\{\mathrm{erf}\left(\frac{h_2+H+h_3{h_4}^2(h_5+H)B_k}{\sqrt{h_3(1+h_3{h_4}^2 B_k)}}\right)\right.$$
$$\left.+\mathrm{sign}\left(H-\frac{h_2+h_3{h_4}^2 h_5 B_k}{1+h_3{h_4}^2 B_k}\right)\mathrm{erf}\left(\sqrt{\frac{1}{h_3}+{h_4}^2 B_k}\left|H-\frac{h_2+h_3{h_4}^2 h_5 B_k}{1+h_3{h_4}^2 B_k}\right|\right)\right\}$$

$$\int_{-H}^{H} h_1 e^{-\frac{(\bar{r}-h_2)^2}{h_3}} Q(h_4(h_5+\bar{r}))\,d\bar{r} \approx \sum_{k=1}^{t} \int_{-H}^{H} h_1 e^{-\frac{(\bar{r}-h_2)^2}{h_3}} A_k e^{-B_k(h_4(h_5+\bar{r}))^2}\,d\bar{r}$$
$$\approx \sum_{k=1}^{t} \frac{h_1 h_3 A_k}{2\sqrt{h_3(1+h_3{h_4}^2 B_k)}} e^{-\frac{B_k {h_4}^2 (h_2+h_5)^2}{1+h_3 {h_4}^2 B_k}} \sqrt{\pi}\left\{\mathrm{erf}\left(\frac{H+h_2+h_3{h_4}^2(H-h_5)B_k}{\sqrt{h_3(1+h_3{h_4}^2 B_k)}}\right)\right.$$
$$\left.+\mathrm{erf}\left(\frac{H-h_2+h_3{h_4}^2(H+h_5)B_k}{\sqrt{h_3(1+h_3{h_4}^2 B_k)}}\right)\right\}$$

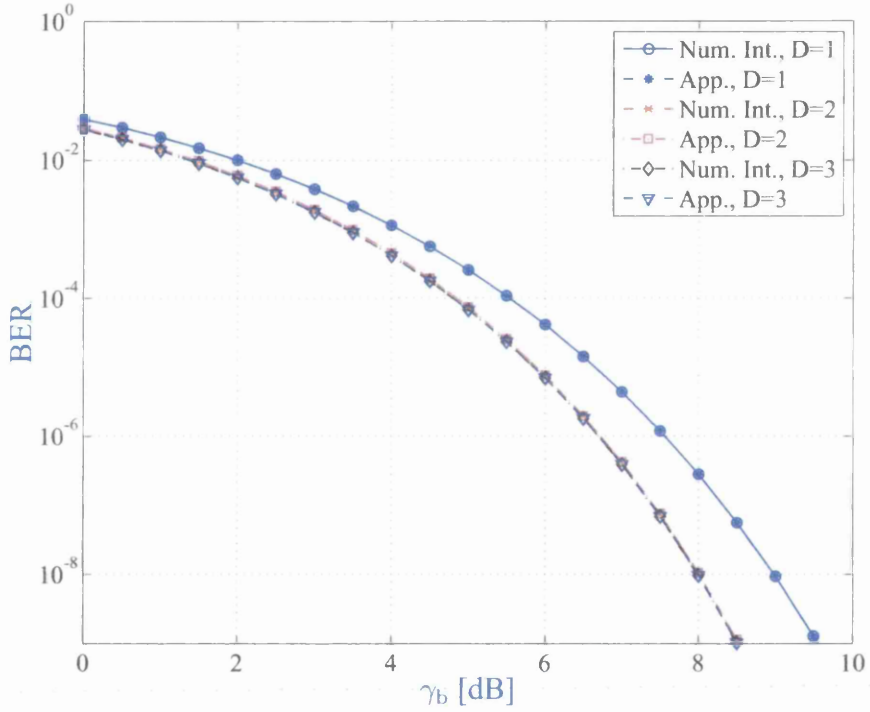

Figure 5.21: The BER versus the SNR γ_b for the different number of retransmissions D.

6

Assessment of Link Performance with a Single Interferer

6.1 Introduction

Co-channel interference is one of the additive distortions of the transmitted signals in wireless communications. Even though such distortion can be suppressed by an appropriate communication system design [123], it can never be eliminated completely. Hence, it is important to evaluate the system bit error rate (BER) performance in the presence of residual co-channel interference. The previous works analyzed the impact of co-channel interference on the system BER performance under various assumptions such as the number of co-channel interferers and their channel fading statistics [124]. For example, the exact BER in the presence of co-channel interference for the narrowband systems is obtained in papers [125], [126] and [127], and for the wideband systems in papers [128], [129] and [130]. In these works, the interference is assumed to be asynchronous with the desired signal, and the system BER is then averaged over the random delays of the interference signals.

In general, the exact BER analysis of communication systems with co-channel interference can be often rather complicated. In order to simplify the analysis, different Gaussian approximations of the interference have been considered [128, 131]. For example, the standard Gaussian approximation and a sum-of-sinusoids approximation

are analyzed in [125]. It is noted in [126] that the standard Gaussian approximation is not suitable for studying the impact of the interference fading distributions on the system BER performance. On the other hand, the reference [132] suggests that the standard Gaussian approximation is sufficiently accurate provided that the desired signal is subject to fading.

In this chapter, we study the impact of a single co-channel interferer on the BER performance of a communication link. In particular, we obtain a novel metric that can be used to assess whether the standard Gaussian approximation overestimates or underestimates the link BER. The proposed metric is a function of the distribution of the interference signal, and it is independent of the distribution of the desired signal. More importantly, unlike in the previous works, the standard Gaussian approximation is constructed as a non-linear transformation of the original interference signal. We assume that both the desired signal as well as the interference signal are binary phase shift keying (BPSK) modulated and subject to independent frequency non-selective fading. In addition, the desired signal and the interference signal are assumed to be time-synchronized which is often the case in the time division multiple access networks with channels reuse and the networks with coordinated transmissions. Finally, numerical examples for the Nakagami and lognormal distributed interference fading amplitude are provided to confirm the validity of the proposed metric.

The rest of this chapter is organized as follows. System model is presented in Section 6.2. Performance evaluation is presented in Section 6.3. Numerical examples are presented in Section 6.4. Chapter conclusions are given in Section 6.5.

6.2 System model

Consider a point-to-point communication link operating over a slowly fading channel, so that the channel fading coefficient is perfectly known to the link receiver. We assess the effect of a single co-channel interferer on the BER performance of such link. Thus, let the received signal at the input of a symbol-by-symbol coherent detector at the link receiver be written as,

$$y = h_0 s_0 + I + w \tag{6.1}$$

where $h_0 \geq 0$ is a channel fading amplitude described by its probability density function (PDF) $f_{h_0}(h_0)$, s_0 is a modulation symbol generated at the link transmitter, I is a sample of the co-channel interference, and w represents an additive white Gaussian noise (AWGN).

We make the following assumptions. The interference is a digitally modulated signal that is symbol-time synchronized with the useful signal, however, the interfering signal and the useful signal are otherwise mutually independent. Thus, the interfering signal can be written as a product of the three random variables, i.e.,

$$I = hzs$$

where $h \geq 0$ is a channel fading amplitude, $z = \cos\theta$ where θ represents a random phase shift between the interfering signal and the useful signal, and s is a modulation symbol. For simplicity, we assume that the transmitted symbols s_0 and s and equally probable BPSK symbols, i.e., $s_0 \in \{+1, -1\}$ and $s \in \{+\sqrt{E_b}, -\sqrt{E_b}\}$. Then, the symbol-by-symbol decisions about the transmitted symbol s_0 by the detector at the link receiver are obtained as,

$$\hat{s}_0 = \text{sign}(y) \tag{6.2}$$

where $\text{sign}(\cdot)$ denotes the sign of a real number. Furthermore, provided that the phase θ is uniformly distributed in the interval $[0, 2\pi)$ the random variable z has zero-mean and the variance $1/2$, and its PDF is [93],

$$f_z(z) = \frac{1}{\pi\sqrt{1-z^2}} \quad \text{for} \quad |z| \leq 1.$$

Correspondingly, the interference I has zero-mean and the variance $\sigma_I^2 = \text{E}[I^2] = \text{E}[h^2]\, E_b/2$ where $\text{E}[\cdot]$ denotes expectation. We also assume that the AWGN w has zero-mean and the variance $\sigma_w^2 = \text{E}[w^2]$.

We can define the average signal-to-noise ratio (SNR) and the average signal-to-interference ratio (SIR) , respectively, as,

$$\text{SNR} = \frac{\text{E}[h_0^2]}{\sigma_w^2} = \gamma_b\, \text{E}\big[h_0^2\big] \quad \text{and} \quad \text{SIR} = \frac{\text{E}[h_0^2]}{\sigma_I^2}$$

where $\gamma_b = \sigma_w^{-2}$ is the SNR per transmitted BPSK symbol without fading, since $\text{E}[s_0^2] = 1$.

6.3 Performance evaluation

The main objective of our analysis is to assess whether the Gaussian approximation of the interfering signal I underestimates or overestimates the BER of the link. Hence, consider a (memoryless) transformation $G(\cdot)$, so that $G(I)$ is exactly Gaussian distributed, and the variances of the random variables I and $G(I)$ are equal. Since I has zero-mean and it is a product of three random variables, an odd-symmetry of the transformation function $G(\cdot)$, i.e., $G(-I) = -G(I)$, is a sufficient condition for the random variable $G(I)$ to also have a zero-mean. Furthermore, we assume that the transformation $G(\cdot)$ is a strictly increasing function in order to simplify our analysis. Note also that the Q-function is defined as,

$$Q(x) = \int_{-\infty}^{x} \frac{1}{\sqrt{2\pi}} \mathrm{e}^{-t^2/2} \mathrm{d}t = \frac{1}{2}\mathrm{erfc}\left(\frac{x}{\sqrt{2}}\right) = \frac{1}{2}\left(1 - \mathrm{erf}\left(\frac{x}{\sqrt{2}}\right)\right)$$

where $\mathrm{erf}(\cdot)$ and $\mathrm{erfc}(\cdot)$ are the error function and the complementary error function, respectively.

Using the law of transformation of random variables [93], we can relate the PDFs of the random variables $G(I)$ and I as,

$$f_{G(I)}(G(I)) = f_I(I)\, \dot{G}(I)^{-1} \tag{6.3}$$

where $\dot{G}(I)^{-1} = \left(\frac{\mathrm{d}}{\mathrm{d}I} G(I)\right)^{-1}$ is the reciprocal function of the derivative $\mathrm{d}G(I)/\mathrm{d}I$. Since we assume that the PDF $f_{G(I)}(G(I))$ of the random variable $G(I)$ is the Gaussian distribution $\mathcal{N}(0, \sigma_I^2)$, we can solve differential equation (6.3) to obtain the required transformation $G(I)$, i.e.,

$$G(I) = \sqrt{2\sigma_I^2}\, \mathrm{erf}^{-1}\left(2d(I)\right) \tag{6.4}$$

where $\mathrm{erf}^{-1}(\cdot)$ is the inverse error function [106], and,

$$d(I) = \int f_I(I)\, \mathrm{d}I + \mathcal{C}$$

and a real valued constant $\mathcal{C}$ is determined from the initial conditions; for example, we require that, $G(I) \to \infty$ for $I \to \infty$, and $G(I) \to -\infty$ for $I \to -\infty$. The function $d(I)$ can be equivalently expressed as,

$$d(I) = \frac{1}{2}\mathrm{erf}\left(\frac{G(I))}{\sqrt{2\sigma_I{}^2}}\right).$$

Note that the cumulative density function (CDF) of the interference I is given as a definite integral,

$$F_I(i) = \Big[d(I)\Big]_{-\infty}^{i} = \int_{-\infty}^{i} f_I(I)\mathrm{d}I.$$

In order to obtain the function $d(I)$, and thus, the required transformation $G(I)$, we have to first compute the PDF of the interference I. Using the law of the total probability, we get,

$$f_I(I) = \frac{1}{2} f_I(I|s = \sqrt{E_b}) + \frac{1}{2} f_I(I|s = -\sqrt{E_b}).$$

It is useful to define an auxiliary random variable $v = hz$, i.e., $I = vs$, in order to express the conditional PDF $f_I(I|s)$ as,

$$f_I(I|s) = \frac{1}{\sqrt{E_b}} f_v\left(\mathrm{sign}(s)\,\frac{I}{\sqrt{E_b}}\right)$$

so that,

$$f_I(I) = \frac{1}{2\sqrt{E_b}}\left(f_v\left(\frac{I}{\sqrt{E_b}}\right) + f_v\left(\frac{-I}{\sqrt{E_b}}\right)\right).$$

In the following, we obtain the transformation $G(I)$ for two specific examples of the distribution of the interference fading amplitude h.

6.3.1 Nakagami distribution

Assume that h has a Nakagami distribution with parameters (Ω, m), i.e., the PDF of h can be written as [8],

$$f_h(h) = \frac{2}{\Gamma(m)}\left(\frac{m}{\Omega}\right)^m h^{2m-1} e^{-\frac{mh^2}{\Omega}} \quad \text{for} \quad h \geq 0$$

where $\Omega = \mathrm{E}[h^2]$, m is the fading figure, and $\Gamma(.)$ is the gamma function. The variance of the interference I is, $\sigma_I^2 = \Omega E_b/2$. For integer values of m, the average fading power can be expressed as $\Omega = 2m\sigma_1^2$ for some value σ_1^2.

The PDF of the random variable v conditioned on the value of z can be written as,

$$f_{v|z}(v|z) = \frac{1}{|z|\,\Gamma(m)}\left(\frac{m}{\Omega}\right)^m \left|\frac{v}{z}\right|^{2m-1} \mathrm{e}^{-\frac{mv^2}{z^2\Omega}}.$$

Hence, the conditional PDF of the interference I can be expressed as,

$$f_{I|z}(I|z) = \frac{1}{|z|\,\Gamma(m)} \left(\frac{m}{E_b\Omega}\right)^m \left|\frac{I}{z}\right|^{2m-1} e^{-\frac{mI^2}{E_b z^2 \Omega}}$$

and we obtain a closed-form expression for the function $d(I)$, i.e.,

$$\begin{aligned} d(I) &= \tfrac{1}{2}\int_{-1}^{1} f_z(z) \frac{-\mathrm{sign}(I)\Gamma\left(m, \frac{mI^2}{E_b z^2 \Omega}\right)}{\Gamma(m)} \mathrm{d}z + \mathcal{C} \\ &= \frac{-\mathrm{sign}(I)}{2} + \frac{1}{2\Gamma(m)} \left(\frac{m}{E_b\Omega}\right)^m |I|^{2m} \mathrm{sign}(I) \left(\frac{\tan(m\pi)\Gamma(m)^2 {}_2\bar{\mathrm{F}}_2\left(m, m; \frac{1}{2}+m, 1+m; \frac{-mI^2}{E_b\Omega}\right)}{\sqrt{\pi}} \right. \\ &\quad \left. -\sqrt{\pi}\cos^{-1}(m\pi) \left(\frac{mI^2}{E_b\Omega}\right)^{\frac{1}{2}-m} {}_2\bar{\mathrm{F}}_2\left(\tfrac{1}{2}, \tfrac{1}{2}; \tfrac{3}{2}-m, \tfrac{3}{2}; \tfrac{-mI^2}{E_b\Omega}\right)\right) + \mathcal{C} \end{aligned}$$

where $\cos^{-1}(t) = 1/\cos(t)$, the constant $\mathcal{C} = \mathrm{sign}(I)/2$, $\Gamma(a,x) = \int_x^\infty t^{a-1}e^{-t}\mathrm{d}t$ is the incomplete gamma function, ${}_p\bar{\mathrm{F}}_q\left(a_1,\ldots,a_p;b_1,\ldots,b_q;z\right) = \frac{{}_p\mathrm{F}_q(a_1,\ldots,a_p;b_1,\ldots,b_q;z)}{\Gamma(b_1)\ldots\Gamma(b_q)}$ is the regularized generalized hypergeometric function, and ${}_p\mathrm{F}_q\left(a_1,\ldots,a_p;b_1,\ldots,b_q;z\right)$ is the generalized hypergeometric function [106]. Note also that, for $m = 1$, the inference channel fading amplitude h is Rayleigh distributed, and thus, the interference I is exactly Gaussian distributed; in this case, $G(I) = I$ is an identity transformation, and the function $d(I) = \frac{1}{2}\mathrm{erf}\left(\frac{I}{\sqrt{2\sigma_I{}^2}}\right)$.

6.3.2 Lognormal distribution

Assume now that h follows a lognormal distribution with parameters $(\bar{u}, \sigma_1)$, i.e.,

$$f_h(h) = \frac{1}{\sqrt{2\pi}h\sigma_1} e^{-\frac{(\ln h - \bar{u})^2}{2\sigma_1^2}} \quad \text{for } h \geq 0.$$

The variance of the interference I is, $\sigma_I^2 = \mathrm{E}[I^2] = \frac{E_b}{2}\mathrm{e}^{2(\bar{u}+\sigma_1^2)}$.

The PDF of the random variable v conditioned on z can be written as,

$$f_{v|z}(v|z) = \frac{1}{\sqrt{2\pi\sigma_1^2}|v|}\, \mathrm{e}^{-\frac{(\ln|\frac{v}{z}|-\bar{u})^2}{2\sigma_1^2}}$$

and the PDF of the interference I conditioned on z can be expressed as,

$$f_{I|z}(I|z) = \frac{1}{\sqrt{8\pi\sigma_1^2}|I|} \mathrm{e}^{-\frac{\left(\ln\left|\frac{I}{z\sqrt{E_b}}\right|-\bar{u}\right)^2}{2\sigma_1^2}}.$$

The function $d(I)$ is given by the following definite integral, i.e.,

$$d(I) = \frac{1}{2}\int_{-1}^{1} \frac{\text{sign}(I)}{2}\text{erf}\left(\frac{\ln\left|\frac{I}{z\sqrt{E_b}}\right| - \bar{u}}{\sqrt{2\sigma_1^2}}\right) f_z(z)\,\mathrm{d}z + \mathcal{C}$$

which can be readily computed numerically, and the constant $\mathcal{C} = \frac{\text{sign}(I)}{4}$. For example, we can use the Gauss numerical integration formula [106, §25.4], i.e.,

$$\int_{-1}^{1} F(t)\mathrm{d}t = \sum_{i=1}^{n} W_i F(t_i) + R_n$$

for some function $F(t)$ where the abscissas t_i, the weights w_i, and the expression for the approximation error R_n are given in [106, §25.4, Table 25.4].

6.3.3 BER performance

Consider the average BER denoted as $\bar{P}_I$ of the link with a single interferer corresponding to the received signal (6.1) and the average BER denoted as $\bar{P}_G$ of the link with a single Gaussian interferer corresponding to the received signal,

$$y = h_0 s_0 + G(I) + w \tag{6.5}$$

For both received signals (6.1) and (6.5), we assume the symbol-by-symbol decisions (6.3). Recall also that we assume that the mean values, $\mathrm{E}[I] = \mathrm{E}[G(I)] = 0$, and the variances, $\mathrm{E}[I^2] = \mathrm{E}\left[G(I)^2\right] = \sigma_I^2$. More importantly, note that the interference terms I and $G(I)$ are correlated with the correlation coefficient, $\rho = \sigma_I^{-2}\,\mathrm{E}_I[I \cdot G(I)]$, where, in general, $\mathrm{E}_x[F(x)]$ denotes expectation of function $F(x)$ over the distribution of a random variable x. In addition, since the transformation $G(\cdot)$ is assumed to be monotonic, we can compute the joint distribution function of the interference terms as,

$$\begin{aligned}\Pr\left(I < u, G(I) < v\right) &= \Pr\left(G(I) < v | I < u\right)\Pr\left(I < u\right) \\ &= \left(\eta(v - G(u)) + \eta(G(u) - v)\Pr\left(I < G^{-1}(v)\right)\right)\Pr\left(I < u\right)\end{aligned}$$

where $\Pr(\cdot)$ denotes the probability, $\eta(x)$ is 1 if $x \geq 0$ and 0 otherwise, and $G^{-1}(\cdot)$ is the inverse of the transformation $G(\cdot)$.

Denote as $P_I(h_0, I)$ and $P_G(h_0, I)$ the conditional BER performance of the link conditioned on the values of the channel fading amplitude h_0 and the interfering term I and $G(I)$ corresponding to the received signal (6.1) and (6.5), respectively. Hence, we can also write,

$$P_I(I) = \mathrm{E}_{h_0}[P_I(h_0, I)] \qquad P_G(I) = \mathrm{E}_{h_0}[P_G(h_0, I)]$$

and thus, for the overall average BER performance is,

$$\bar{P}_I = \mathrm{E}_I[P_I(I)] \qquad \bar{P}_G = \mathrm{E}_I[P_G(I)]$$

where $\mathrm{E}_x[F(x)]$ denotes expectation of a function $F(x)$ over the distribution of a random variable x. Note that we implicitly assume that the probabilities $P_I(h_0, I)$ and $P_G(h_0, I)$ are independent of the specific transmitted symbol s_0, i.e., for an $|\mathcal{S}|$-ary modulation constellation $\mathcal{S}$ of equi-probable symbols, the conditional BERs,

$$P_I(h_0, I) = \frac{1}{|\mathcal{S}|} \sum_{s_0 \in \mathcal{S}} P_I(h_0, I, s_0) \qquad P_G(h_0, I) = \frac{1}{|\mathcal{S}|} \sum_{s_0 \in \mathcal{S}} P_G(h_0, I, s_0).$$

We have the following proposition.

Proposition 1. *Conditioned on the interference terms I and $G(I)$, the BERs, $P_I(I) < P_G(I)$ if $I < G(I)$, and, $P_I(I) > P_G(I)$ if $I > G(I)$.* ■

Proof. Assuming the received signals (6.1) and (6.5), and the symbol-by-symbol detector (6.2) for the transmitted BPSK symbols s_0, it is straightforward to show that the conditional BERs can be computed as [8],

$$\begin{aligned} P_I(h_0, I) &= \frac{1}{2}Q((h_0 + I)\gamma_b) + \frac{1}{2}Q((h_0 - I)\gamma_b) \\ P_G(h_0, I) &= \frac{1}{2}Q((h_0 + G(I))\gamma_b) + \frac{1}{2}Q((h_0 - G(I))\gamma_b). \end{aligned}$$

Then, for any $h_0 \geq 0$, the conditional BER difference,

$$\Delta P(h_0, I) = P_I(h_0, I) - P_G(h_0, I) \geq 0 \text{ if } |I| \geq |G(I)|$$

and, for $|I| \geq |G(I)|$, the maximum value of $\Delta P(h_0, I)$ occurs for $h_0 = (|I| + |G(I)|)/2$. Similarly, for any $h_0 \geq 0$, we can show that,

$$\Delta P(h_0, I) \leq 0 \text{ if } |I| \leq |G(I)|.$$

Consequently, since the PDF $f_{h_0}(h_0) \geq 0$, we have that,

$$\mathrm{E}_{h_0}[\Delta P(h_0, I)] = \Delta P(I) \begin{cases} \geq 0 & \text{if } |I| \geq |G(I)| \\ \leq 0 & \text{if } |I| \leq |G(I)| \end{cases}.$$

■

6.3.4 Proposed performance metric

Our aim is to assess whether the Gaussian approximation of the interference underestimates or overestimates the (true) BER. In particular, we assess the sign of the average BER difference,

$$\Delta\bar{P} = \mathrm{E}_I[\Delta P(I)] = \mathrm{E}_I[P_I(I) - P_G(I)]$$

since $\Delta\bar{P} > 0$ indicates that the Gaussian approximation underestimates the BER, and $\Delta\bar{P} < 0$ indicates that the standard Gaussian approximation overestimates the BER.

Assuming Proposition 1, we have that the sign of the conditional BER difference $\Delta P(I)$ is given by the sign of the difference, $I - G(I)$. In addition, using eq. (6.4), we can show that the condition $I < G(I)$ and $I > G(I)$, respectively, is equivalent to, $\frac{1}{2}\mathrm{erf}\left(I/\sqrt{2{\sigma_I}^2}\right) < d(I)$, and, $\frac{1}{2}\mathrm{erf}\left(I/\sqrt{2{\sigma_I}^2}\right) > d(I)$. Hence, in order to assess whether the standard Gaussian approximation underestimates or overestimates the link BER, we consider the function,

$$\mathcal{M}(I) = \frac{1}{2}\mathrm{erf}\left(\frac{I}{\sqrt{2\sigma_I^2}}\right) - d(I).$$

After some manipulations, we equivalently obtain the expression,

$$\mathcal{M}(I) = Q(G'(I)) - Q(I')$$

where

$$G'(I) = \frac{G(I)}{\sigma_I} \quad \text{and} \quad I' = \frac{I}{\sigma_I}$$

are the normalized interference terms having the unit variances. For instance, if the interference fading amplitude h is Rayleigh distributed, then $G(I) = I$ and $\mathcal{M}(I) = 0$ for $\forall I$.

Since the interference I and its transformation $G(I)$ are random variables, we consider the average metric,

$$\bar{\mathcal{M}} = \mathrm{E}_I[\mathcal{M}(I)] = \int_0^\infty \mathcal{M}(I) f_I(I) \mathrm{d}I. \tag{6.6}$$

The metric (6.6) may have to be evaluated numerically for the specific distribution of the interference I, i.e., for the specific distribution of the interference fading amplitude h. However, for numerical convenience, we can instead evaluate an upper bound of the metric (6.6), i.e., let,

$$\bar{\mathcal{M}} \leq \int_0^\infty \mathcal{M}(I) \mathrm{d}I = \bar{\mathcal{M}}_1. \tag{6.7}$$

Note that the integration in (6.7) does not converge when calculated term-by-term. For a Nakagami distributed interference fading amplitude h, we can obtain a closed form expression of the upper bound $\bar{\mathcal{M}}_1$, i.e.,

$$\bar{\mathcal{M}}_1 = \frac{1}{2}\sqrt{\frac{E_b\Omega}{\pi}}\left(\frac{2\sqrt{m\pi}\cos^{-1}(m\pi)}{\Gamma(\frac{1}{2}-m)\Gamma(1+m)} - 1\right).$$

Note that the limits, $\lim_{m\to 1/2}\frac{\cos^{-1}(m\pi)}{\Gamma(1/2-m)} = \lim_{m\to 3/2}\frac{\cos^{-1}(m\pi)}{\Gamma(1/2-m)} = \frac{1}{\pi}$, and, $\lim_{\mathrm{SIR}\to\infty}\bar{\mathcal{M}}_1 = \lim_{\sigma_I^2\to 0}\bar{\mathcal{M}}_1 = 0$. Hence and importantly, the upper bound $\bar{\mathcal{M}}_1$ can be used to indicate whether the standard Gaussian approximation of the interference overestimates or underestimates the link BER. This is formulated more precisely in the following proposition.

Proposition 2. *Consider the average BER performance difference, $\Delta\bar{P} = \mathrm{E}_I[\Delta P(I)]$. The positive values $\bar{\mathcal{M}}_1 > 0$ indicate that the Gaussian approximation of the interference underestimates the link BER, $\bar{P}_I$, and the negative values $\bar{\mathcal{M}}_1 < 0$ indicate that the Gaussian approximation of the interference $G(I)$ overestimates the link BER, $\bar{P}_I$.* ■

Proof. Using Proposition 1 and eq. (6.4), we can show that if $G(I) > I$ or $G(I) < I$, then the integrand in (6.7) is less than 0 or greater than 0, respectively. Consequently, the sign of $\bar{\mathcal{M}}_1$ is indicative of the sign of the average BER difference $\Delta\bar{P}$. ■

Furthermore, the smaller values of magnitude $|\bar{\mathcal{M}}_1|$ suggest that, in general, the standard Gaussian approximation of the interference will less bias the average BER of the link. However, note that the value $\bar{\mathcal{M}}_1 = 0$ cannot be used to detect whether the interference is Gaussian distributed.

6.4 Numerical examples

In our numerical examples, we assume that the transmitted signal is subject to a Rayleigh fading h_0 of the unit average power,i.e., $\mathrm{E}[h_0^2] = 1$. Fig. 6.1 and Fig. 6.2 show the average BER $\bar{P}_I$ and $\bar{P}_G$ of the link versus SIR for the SNR $\gamma_b = 10$dB assuming that the interference fading amplitudes are either Nakagami or lognormally distributed.

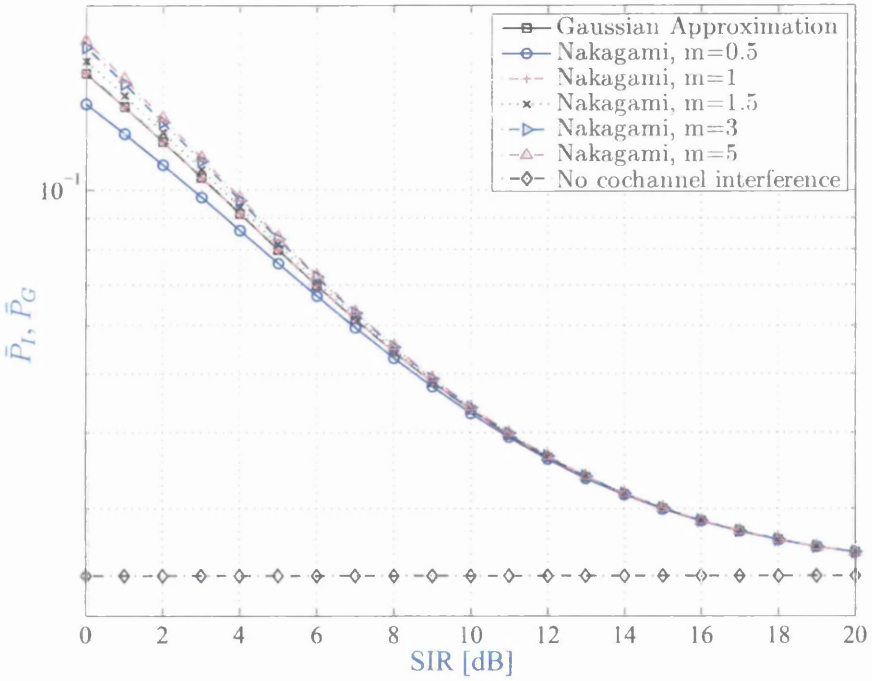

Figure 6.1: The link average BER versus SIR for the Nakagami distributed interference fading amplitude and the SNR $\gamma_b = 10$dB.

We observe that, for the Nakagami distribution, depending on the value of the parameter m, the standard Gaussian approximation corresponding to the BER $\bar{P}_G$ can both overestimate and underestimate the link BER $\bar{P}_I$. On the other hand, for the lognormal distribution, the larger the value of the parameter $\bar{u}$, the more the Gaussian approximation overestimates the link BER. The average BER difference $\Delta\bar{P} = \bar{P}_I - \bar{P}_G$ curves corresponding to the BER curves in Fig. 6.1 and Fig. 6.2 are shown in Fig. 6.3 and Fig. 6.4. As expected, for the Nakagami distribution with $m = 1$, the Gaussian approximation is exact, and, for both interference fading distributions considered, the

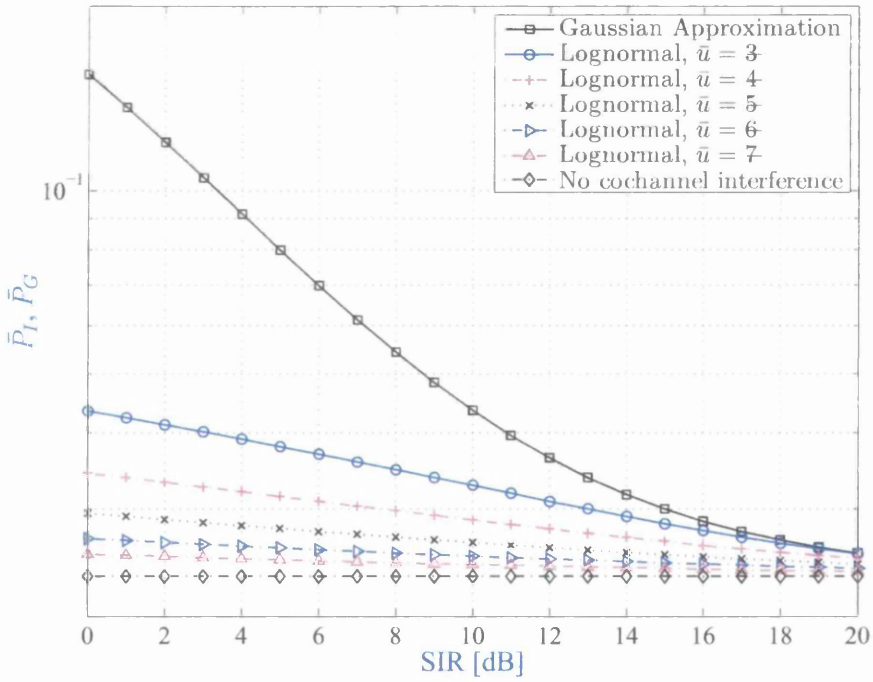

Figure 6.2: The link average BER versus SIR for the lognormal distributed interference fading amplitude and the SNR $\gamma_b = 10$dB.

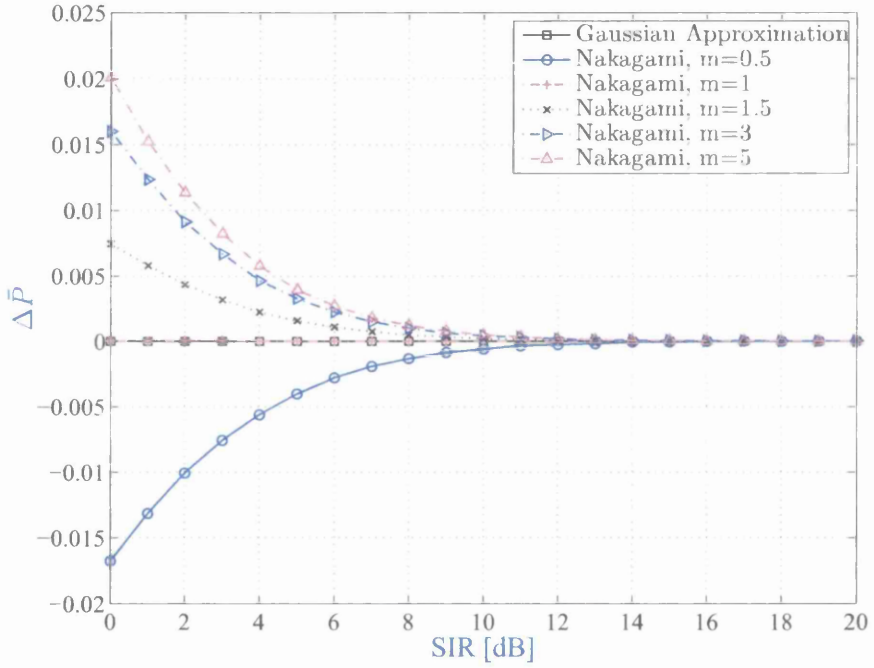

Figure 6.3: The link average BER difference versus SIR for the Nakagami distributed interference fading amplitude and the SNR $\gamma_b = 10$dB.

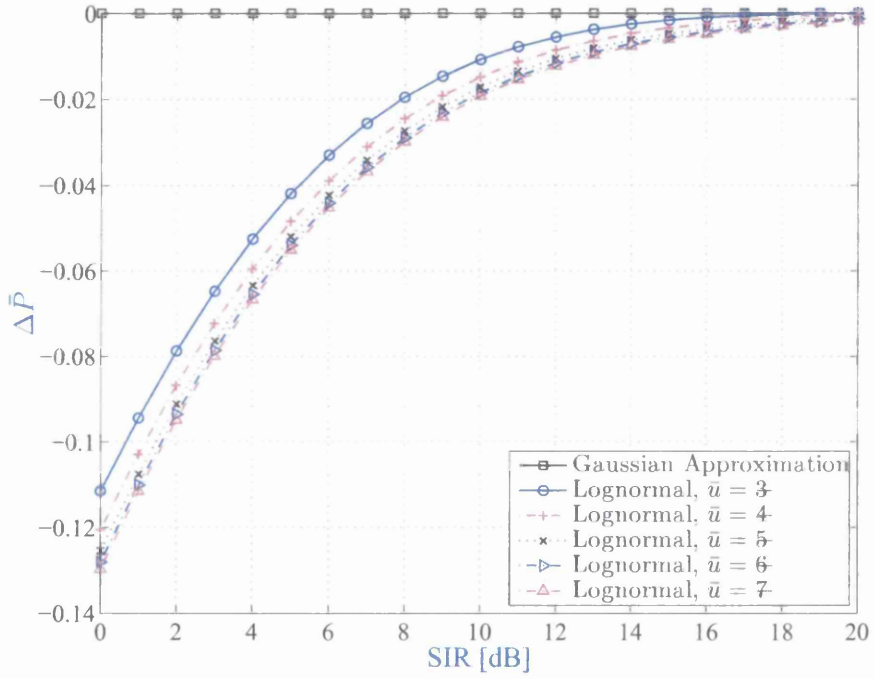

Figure 6.4: The link average BER difference versus SIR for the lognormal distributed interference fading amplitude and the SNR $\gamma_b = 10$dB.

Gaussian approximation becomes more accurate with increasing values of SIR. The selected range of distributions parameters in Fig. 6.3 and Fig. 6.4 shows that the estimation error of the error rate,when using Gaussian approximation, can vary in a range of order 10^{-2} for Nakagami case and 10^{-1} for lognormal case.

The proposed metric curves $\bar{\mathcal{M}}_1$ versus SIR corresponding to the average BER difference curves in Fig. 6.3 and Fig. 6.4 are shown in Fig. 6.5 and Fig. 6.6. More

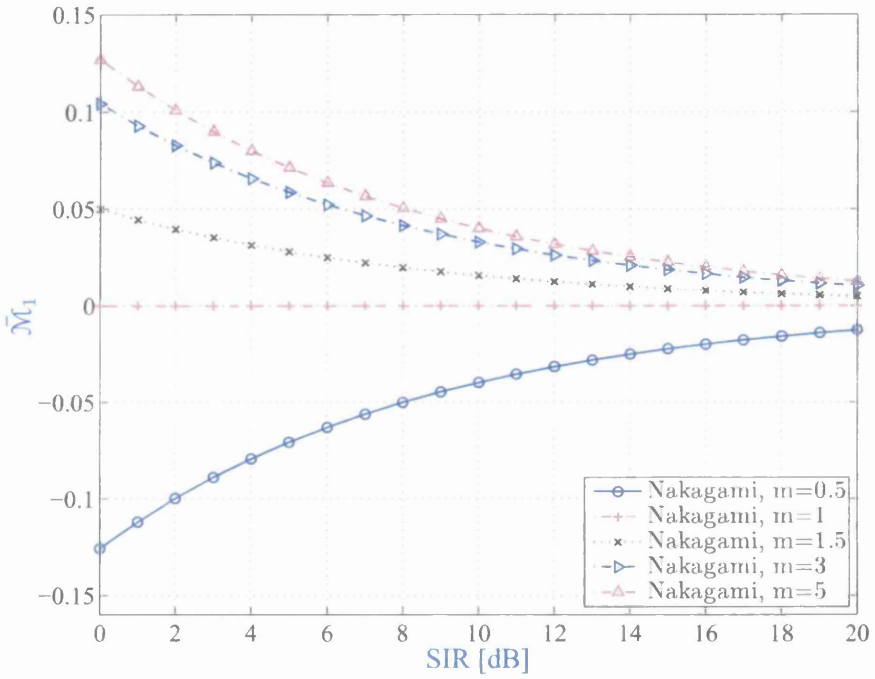

Figure 6.5: The metric $\bar{\mathcal{M}}_1$ versus SIR for the Nakagami distributed interference fading amplitude and the SNR $\gamma_b = 10$dB.

importantly, we observe that the proposed metric curves $\bar{\mathcal{M}}_1$ in Fig. 6.5 and Fig. 6.6 can be used to accurately predict whether the Gaussian approximation of the interference overestimates or underestimates the link average BERs in Fig. 6.1 and Fig. 6.2 which further confirms the validity of Proposition 2.

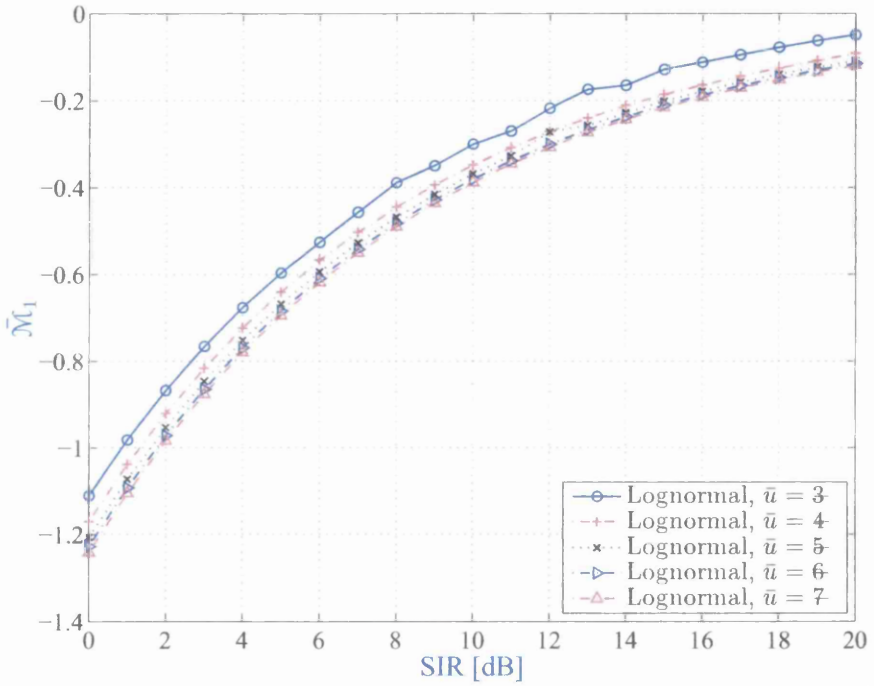

Figure 6.6: The metric $\bar{\mathcal{M}}_1$ versus SIR for the lognormal distributed interference fading amplitude and the SNR $\gamma_b = 10$dB.

6.5 Conclusions

A novel metric was derived that can indicate whether the standard Gaussian approximation of the interference underestimates or overestimates the average BER of the link operating over a frequency non-selective fading channel. Interestingly, the proposed metric is computed for a given distribution of the interfering signal. However, it is otherwise independent of the actual distribution of the desired signal. A closed-form expression of the proposed metric was obtained for the Nakagami distribution of the interference fading amplitude. Numerical examples confirming the validity of the proposed metric were obtained for the case of the Nakagami and lognormally distributed interference fading amplitudes. In addition, the interferer distribution construction is shown to have a significant impact on the error rate performance difference from Gaussian approximation. In particular, the lognormal interferer distribution which represents shadowing effect, has more significant impact on error rate difference than Nakagami interferer distribution which represents multi-path fading effect.

7

Conclusions and Future Work

This chapter gives the overall thesis conclusions and provides suggestions for the future work. It is organized as follows. Section 7.1 presents the main findings of the thesis. Section 7.2 suggests some possible future extended research based on the work that has been done in this thesis.

7.1 Summary of main findings

In Chapter 3, statistics of the conditional error rates of digital modulations over fading channels were considered. The probability density function and the higher order moments of the conditional error rates were obtained using the Prony approximation. For a Ricean distributed channel fading amplitude at the detector input, non-monotonic behavior of the moments of the conditional bit error rates versus some channel model parameters was observed. The non-monotonic behavior of the moments of the conditional BER versus the standard deviation per dimension of the Ricean channel fading has the following practical consequences on the design of communication systems.

The first order non-central moment corresponding to the average BER can be minimized for small values of the standard deviation and non-zero values of the non-centrality (line of sight) parameter; this renders the channel to be more benign and to behave as an AWGN channel model. In practice, the smaller values of standard deviation can be equivalently achieved by decreasing the transmission power. The

transmission power reduction is particularly feasible for line-of-sight communication links using low-order linear modulations and having larger values of the non-centrality parameter.

The second central moment (i.e., the variance) of the conditional BER is a measure of the spread of the random conditional BER values about their mean. The small spread of the conditional BER values corresponds to the small variations of the instantaneous SNR values about their mean; this is desirable when the transmission power control and the receiver automatic gain control are used. The variance of the conditional BER is important in delay limited communications when the receiver is processing received sequences of relatively small length. When the BER variance is large, the conditional BER values can deviate significantly from their expected value (i.e., their first non-central moment).

The Bollinger bands considered can be used to describe the BER of the communication systems operating over time-varying channels. More importantly, the upper bound of the Bollinger band represents the worst case BER performance corresponding to the deep fades, and the lower bound of the Bollinger band indicates more benign channel conditions.

Two problems of the delay limited transmission were investigated in Chapter 4 and Chapter 5. In Chapter 4, the error rate performance measures were investigated for communication systems with non-ergodic transmissions. An equivalent system model for transmission of a single finite length sequence of bits over a BSC was adopted. Such system model was shown to represent the transmission of a finite number of frames employing a properly designed FEC coding over a block fading channel. The instantaneous BER measure was defined for the equivalent system model as a ratio of bits in error to the total number of bits received so far. Since the actual number of bits in error is not known in practical receivers, the credible interval estimators of the instantaneous BER for a single received sequence of finite length were investigated. The DOE measure was introduced to quantify the level of ergodicity for the instantaneous BER. A threshold value of the DOE was then used to define the non-ergodic and ergodic zones of operation of the data detector processing the sequence of received bits. For the case of a BSC and assuming perfect knowledge of its crossover probability at the receiver, three credible interval estimators of the instantaneous BER were obtained.

Several properties of the DOE measure were proved. In particular, it was shown that the channel uncertainty at the receiver reduces ergodicity of the received sequence, so that a longer received sequence is required before the instantaneous BER converges to its expected value. In addition, it was proved that the optimum maximum-likelihood detector has the fastest transition from the non-ergodic to ergodic zone among all data detectors.

The system design implications of the non-ergodic BER analysis were illustrated using several examples. The design goal was to guarantee a worst case instantaneous BER performance with a given probability. In particular, the parameters of a hypothetical adaptive binary linear block code were obtained for each transmitted packet using an upper bound of the instantaneous BER rather than using the expected BER that is only meaningful for asymptotically large number of transmitted packets. In addition, the adaptive transmitter power was used to control the crossover probability of an equivalent BSC to guarantee the worst case instantaneous BER with a given probability. Consequently, by varying the parameters of a FEC coding, and by varying the transmitter power, it is possible to achieve the transmission ergodicity for a smaller number of transmitted packets.

In Chapter 5, a novel retransmission scheme using random permutations at the receiver to decide which bits in the packet should be retransmitted was proposed and its BER performance as well as the throughput have been analyzed. The proposed scheme does not employ the FEC coding, nor does not relay on the CRC bits to detect the transmission errors. However, the proposed scheme assumes a delay limited number of retransmissions, and it was designed assuming a reliable reverse link to deliver error-free feedback messages from the destination to the source. Thus, using the random permutations, it is guaranteed that only the bits within the received packet having small reliabilities are selected for retransmission. The retransmitted bits are combined at the destination receiver using a low complexity diversity combining. This has an overall benign effect on the implementation complexity and the transmission efficiency of the proposed scheme.

Three strategies to select the parameters of the proposed retransmission scheme were considered. These parameters were optimized to achieve the minimum BER. The performance of the proposed retransmission scheme was compared to the block

repetition code corresponding to a conventional ARQ retransmission strategy. It was shown that, for the same number of retransmissions, and the same packet length, the proposed scheme always outperforms such repetition coding, and, in some scenarios, the performance improvement is found to be significant. Numerical examples were used to verify the derived mathematical expressions and approximations by computer simulations. Most of our analysis has been done for the case of AWGN channel, however, the case of a slow Rayleigh block fading channel was also investigated. However, the proposed scheme appears to provide the throughput and the BER reduction gains only for the medium to large SNR values.

In Chapter 6, a novel metric was derived that can indicate whether the standard Gaussian approximation of the interference underestimates or overestimates the average BER of the link operating over a frequency non-selective fading channel. Interestingly, the proposed metric is computed for a given distribution of the interfering signal. However, it is otherwise independent of the actual distribution of the desired signal. A closed-form expression of the proposed metric was obtained for the Nakagami distribution of the interference fading amplitude. Numerical examples confirming the validity of the proposed metric were obtained for the case of the Nakagami and lognormally distributed interference fading amplitudes.

7.2 Future work

The Bollinger bands investigated in Chapter 3 can be seen as a form of the statistical interval estimators. Therefore, these bands can be interpreted in terms of the probability and be compared with the credible intervals proposed in Chapter 4. In addition, since the Bollinger bands have a potential to represent the error rate performance conditioned on the fading, one may consider developing receiver techniques based on the Bollinger bands. Moreover, the presented non-ergodic analysis in Chapter 4 can be made more feasible by assuming the usage of the confidence intervals to estimate the cross over probability.

The proposed retransmission scheme in Chapter 5 has the main disadvantage of possibly long waiting delay times. Therefore, one may consider using this unused

waiting time to transmit additional information to improve the total throughput as in the go-back-N ARQ or selective repeat ARQ. In addition, although the proposed scheme is designed for the truncated ARQ, the performance analysis is based on the ergodic measures. Therefore, one may consider evaluating the instantaneous error rate performance of the proposed scheme based on the interval estimators.

The proposed error rate metric in Chapter 6 can be used to assess the error rate performance analytically for a single interferer case in comparison with the infinite number of interferers. However, even though it can give an indication of the system performance, it does not provide the exact system performance independently from the Gaussian approximation. One may consider improving the proposed error rate metric to evaluate the exact error rate performance.

Appendix A

Review of Some Probability Distributions

The random variables are usually described by their probability density function (PDF) for continuous random variables, probability mass function (PMF) for discrete random variables, cumulative distribution function (CDF) for continuous random variables, cumulative mass function (CMF) for discrete random variables and moments. There are some distributions that have been used very frequently to model the wireless communication channels. In this appendix, we summarize those that have been assumed in the thesis work using the references [8, 133, 134].

A.1 Binomial distribution

Assume X is a discrete random variable that has two possible outcome values with probabilities p and $1-p$ respectively. Suppose that the random variable Y is defined as,

$$Y = \sum_{i=1}^{n} X_i. \tag{A.1}$$

where X_i, $i = 1, 2, \ldots, n$, are statistically independent and identically distributed random variable. Then, the random variable Y has the binomial PMF $f_Y(y)$ defined as,

$$f_Y(y) = \sum_{k=0}^{n} \binom{n}{k} p^k (1-p)^{n-k} \delta(y-k). \tag{A.2}$$

where $\binom{n}{k}$ is the binomial coefficient, and $\delta(.)$ is the delta function. The CMF of Y $F_Y(y)$, is,

$$F_Y(y) = \sum_{k=0}^{[y]} \binom{n}{k} p^k (1-p)^{n-k}. \tag{A.3}$$

where $[y]$ is the largest integer m such that $m \leq y$. The first two moments are,

$$\mathrm{E}[Y] = np. \tag{A.4}$$

$$\mathrm{E}[Y^2] = np(1-p) + n^2p^2. \tag{A.5}$$

$$\sigma_Y{}^2 = np(1-p). \tag{A.6}$$

and the characteristic function $\phi_Y(v)$ is,

$$\phi_Y(v) = (1 - p + pe^{Jv})^n. \tag{A.7}$$

where $J = \sqrt{-1}$.

The binomial distribution is usually used to model the communication system channel in the most simplest forms, i.e., the binary symmetric channel (BSC) model.

A.2 Uniform distribution

The uniform distribution can be used for either continuous or discrete random variables. It is also called the equally likely outcomes distribution. If X is a continuous

uniformly distributed random variable, then X has the PDF,

$$f_X(x) = \begin{cases} \frac{1}{b-a} & \text{for } a \leq x \leq b \\ 0 & \text{for } x < a \text{ or } x > b. \end{cases} \tag{A.8}$$

where a and b is the minimum and maximum value of the random variable X, respectively. The CDF of X is,

$$F_X(x) = \begin{cases} 0 & \text{for } x < a \\ \frac{x-a}{b-a} & \text{for } a \leq x < b \\ 1 & \text{for } x \geq b. \end{cases} \tag{A.9}$$

The first two moments are,

$$\mathrm{E}[X] = \frac{a+b}{2} \tag{A.10}$$

$$\mathrm{E}[X^2] = \frac{a^2+b^2+ab}{3} \tag{A.11}$$

$$\sigma_X{}^2 = \frac{(a-b)^2}{12} \tag{A.12}$$

The characteristic function $\phi_X(v)$ is,

$$\phi_X(v) = \frac{e^{Jvb} - e^{Jva}}{Jv(b-a)} \tag{A.13}$$

The continuous uniform distribution is usually used to model the randomness of the phase under fading conditions in the wireless communication channels.

However, if K is a discrete uniformly distributed random variable, then K has the PMF,

$$f_K(k) = \begin{cases} \frac{1}{n} & \text{for } a \leq k \leq b \\ 0 & \text{otherwise.} \end{cases} \tag{A.14}$$

where $n = b - a + 1$ is the number of possible outcomes, a and b are the minimum and maximum values of the random variable K, respectively. The CMF of K is,

$$F_K(k) = \begin{cases} 0 & \text{for } k < a \\ \frac{k-a+1}{n} & \text{for } a \leq k \leq b \\ 1 & \text{for } k > b. \end{cases} \tag{A.15}$$

The first two moments are,

$$\mathrm{E}[K] = \frac{a+b}{2}. \tag{A.16}$$

$$\mathrm{E}[K^2] = \frac{4n^2+3n+1}{6}. \tag{A.17}$$

$$\sigma_K{}^2 = \frac{n^2-1}{12}. \tag{A.18}$$

and the characteristic function $\phi_K(v)$ is,

$$\phi_K(v) = \frac{e^{Jav} - e^{J(b+1)v}}{n(1-e^{Jv})}. \tag{A.19}$$

The discrete uniform distribution is usually used in random number generators.

A.3 Gaussian (normal) distribution

The Gaussian or normal random variable X has the PDF,

$$f_X(x) = \frac{1}{\sqrt{2\pi\sigma_X{}^2}} e^{-\frac{(x-\mu_X)^2}{2\sigma_X{}^2}}. \tag{A.20}$$

where μ_X is the mean and $\sigma_X{}^2$ is the variance of the random variable X. The CDF of X is,

$$F_X(x) = 1 - Q(\frac{x-\mu_X}{\sigma_X}). \tag{A.21}$$

where $Q(.)$ is the Q function.

The n-th central moment M_n of X can be expressed as,

$$M_n = \begin{cases} 1.3.5\ldots(n-1)\sigma_X{}^n & \text{for odd n} \\ 0 & \text{for even n.} \end{cases} \tag{A.22}$$

The n-th moment can be expressed in terms of the central moments as,

$$\mathrm{E}[X^n] = \sum_{i=0}^{n} \binom{n}{i} \mu_X{}^i M_{n-i}. \tag{A.23}$$

Note that Eq. (A.23) is true in general for any random variable. The characteristic function $\phi_X(v)$ is,

$$\phi_X(v) = e^{Jv\mu_X - \frac{v^2\sigma_X{}^2}{2}}. \tag{A.24}$$

The Gaussian distribution is used to model the noise statistics, i.e. additive white Gaussian noise (AWGN) model, in many wireless communication systems.

A.4 Chi-square distribution

The Chi-square distribution is a form of transforming the Gaussian distribution. More precisely, let X_i are statistically independent and identically distributed Gaussian random variables, each with variance σ^2, where $i = 1, 2, \ldots, n$, and n denotes the number of random variables or the distribution degrees of freedom. Then, define Y to be a random variable,

$$Y = \sum_{i=1}^{n} X_i{}^2. \tag{A.25}$$

The distribution of Y is called the Chi-square distribution with n degrees of freedom. The chi-square distribution can be the central Chi-square distribution when X_i has zero mean, or the non-central Chi-square distribution when X_i has nonzero mean.

A.4.1 Central chi-square distribution

The central Chi-square random variable Y with n degrees of freedom has the PDF,

$$f_Y(y) = \frac{1}{\sigma^n 2^{\frac{n}{2}}\Gamma(\frac{n}{2})} y^{\frac{n}{2}-1} e^{-\frac{y}{2\sigma^2}} \quad y \geq 0. \tag{A.26}$$

The CDF of Y for even n is,

$$F_Y(y) = 1 - e^{-\frac{y}{2\sigma^2}} \sum_{k=0}^{\frac{n}{2}-1} \frac{1}{k!} \left(\frac{y}{2\sigma^2}\right) \quad y \geq 0. \tag{A.27}$$

where $(.)!$ denotes the factorial. The first two moments are,

$$\mathrm{E}[Y] = n\sigma^2. \tag{A.28}$$

$$\mathrm{E}[Y^2] = 2n\sigma^4 + n^2\sigma^4. \tag{A.29}$$

$$\sigma_Y{}^2 = 2n\sigma^4. \tag{A.30}$$

and the characteristic function of Y is,

$$\phi_Y(v) = \frac{1}{(1 - J2v\sigma^2)^{\frac{n}{2}}} \tag{A.31}$$

The central Chi-square distribution is usually used to model the fading power statistics in the non-line of sight communication scenarios.

Rayleigh distribution

The Raleigh distributed random variable Z is obtained by direct transformation to of the central Chi-square random variable Y as,

$$Z = \sqrt{Y}. \tag{A.32}$$

Next, we consider the Rayleigh distribution assuming two degrees of freedom ($n = 2$). Thus, the PDF of the Rayleigh random variable Z is,

$$f_Z(z) = \frac{z}{\sigma^2} e^{-\frac{z^2}{2\sigma^2}} \quad z \geq 0. \tag{A.33}$$

The CDF of Z is,

$$F_Z(z) = 1 - e^{-\frac{z^2}{2\sigma^2}} \quad z \geq 0. \tag{A.34}$$

The k-th moment of Z is,

$$\mathrm{E}[Z^k] = (2\sigma^2)^{\frac{k}{2}} \Gamma(1 + \frac{k}{2}). \tag{A.35}$$

and the variance is,

$$\sigma_Z{}^2 = (2 - \frac{\pi}{2})\sigma^2. \tag{A.36}$$

The characteristic function of Z is,

$$\phi_Z(v) = -e^{-\frac{v^2\sigma^2}{2}} \sum_{i=0}^{\infty} \frac{\left(\frac{v^2\sigma^2}{2}\right)^i}{(2i-1)k!} + J\sqrt{\frac{\pi}{2}} v\sigma^2 e^{-\frac{v^2\sigma^2}{2}}. \tag{A.37}$$

The Rayleigh distribution is usually used to model the fading amplitude statistics in the non-line of sight wireless commutation scenarios.

A.4.2 Non-central chi-square distribution

The non-central Chi-square distributed random variable Y with n degrees of freedom, has the PDF,

$$f_Y(y) = \frac{1}{2\sigma^2}\left(\frac{y}{s^2}\right)^{\frac{n-2}{4}} e^{-\frac{s^2+y}{2\sigma^2}} I_{\frac{n}{2}-1}\left(\frac{s\sqrt{y}}{\sigma^2}\right) \quad y \geq 0. \tag{A.38}$$

where $I_\alpha(.)$ is the αth order modified Bessel function of the first kind, $s^2 = \sum_{i=1}^{n} {m_i}^2$ is the non-centrality parameter and m_i are the mean values of the X_i in (A.25).

The CDF of Y for even n is,

$$F_Y(y) = 1 - Q_{\frac{n}{2}}\left(\frac{s}{\sigma}, \frac{\sqrt{y}}{\sigma}\right) \tag{A.39}$$

where $Q_{\frac{n}{2}}(.,.)$ is the generalized Marcum's Q function. The first two moments are,

$$\mathrm{E}[Y] = n\sigma^2 + s^2. \tag{A.40}$$

$$\mathrm{E}\left[Y^2\right] = 2n\sigma^4 + 4\sigma^2 s^2 + (n\sigma^2 + s^2)^2. \tag{A.41}$$

$${\sigma_Y}^2 = 2n\sigma^4 + 4\sigma^2 s^2. \tag{A.42}$$

The characteristic function of Y is,

$$\phi_Y(v) = \frac{1}{(1 - J2v\sigma^2)^{\frac{n}{2}}} e^{\frac{Jvs^2}{1-J2v\sigma^2}}. \tag{A.43}$$

The non-central Chi-square distribution is used to model the fading power statistics in the line-of-sight communication scenarios.

Rice distribution

The Rice distribution is related to the non-central Chi-square distribution similarly as the Rayleigh distribution is related to the central Chi-square distributions in (A.32). The Ricean distributed random variable Z with n degrees of freedom has the PDF,

$$f_Z(z) = \frac{z^{\frac{n}{2}}}{\sigma^2 s^{\frac{n-2}{2}}} e^{-\frac{z^2+s^2}{2\sigma^2}} I_{\frac{n}{2}-1}(\frac{zs}{\sigma^2}) \quad z \geq 0. \tag{A.44}$$

The CDF of Z for even n,

$$F_Z(z) = 1 - Q_{\frac{n}{2}}\left(\frac{s}{\sigma}, \frac{z}{\sigma}\right) \tag{A.45}$$

The Rice distribution is usually used to model the fading amplitude statistics in the line-of-sight wireless commutation scenarios.

A.5 Nakagami distribution

The Nakagami distributed random variable X has the PDF,

$$f_X(x) = \frac{2}{\Gamma(m)} \left(\frac{m}{\Omega}\right)^m x^{2m-1} e^{-\frac{mx^2}{\Omega}} \tag{A.46}$$

where $\Omega = \mathrm{E}[X^2]$, m is called the fading figure and it is defined as the ratio of moments, i.e.,

$$m = \frac{\Omega^2}{\mathrm{E}[(X^2 - \Omega)^2]}. \tag{A.47}$$

The Nakagami distribution is usually used to model the fading amplitude statistics in different scenarios in wireless communication systems. As a special case, for $m = 1$, the Nakagami distribution becomes the Rayleigh distribution.

A.6 Lognormal distribution

The lognormal random variable Y is defined as the natural logarithm of a Gaussian distributed random variable X with mean μ_X and variance σ_X. The PDF of Y is,

$$f_Y(y) = \begin{cases} \frac{1}{\sqrt{2\pi\sigma_X{}^2 y^2}} e^{-\frac{(\ln(y)-\mu_X)^2}{2\sigma_X{}^2}} & y \geq 0 \\ 0 & r < 0. \end{cases} \tag{A.48}$$

where $\ln(.)$ denotes the natural logarithm.

The lognormal distribution is usually used to model the effect of shadowing in the wireless communication systems.

Bibliography

[1] M. Deru and P. Torcellini, "Performance Metrics Research Project - Final Report," National Renewable Energy Laboratory, Tech. Rep. NREL/TP-550-38700, Oct. 2005. 1

[2] M. A. M. Hassanien and P. Loskot, "Higher Order Moments of Error Rates of Digital Modulations ," in *IEEE VTC-2010 Spring Conf. 71th* , May 2010, pp. 1–5. 6

[3] M. A. M. Hassanien and P. Loskot, "Non-Ergodic Error Rate Analysis of Finite Length Received Sequences," in *Int. Conf. Wireless Comm. Signal Proces.*, Nov. 2009, pp. 1–5. 7, 27, 28

[4] M. A. M. Hassanien and P. Loskot, "Non-ergodic Error Rate Analysis of a Single Finite Length Sequence Over BSC," *in Preparation to be Submitted to IEEE Trans. Commun.*, Dec. 2011. 7

[5] M. A. M. Hassanien and P. Loskot, "Improving Link Reliability Complexity Trade-Off by Exploiting Reliable Feedback Signaling," in *ISWCS* , Sep. 2010, pp. 775–779. 7

[6] M. A. M. Hassanien and P. Loskot, "Improving Link Reliability Complexity Trade-Off by Exploiting Reliable Feedback Signaling," in *in Preparation to be Submitted to IEEE Trans. Sign. Proc.*, Jan. 2012. 7

[7] M. A. M. Hassanien and P. Loskot, "Assessment of the Link Performance with a Single Interferer," *Submitted to IEEE Trans. Commun.*, Jul. 2011. 8

[8] J. G. Proakis, *Digital Communications*, 4th ed. McGraw-Hill, 2001. 11, 20, 21, 32, 40, 43, 45, 68, 77, 111, 114, 129

[9] A. Papoulis, *Probability, Random Variables and Stochastic Processes*, 3rd ed. McGraw-Hill, 1991. 11, 12, 41, 45

[10] W. Gardner, *Introduction To Random Processes With Applications To Signals and Systems*. Macmillan Publishing Company, 1986. 11, 12, 13, 15, 41, 53

[11] R. E. Ziemer and W. H. Tranter, *Principles of Communications*, 5th ed. Willey & sons, 2002. 11, 15

[12] A. Wolf, "Mean ergodic Theorems and Tests for a Certain Class of Random Processes," in *Proc. of the IEEE J.*, vol. 51, no. 6, 1963, pp. 403–404. 12

[13] M. K. Simon and M.-S. Alouini, *Digital Communication over Fading Channels*, 2nd ed. Willey & sons, 2005. 13

[14] E. Lehmann and G. Casella, *Theory of Point Estimation*, 2nd ed. Springer, 1998. 14

[15] F. A. G. A. M. Mood and D. C. Boes, *Introduction to the Theory of Statistics*, 3rd ed. McGraw-Hill, 1974. 14

[16] S. M. Kay, *Fundamentals of Statistical Signal Processing,Volume II: Detection Theory*. Prentice Hall, 1998. 15

[17] S. M. Kay, *Fundamentals of Statistical Signal Processing,Volume I: Estimation Theory*. Prentice Hall, 1993. 15

[18] H. L. V. Trees, *Detection, Estimation, and Modulation Theory, Part I*. Wiley-Interscience, 2001. 15

[19] N. Mukhopadhyay, *Probability and Statistical Inference*. Marcel Dekker Inc., 2000. 15, 41, 44

[20] O. Kallenberg, *Foundations of Modern Probability*. Springer, 1997. 15, 41, 44

[21] D. Karlen, "Credibility of Confidence Intervals," in *Proc. C. Adv. Statistical Tec. in Particle Phy.*, 2002, pp. 53–57. 16

[22] T. Bayes, "Essay Towards Solving a Problem in the Doctrine of Chances," *Phil. Trans.*, pp. 370–418, 1764. 16

[23] A.Glavieux, *Channel Coding in Communication Network*, 1st ed. London ISTE Ltd, 2007. 16, 17

[24] C. E. Shannon, "Mathematical theory of communication," *Bell Syst. Tech*, pp. 379–423, 1948. 16, 21

[25] S. Lin and D. J. Costello, *Error control coding: Fundamentals and Applications*. New Jersey:Pearson Education Inc, 2004. 16, 17

[26] S. Moon, *Error Correction Coding:Mathematical Methods and Algorithms*, 2nd ed. New Jersey:Willey & sons, 2005. 17

[27] A. S. Tanenbaum, *Computer Networks (International Edition)*, 4th ed. Pearson Education, 2002. 17

[28] J. F. Kurose and K. W. Ross, *Computer Networking: International Version: A Top-Down Approach*, 5th ed. Pearson Education, 2009. 17

[29] R. Comroe and D. Costello, " ARQ Schemes for Data Transmission in Mobile Radio Systems," *IEEE J. Select. Areas Commun.*, pp. 472–481, 1984. 17, 18

[30] S. P. P. Frenger and E. Dahlman, "Performance Comparison of HARQ with Chase Combining and Incremental Redundancy for HSDPA," in *Vehicular Technology Conference, 2001. VTC 2001 Fall. IEEE VTS 54th*, vol. 3, 2001, pp. 1829 –1833. 18

[31] J. S. E. Dahlman, S. Parkvall and P. Beming, *3G Evolution: HSPA and LTE for Mobile Broadband*, 2nd ed. Academic Press, 2008. 18

[32] P. L. Ecuyer, "Uniform Random Number Generators," in *Proc. of the 1998 Winter Simulation Conference, IEEE Press*, Dec. 1998, pp. 97 –104. 19

[33] P. L. Ecuyer, "Uniform Random Number Generation," *Annals of Operations Research*, vol. 53, pp. 77 –120, 1994. 19

[34] J. N. Laneman, "Cooperative diversity in wireless networks: Algorithms and architectures," Ph.D. dissertation, MIT, 2002. 21

[35] E. E. A.Sendonaris and B.Aazhang, " User Cooperation Diversity. Part I. System Description," *IEEE Trans. Commun.*, vol. 51, pp. 1927 –1938, Nov. 2003. 21

[36] E. E. A.Sendonaris and B.Aazhang, " User Cooperation Diversity. Part II. Implementation Aspects and Performance Analysis," *IEEE Trans. Commun.*, vol. 51, no. 11, pp. 1939 –1948, Nov. 2003. 21

[37] S. Hanly and D. Tse, "Multi-access Fading Channels, Part II: Delay-limited Capacities," *IEEE Trans. Inform. Theory*, vol. 44, no. 7, pp. 2816–2831, Nov. 1998. 21, 22

[38] T. M. G. Wunder and Z. Chan, "Delay-limited Transmission in OFDM Systems: Performance Bounds and Impact of System Parameters," *IEEE Trans. Commun.*, vol. 8, no. 7, pp. 3747–3757, Jul. 2009. 21

[39] E. Jorswieck and H. Boche, "Delay-limited Capacity: Multiple Antennas, Moment Constraints, and Fading Statistics," *IEEE Trans. Commun.*, vol. 6, no. 12, pp. 1536–1276, Dec. 2007. 22, 23

[40] I. M. J. K. S. Gilhousen, R. Padovani, A. J. Viterbi, L. A. Weaver, and C. E. Wheatley, "On the Capacity of a Cellular CDMA System," *IEEE Trans. Vehic. Tech.*, vol. 40, pp. 303–312, May 1991. 22

[41] S. V. Hanly, "An Algorithm for Combined Cell-site Selection and Power Control to Maximize Cellular Spread Spectrum Capacity," *IEEE J. Select. Areas Commun.,Special Issue on the Fundamentals of Networking*, vol. 13, Sep. 1995. 22

[42] R. Yates, "A Framework for Uplink Power Control in Cellular Radio Systems," *IEEE J. Select. Areas Commun.,Special Issue on the Fundamentals of Networking*, vol. 13, Sep. 1995. 22

[43] S. V. Hanly and D. Tse, "Multi-access Fading Channels: Shannon and Delay-limited Capacities," in *Proc. 33rd Allerton Conf.*, Oct. 1995. 22

[44] J. H. Yeo, " Ergodic, Delay-limited and Outage Capacities," in *Lecture notes,Department of Electronic and Electrical Engineering Phang University of Science and Technology*, Jan. 2010. 22

[45] J. P. E. Biglieri and S. S. Shitz, "Fading Channels: Information Theoretic and Communications Aspects," *IEEE Trans. Inform. Theory*, vol. 44, no. 6, pp. 2619–2692, Oct. 1998. 22, 40, 42

[46] G. T. G. Caire and E. Biglieri, "Optimum Power Control over Fading Channels," *IEEE Trans. Inform. Theory*, vol. 45, no. 5, pp. 1468–1489, Jul. 1999. 23

[47] G. C. E. Biglieri and G. Taricco, "Limiting Performance of Block Fading Channels with Multiple Antennas," *IEEE Trans. Inform. Theory*, vol. 47, no. 4, pp. 1273–1289, May 2001. 23

[48] J. H. Sung and J. R. Barry, "Approaching the Zero-outage Capacity of MIMO-OFDM without Water-filling," *IEEE Trans. Inform. Theory*, vol. 54, no. 4, pp. 1423–1436, Apr. 2008. 23

[49] R. Berry and R. Gallager, " Communication over Fading Channels with Delay Constraints," *IEEE Trans. Inform. Theory*, vol. 48, no. 5, pp. 1135–1149, Nov. 2002. 23

[50] R. Berry, " Optimal Power-delay Trade-offs in Fading Channels: Small Delay Asymptotics," in *Information Theory and Applications*, Feb. 2006. 23

[51] A. S. D. Rajan and B. Aazhang, " Delay-Bounded Packet Scheduling of Bursty Traffic over Wireless Channels," *IEEE Trans. Inform. Theory*, vol. 50, no. 1, pp. 125–144, 2004. 23

[52] R. Negi and S. Goel, " An Information-theoretic Approach to Queuing in Wireless Channels with Large Delay Bounds," in *Proc. IEEE Global Telecommun. Conf.*, vol. 1, 2004, pp. 116–122. 23

[53] I. Bettesh and S. Shamai, " Optimal Power and Rate Control for Minimal Average Delay: The Single-user Case," *IEEE Trans. Inform. Theory*, vol. 52, no. 9, pp. 4115–4141, 2006. 23

[54] J. T. L. Liu, P. Parag, W. Y. Chen, and J. F. Chamberland, " Resource Allocation and Quality of Service Evaluation for Wireless Communication Systems using Fluid Models," *IEEE Trans. Inform. Theory*, vol. 53, no. 5, pp. 1767–1777, 2007. 23

[55] P. E. Somsak Kittipiyakul and T. Javidi, " High-SNR Analysis of Outage-limited Communications With Bursty and Delay-Limited Information," *IEEE Trans. Inform. Theory*, vol. 55, no. 2, pp. 746–763, Feb. 2009. 23

[56] J. M. Abbas El Gamal, B. Prabhakar, and D. Shah, " Throughput-delay Tradeoff in Wireless Networks," in *IEEE Conf. INFOCOM*, Mar. 2004. 23

[57] P. Gupta and P. R. Kumar, " The Capacity of Wireless Networks," *IEEE Trans. Inform. Theory*, vol. 46, no. 2, pp. 388–404, Mar. 2000. 23

[58] M. Grossglauser and D. Tse, " Mobility Increases the Capacity of Ad-hoc Wireless Networks," *IEEE INFOCOM*, pp. 1360–1369, 2001. 23

[59] M. G. S. N. Diggavi and D. Tse, " Even One Dimensional Mobility Increases Ad Hoc Wireless Capacity," in *Proceedings of ISIT 2002,Laussane, Switzerland*, Jul. 2002. 23

[60] S. Jagabathula and D. Shah, " Optimal Delay Scheduling in Networks with Arbitrary Constraints," in *ACM SIGMETRICS*, 2008. 23

[61] P. Jayachandran and M. Andrews, " Minimizing End-to-End Delay in Wireless Networks using a Coordinated EDF Schedule," in *IEEE Proc. INFOCOM*, 2010. 23

[62] K. J. L. B. Le and E. Modiano, " Delay Analysis of Maximum Weight Scheduling in Wireless Ad Hoc Networks," in *Annual Conf. on Information Sciences and Systems (CISS)*, 2009, pp. 389–394. 24

[63] S. P. Guanhong Pei, V. S. Anil Kumar and A. Srinivasan, " Approximation Algorithms for Throughput Maximization in Wireless Networks with Delay Constraints," in *IEEE Proc. INFOCOM*, vol. 46, 2011, pp. 1116–1124. 24

[64] L.-S. T. Chia-Jung Chang and D. shan Shiu, " Finite Length Analysis of Generalized Expanding Window Fountain Codes," in *IEEE VTC 2009-Fall 70th*, Sep. 2009. 24

[65] N. Ahmed and R. G. Baraniuk, " Throughput Measures for Delay-constrained Communications in Fading Channels," in *Allerton Conf. on Commun.*, Oct. 2003. 24

[66] A. H. Behrouz Mahamy and M. Debbah, " Outage Probability Analysis of Multi-Relay Delay-Limited Hybrid-ARQ Channels," in *IEEE VTC 2010-Fall 72nd*, Sep. 2010. 24

[67] J. M. Pack Sangheon, Shen Xuemin, " Optimizing Truncated ARQ Scheme Over Wireless Fading Channels ," *IEEE Trans. Vehic. Tech.*, vol. 57, no. 2, pp. 1302–1305, Mar. 2008. 24

[68] S. D. Roy and S. Kundu, " Packet Data with Truncated Power Control and Truncated ARQ in Presence of Soft Hand-off," *International Journal of Energy, Information and Communications*, vol. 2, no. 2, May 2011. 24

[69] T. S. Rappaport, *Wireless Communications: Principles and Practice*, 2nd ed. Prentice Hall, 2001. 24

[70] J. Oeting, "Cellular mobile radio - an emerging technology," *IEEE Commun. Mag.*, pp. 10–15, Nov. 1983. 24

[71] V. H. MacDonald, " The Cellular Concept ," *The Bell Systems Technical Journal*, vol. 58, no. 1, pp. 15–43, Jan. 1979. 24

[72] S. Tekinay and B. Jabbari, " Handover and Channel Assignment in Mobile Cellular Networks," *IEEE Commun. Mag.*, pp. 42–46, Nov. 1991. 26

[73] L. J. G. I. Chin-Lin and R. D. Gitlin, " A Microcell/Macrocell Cellular Architecture for Low and Hight Wireless Users," *IEEE Trans. Vehic. Tech.*, vol. 11, no. 6, pp. 885–891, Aug. 1993. 26

[74] C. W. Sung and W. S. Wong, " User Speed Estimation and Dynamic Channel Allocation in Hierarchical Cellular System," in *IEEE Proc. Vehic. Tech. 44th*, Aug. 1994, pp. 91–95. 26

[75] S. S. Rappaport, " Blocking, Hand-off and Traffic Performance for Cellular Communication Systems with Mixed Platforms," in *IEEE Proc. Commun.,Speech and Vision*, vol. 10, no. 5, Oct. 1993, p. 389. 26

[76] K. M. B. Shiri Artstein, F. Barthe, and A. Naor, " Solution of Shannon's Problem on the Monotonicity of Entropy," in *J. Amer. Math. Soc.*, May 2004, pp. 975–982. 26

[77] H. Fischer, *A History of the Central Limit Theorem: From Classical to Modern Probability Theory*, 1st ed. Springer, 2010. 26

[78] V. A. Aalo and J. Zhang, " On the effect of Co-channel Interference on Average Error Rates in Nahgami-fading Channels," *IEEE Commun. Lett.*, vol. 3, pp. 136–138, 1999. 26

[79] R. Y. Tokgoz and B.D., " The Effect of Imperfect Channel Estimation on the Performance of Maximum Ratio Combining in the Presence of Co-channel Interference," *IEEE Trans. Vehic. Tech.*, vol. 55, no. 5, pp. 1527–1534, 2006. 26

[80] R. J. X. Rui and J. Geng, " Symbol Error Rate Analysis of Multiple-input Multiple-output Maximal Ratio Combining Systems with Self Interference and Co-channel Interference," *IET Commun.*, vol. 1, no. 4, pp. 1751–8628, Aug. 2007. 26

[81] R. Prasad and A. Kegel, " Improved Assessment of Interference Limits in Cellular Radio Performance," *IEEE Trans. Vehic. Tech.*, vol. 40, pp. 412–419, May 1991. 26

[82] X. Yang and A. Petropulu, " Co-channel Interference Modeling and Analysis in a Poisson Field of Interferers in Wireless Communications," *IEEE Trans. Signal Proc.*, vol. 51, no. 1, pp. 64–76, May 2003. 26

[83] J. Ilow and D. Hatzinakos, " Analytic Alpha-stable Noise Modeling in a Poisson Field of Interferers or Scatterers," *IEEE Trans. Signal Proc.*, vol. 46, no. 6, pp. 1601–1611, Jun. 1998. 26

[84] A. C. K. Gulati, B. L. Evans, and K. R. Tinsley, " Statistical Modeling of Co-Channel Interference," in *Proc. IEEE Global Commun. Conf.*, Dec. 2009, pp. 1–6. 26

[85] J. G. A. S. Weber and N. Jindal, " The Effect of Fading, Channel Inversion, and Threshold Scheduling on Ad Hoc Networks," *IEEE Trans. Inform. Theory*, vol. 53, no. 11, pp. 4127–4149, 2007. 26

[86] A. C. K. Gulati, R. W. Heath, B. L. Evans, K. R. Tinsley, and X. E. Lin, " MIMO Receiver Design in the Presence of Radio Frequency Interference," in *Proc. IEEE Global Commun. Conf.*, Dec. 2008. 26

[87] J. H. W. R. S. Blum and N. R. Sollenberger, " On the Capacity of Cellular Systems with MIMO," *IEEE Commun. Lett.*, vol. 6, no. 6, pp. 242–244, Jun. 2002. 26

[88] S. Sigdel and W. A. Krzymien, " Interference Suppression Through Adaptive Subset Antenna Transmission in Interference Limited MIMO Wireless Environments," in *IEEE VTC-2006 Fall Conf. 64th*, Sep. 2006, p. 1. 26

[89] C. R. Tanya Mayer and T. T. Ha, " Co-Channel Interference Reduction on the Forward Channel of a Wideband CDMA Cellular System," in *IEEE Military Commun. Conf. Proc.*, 1999, p. 785. 26

[90] N. S. Alan Carter, Derek Hilborn and A. Abu-Dayya, " A Diversity Co-Channel Interference Canceller for AMPS Cellular Systems," in *IEEE VTC-1998 Fall Conf. 48th*, May 1998, p. 26. 26

[91] M. K. Simon and M.-S. Alouini, *Digital Communication over Fading Channels: A Unified Approach to Performance Analysis*. Wiley, 2000. 27

[92] P. Loskot and N. C. Beaulieu, "Prony and polynomial approximations for evaluation of the average probability of error over slowly fading channels," *IEEE Trans. Vehic. Tech.*, vol. 58, pp. 1269–1280, Mar. 2009. 28, 29, 30, 40, 41, 104

[93] A. Papoulis and S. U. Pillai, *Probability, Random Variables, and Stochastic Processes*, 4th ed. McGraw-Hill, 2002. 28, 29, 30, 109, 110

[94] J. Bollinger, *Bollinger on Bollinger Bands*. McGraw-Hill Professional, 2001. 28, 31

[95] D. E. Knuth, *The Art of Computer Programming*, 3rd ed. Addison-Wesley, Mar. 2011. 31

[96] H. Y. T. Ngan and G. K. H. Pang, "Novel Method for Patterned Fabric Inspection using Bollinger Bands," *Society of Photo-Optical Engineers*, vol. 45, Sep. 2006. 31

[97] E. Kreyszig, *Advanced Engineering Mathematicas*, 7th ed. John Wiley & Sons , Inc., 1993. 33

[98] M. Chiani, D. Dardari, and M. K. Simon, "New Exponential Bounds and Approximations for the Computation of Error Probability in Fading Channels," *IEEE Trans. Wireless Commun.*, vol. 2, no. 4, pp. 840–845, Jul. 2003. 33

[99] J. J. Boutros, A. G. Fàbregas, E. Biglieri, and G. Zémor, "Low-density parity-check codes for nonergodic block-fading channels," *IEEE Trans. Inform. Theory*, vol. 56, no. 9, pp. 4286–4300, Sep. 2010. 40, 42, 43

[100] J. Kieffer, "Epsilon-Capacity of a Class of Non-ergodic Channels," in *Proc. ISIT*, 2006, pp. 1268–1271. 40

[101] W. M. Bolstad, *Introduction to Bayesian Statistics*, 2nd ed. John Wiley & Sons, Inc., 2007. 41, 44, 45, 46, 47

[102] K. R. Koch, *Introduction to Bayesian Statistics*, 2nd ed. Springer, 2007. 41, 44

[103] M. C.Jeruchim, P. Balaban, and K. S. Shanmugan, *Simulation of Communication Systems: Modeling, Methodology, and Techniques*, 2nd ed. Kluwer Academic Publishers, 2002. 41, 44, 45, 53

[104] K. L. Kosbar and T. F. Chang, "Interval Estimation and Monte Carlo Simulation of Digital Communication Systems," in *Proc. MILCOM*, 1992, pp. 3.3.1–3.3.5. 41

[105] Billingsley and Patrick, *Convergence of Probability Measures*, 2nd ed. John Wiley & Sons , Inc., 1999. 44

[106] M. Abramowitz and I. A. Stegun, *Handbook of Mathematical Functions with Formulas, Graphs, and Mathematical Tables*. Dover, 1974. 46, 110, 112, 113

[107] R. Kass and J.M.Buhrman, "Mean, Median and Mode in Binomial Distributions," *Statistica Neerlandica*, vol. 34, pp. 13–18, Apr. 2008. 50

[108] M. Mitzenmacher and E. Upfal, *Probability and Computing: Randomized Algorithms and Probabilistic Analysis*. Cambridge University Press, 2005. 53

[109] T. M. Cover and J. A. Thomas, *Elements of Information theory*, 2nd ed. John Wiley & Sons, 1991. 68

[110] S. Lin and D. J. Costello, *Error Control Coding: Fundamentals and Applications*. Prentice-Hall, 1983. 68

[111] A. Goldsmith and P. Varaiya, "Capacity of Fading Channels with Channel Side Information," *IEEE Trans. Inform. Theory*, vol. 43, no. 6, pp. 1986–1992, Nov. 1997. 69

[112] S. Fujii, T. Kaneko, and Y. Hayashida, "Effectiveness of Copy-transmission in Go-Back-N ARQ System with Selective Repeat in Intra-block and with Limited Retransmissions," in *Proc. Int. Conf. Commun. Syst. Networks*, 2010, pp. 1–6. 69

[113] I. Khazali and A. Agarwal, "Control Messages Delivery Protocol," in *Proc. Bien. Symp. Commun.*, 2010, pp. 251–254. 69

[114] J. L. Lugand, D. J. Costello and R. H. Deng, "Parity Retransmission Hybrid ARQ Using Rate 1/2 Convolutional Codes on a Non-stationary Channel," *IEEE Trans. Commun.*, vol. 37, pp. 755–765, Jul. 1989. 69

[115] Q. Yang and V. K. Bhargava, "Delay and Coding Gain Analysis of a Truncated Type-II Hybrid ARQ Protocol," *IEEE Trans. Vehic. Tech.*, vol. 37, pp. 177–183, Feb. 1989. 69

[116] S. I. F. Adachi and K. Ohno, "Performance Analysis of a Time Diversity ARQ in Land Mobile Radio," *IEEE Trans. Commun.*, vol. 42, pp. 22–32, Feb. 1993. 69

[117] E. Malkamäki and H. Leib, "Performance of Truncated Type-II Hybrid ARQ Schemes with Noisy Feedback over Block Fading Channels," *IEEE Trans. Commun.*, vol. 48, no. 9, Sep. 2000. 69

[118] C. Wengerter, A. G. E. von Elbwart, E. Seidel, G. Velev, and M. Schmitt, "Advanced Hybrid ARQ Technique Employing a Signal Constellation Rearrangement," in *Proc. VTC*, vol. 4, 2006, pp. 2002–2006. 69

[119] J. Jung, H. Park, and J. Lim, "A Novel Hybrid ARQ Scheme Based on Shift Column Permutation Bit Interleaving for OFDM Systems," in *Proc. VTC*, 2006, pp. 1–5. 69

[120] D. J. C. MacKay, *Information Theory, Inference, and Learning Algorithms*. Cambridge Univ. Press, 2003. 69

[121] K. C. Beh, A. Doufexi, and S. M. D. Armour, "Performance Evaluation of Hybrid ARQ Schemes of 3GPP LTE OFDMA System," in *Proc. PIMRC*, 2007, pp. 1–5. 69

[122] S. Benedetto and E. Biglieri, *Principles of Digital Transmission with Wireless Applications*, 2nd ed. Kluwer Academic, 1999. 71

[123] P. Hoeher, S. Badri-Hoeher, X. Wen, and C. Krakowski, "Single-antenna Co-channel Interference Cancellation for TDMA Cellular Radio Systems," *IEEE Wireless Comms. Mag.*, vol. 12, pp. 30–37, Apr. 2005. 107

[124] Y. Yao and A. U. H. Sheikh, "Investigation into Co-channel Interference in Micro-cellular Mobile Systems," *IEEE Trans. Vehic. Tech.*, vol. 41, no. 2, pp. 114–123, May 1992. 107

[125] N. C. Beaulieu and A. A. Abu-Dayya, "Bandwidth-efficient QPSK in Co-channel Interference and Fading," *IEEE Trans. Commun.*, vol. 43, no. 9, pp. 2464–2474, Sep. 1995. 107, 108

[126] N. C. Beaulieu and J. Cheng, "Precise Error Rate Analysis of Bandwidth Efficient BPSK in Nakagami Fading and Co-channel Interference," *IEEE Trans. Commun.*, vol. 52, no. 1, pp. 149–158, Jan. 2004. 107, 108

[127] Z. Du, J. Cheng, and N. Beaulieu, "BER Analysis of BPSK Signals in Ricean-Faded Cochannel Interference," *IEEE Trans. Commun.*, vol. 55, pp. 1994–2001, Oct. 2007. 107

[128] G. Zang and C. Ling, "Performance Evaluation for Band-limited DS-CDMA Systems Based on Simplified Improved Gaussian Approximation," *IEEE Trans. Commun.*, vol. 51, no. 7, pp. 1204–1213, Jul. 2003. 107

[129] X. Liu and L. Hanzo, "A Unified Exact BER Performance Analysis of Asynchronous DS-CDMA Systems Using BPSK Modulation over Fading Channels," *IEEE Trans. Wireless Commun.*, vol. 6, no. 10, pp. 3504–3509, Oct. 2007. 107

[130] B. Smida, L. Hanzo, and S. Affes, "Exact BER Performance of Asynchronous MC-DS-CDMA over Fading Channels," *IEEE Trans. Wireless Commun.*, vol. 9, no. 4, pp. 1249–1254, Apr. 2010. 107

[131] Y. C. Yoon, "An Improved Gaussian Approximation for Probability of Bit-Error Analysis of Asynchronous Bandlimited DS-CDMA Systems with BPSK Spreading," *IEEE Trans. Wireless Commun.*, vol. 1, no. 3, pp. 373–382, Jul. 2002. 107

[132] A. Giorgetti and M. Chiani, "Influence of Fading on the Gaussian Approximation for BPSK and QPSK with Asynchronous Co-channel Interference," *IEEE Trans. Wireless Commun.*, vol. 4, no. 2, pp. 384–389, Mar. 2005. 108

[133] M. K. Simon, *Probability Distributions Involving Gaussian Random Variables*, 1st ed. Springer, 2002. 129

[134] H. Pham, *Handbook of Engineering Statistics*. Springer, 2006. 129